DYNAMIC PULL ANALYSIS FOR ESTIMATING SEISMIC RESPONSE

A THESIS SUBMITTED TO
THE GRADUATE SCHOOL OF NATURAL AND APPLIED SCIENCES
OF
MIDDLE EAST TECHNICAL UNIVERSITY

BY

CAN DEĞİRMENCİ

IN PARTIAL FULFILLMENT OF THE REQUIREMENTS
FOR
THE DEGREE OF MASTER OF SCIENCE
IN
CIVIL ENGINEERING

NOVEMBER 2006

Approval of the Graduate School of Natural and Applied Sciences

Prof. Dr. Canan Özgen
Director

I certify that this thesis satisfies all the requirements as a thesis for the degree of Master of Science.

Prof. Dr. Erdal Çokca
Head of Department

This is to certify that we have read this thesis and that in our opinion it is fully adequate, in scope and quality, as a thesis for the degree of Master of Science.

Prof. Dr. Haluk Sucuoğlu
Supervisor

Examining Committee Members

Assoc. Prof. Dr. Ahmet YAKUT	(METU,CE)	
Prof. Dr. Haluk SUCUOĞLU	(METU,CE)	
Assoc. Prof. Dr. Sinan AKKAR	(METU,CE)	
Asst. Prof. Dr. Altuğ ERBERİK	(METU,CE)	
M.S. Joseph KUBİN	(PROTA)	

I hereby declare that all information in this document has been obtained and presented in accordance with academic rules and ethical conduct. I also declare that, as required by these rules and conduct, I have fully cited and referenced all material and results that are not original to this work.

Name, Last name: Can DEĞİRMENCİ

Signature:

ABSTRACT

DYNAMIC PULL ANALYSIS FOR ESTIMATING THE SEISMIC RESPONSE

Değirmenci, Can
M.S., Department of Civil Engineering
Supervisor: Prof. Dr. Haluk Sucuoğlu

November 2006, 144 pages

The analysis procedures employed in earthquake engineering can be classified as linear static, linear dynamic, nonlinear static and nonlinear dynamic. Linear procedures are usually referred to as force controlled and require less analysis time and less computational effort. On the other hand, nonlinear procedures are referred to as deformation controlled and they are more reliable in characterizing the seismic performance of buildings. However, there is still a great deal of unknowns for nonlinear procedures, especially in modelling the reinforced concrete structures.

Turkey ranks high among all countries that have suffered losses of life and property due to earthquakes over many centuries. These casualties indicate that, most regions of the country are under seismic risk of strong ground motion. In addition to this phenomenon, recent studies have demonstrated that near fault ground motions are more destructive than far-fault ones on structures and these effects can not be captured effectively by recent nonlinear static procedures.

The main objective of this study is developing a simple nonlinear dynamic analysis procedure which is named as “Dynamic Pull Analysis” for estimating the seismic response of multi degree of freedom (MDOF) systems. The method is tested on a six-story reinforced concrete frame and a twelve-story reinforced concrete frame that are designed according to the regulations of TS-500 (2000) and TEC (1997).

Keywords: Nonlinear analysis procedures, pushover, modal pushover analysis, dynamic pull analysis, near-fault ground motions

ÖZ

DİNAMİK ÇEKME ANALİZİ İLE SİSMİK TEPKİLERİN TAHMİNİ

Değirmenci, Can
Yüksek Lisans, İnşaat Mühendisliği Bölümü
Tez Yöneticisi: Prof. Dr. Haluk Sucuoğlu

Kasım 2006, 144 sayfa

Deprem mühendisliğinde kullanılan yöntemler doğrusal statik, doğrusal dinamik, doğrusal olmayan statik ve doğrusal olmayan dinamik yöntemler olarak sınıflandırılabilir. Doğrusal yöntemler genellikle kuvvet kontrollu olmakta ve az analiz zamanına ve az hesaplama emeğine gerek duymaktadır. Diğer taraftan, doğrusal olmayan yöntemler deplasman kontrollü olup, binaların sismik performansını belirleme açısından daha güvenilir sayılmaktadır. Fakat, özellikle betonarme yapıların modellenmesinde doğrusal olmayan yöntemler hala birçok bilinmez barındırmaktadır.

Türkiye depremlerden dolayı olan can ve mal kayıpları bakımından yüzyıllardır tüm ülkeler arasında üst sıralarda yeralmaktadır. Bu kayıplar göstermiştir ki ülkenin birçok bölgesi güçlü yer hareketleri riski altındadır. Bununla birlikte, son dönemde yapılan çalışmalar göstermiştir ki, yakın fay yer hareketleri uzak fay yer hareketlerine göre yapılar üzerinde daha yıkıcı olmakta

ve bu etkiler güncel doğrusal olmayan statik yöntemler tarafından etkili bir şekilde tespit edilememektedir.

Bu çalışmanın temel amacı, çok dereceli sistemlerin (ÇDS) sismik tepkilerin tahmini için "Dinamik Çekme Analizi" diye adlandırılan basit bir doğrusal olmayan dinamik analiz yönteminin geliştirilmesidir. Bu yöntem, TS-500 (2000) and TEC (1997) yönetmeliklerine göre tasarlanmış altı ve on iki katlı betonarme çerçeveler üzerinde test edilmişdir.

Anahtar kelimeler: Doğrusal olmayan analiz yöntemleri, doğrusal olmayan artımsal itme analizi, modal doğrusal olmayan artımsal itme analizi, dinamik çekme analizi, yakın fay yer hareketleri

To my sponsors and full time supporters; my family ☺

ACKNOWLEDGEMENTS

This study was performed under the supervision of Prof. Dr. Haluk Sucuoğlu. I would like to express my sincere appreciation for his support, guidance and insights throughout the study.

Mehmet Selim Günay is highly acknowledged for their complimentarily helps in the thesis study.

I would like to thank my friends at METU; Zeynep Düzce, Serdar Çullu, Özgür Lütfi Ertuğrul.

Thanks go to Aydan Özmen, Robert Jury and David Hopkins for sharing their worthy experiences with me during the Teknokent days.

I thank K. Mete Bastırmacı and Doğan Okay for every moment of very enjoyable co-operations and educating me for different phase of the business world

My homemates, Erkan Karagöz and Salih Serkan Artagan deserve thanks for all the moments shared together.

My dear parents, my sister and my grandparents deserve the greatest thanks for their endless love, support, friendship, understanding and endurance.

TABLE OF CONTENTS

LIST OF TABLES

LIST OF FIGURES

CHAPTER 1

INTRODUCTION

1.1 Statement of Problem

Recently, countries that are under significant earthquake risk such as United States, Japan, Italy and Turkey move towards the implementation of Performance Based Earthquake Engineering philosophies in seismic design of civil structures. For this reason, new seismic design provisions will require structural engineers to perform nonlinear analyses of the structures that they are designing.

Today, the analysis procedures employed in the earthquake engineering profession can be classified as linear static, linear dynamic, nonlinear static and nonlinear dynamic. Linear procedures are usually referred as force controlled, while nonlinear procedures are referred as deformation controlled. Nonlinear procedures are more reliable on characterizing the seismic performance of buildings than the linear procedures, while linear procedures require less time and less computational effort. Although, a significant amount of research is performed for developing nonlinear procedures, there is a great deal of unknowns especially in modelling purpose of reinforced concrete structures. Modelling shear walls, shear deformations, non structural members are still a challenge.

Nonlinear static procedure, which is called "Pushover Analysis" in literature, consists of a series of analyses, to obtain a force-displacement curve (capacity curve) of the overall structure. Nonlinear force-deformation properties of all lateral force-resisting elements are created and gravity loads are applied initially. A predefined lateral load pattern that is distributed along the building height is then applied. Each load step, lateral loads are homogenously increased. After certain step, some members start to yield. Then structural model is modified at each step according to nonlinear response of members that reduces the global stiffness. Procedure is repeated until a control displacement at the top of building reaches a certain level of deformation, or structure becomes unstable. The roof displacement is plotted against base shear to obtain the global capacity curve; i.e., pushover curve.

The nonlinear static procedure must be used with attention. The pushover analysis is a representation of a static "approximation" of the response of a structure when subjected to dynamic earthquake loads. This approximate analysis method has a great advantage when compared to the exact nonlinear dynamic analysis. However, it has some limitations that affect the accuracy of results such as the estimating of approximate response, selection of lateral load patterns and identification of failure mechanisms due to higher modes of vibration. To eliminate these weaknesses, several methods were proposed such as modal pushover analysis (Chopra and Goel, 2001) which is aimed to solve higher mode effect and adaptive pushover methodology which is aimed to solve selection of load patterns.

Turkey ranks high among countries, which have suffered losses of life and property due to earthquakes over many centuries. For example in the last century, earthquakes caused over 110,000 deaths, about 250,000 hospitalized injuries and close to 600,000 destroyed housing unit in Turkey. These causalities indicate that, most of the regions of country are under risk of strong ground motion shaking. Recent studies have demonstrated that near fault ground motions impose large demands on structures compared to ordinary ground motions. In addition to large inelastic displacement demand, commonly used displacement estimation techniques that are successful for far field earthquakes are unable to capture the sequence of displacement profile (Alavi and Krawinkler, 2001). For this reason, effects of near fault ground motions must carefully be examined for reducing further losses in Turkey by the new generation of earthquake engineers.

1.2 Review of Past Studies

1.2.1 Simplified Nonlinear Analysis Procedures

Structures exposed to severe seismic actions usually respond inelastically. Hence, nonlinear analysis procedures and simplification of these procedures is a subject that has been studied since 1960's. The proposed simplified nonlinear analysis procedures and structural models are usually based on the reduction of MDOF model of structures to an equivalent SDOF system. The studies of Jacobsen (1960) and Rosenblueth and Herrera (1964) are two examples of this time period.

The concept of equivalent viscous damping was originally proposed by Jacobsen (1960) to obtain approximate solutions for the steady state vibration of SDOF systems with linear restoring force-deformation and nonlinear damping force-velocity relationships under harmonic loading. In this method, the equivalent damping was determined by equating the energy per cycle of the nonlinearly damped oscillator to the energy per cycle of a linearly damped oscillator having the same period with the original system and equivalent-damping ratio. Then, he extended the concept of equivalent damping to SDOF systems with nonlinear restoring force-deformation relationships by considering a period shift in combination with equivalent viscous damping

Rosenblueth and Herrera (1964) proposed a procedure in which the maximum deformation of inelastic SDOF system was estimated as the maximum deformation of a linear elastic SDOF system with longer period of vibration (T_{eq}) and higher damping coefficient (ζ_{eq}). In this procedure, series of analyses were conducted by changing values of T_{eq} and ζ_{eq} and by results of these analysis series, deformation of inelastic systems were estimated. Rosenblueth and Herrera (1964) used the secant stiffness at maximum deformation to represent period shift, and equivalent-damping ratio was calculated by equating the energy dissipated per cycle in nonlinear and equivalent linear SDOF system subjected to harmonic loading.

Gülkan and Sozen (1974) stated that the response of reinforced concrete structures to strong earthquake motions was influenced by two basic phenomena, which were reduction in stiffness and increase in energy dissipation capacity. They also stated that the maximum dynamic response of reinforced concrete structures, which can be represented by SDOF systems, can be approximated by linear response analysis using a reduced stiffness and a substitute damping. Gülkan and Sozen expressed that the equivalent viscous damping approach had considerable potential as a vehicle to interpret the response of RC systems from the design point of view, and used the equivalent damping approach to estimate the design base shear corresponding to inelastic response. They developed an empirical equation for equivalent damping ratio using secant stiffness of Takeda hysteresis model. They conducted dynamic experiments with one story, one bay frames. Results obtained from experiments supported proposed procedure.

Shibata and Sözen (1976) proposed the Substitute-Structure Method as a procedure for determination of design forces and for improving the reduced stiffness and equivalent damping analogy of Gülkan and Sözen (1974) for MDOF systems. This procedure can be used for just 2-D models structures which are regular in plan and elevation.

Newmark and Hall (1982) proposed procedures on displacement modification factors. Main purpose of the procedures is estimating the inelastic displacement demand of MDOF system by using equivalent elastic SDOF representation. This equivalent SDOF system has the same lateral stiffness and damping coefficient as that of MDOF one and its maximum deformation is converted to find maximum deformation of inelastic MDOF system by using certain displacement modification factors. A similar study was conducted by Miranda (2000). Miranda has developed C1 values which is a modification factor to relate expected maximum inelastic displacements to displacements calculated from linear elastic spectral response for oscillators having bilinear load-deformation relations located on firm sites, and has developed C1 values for stiffness degrading systems.

Fajfar and Fischinger (1987) introduced the N2 Method in the seismic evaluation of the nonlinear seismic response of a seven story RC frame-wall building. It was observed that the N2 Method underestimated the shear forces along the height of the building in this study. The method was explained in detail with some modifications by Fajfar and Gaspersic (1996). This method can be used for planar structures that oscillate predominantly in the first mode. It uses the elastic spectrum and nonlinear static analysis. The capacity curve of a MDOF system is converted to the capacity curve of a SDOF system and global demand is determined using R-μ-T relations. Then the local demands are determined by performing nonlinear static analysis up to the determined global displacement demand. A global damage index is determined at the end of the method.

In the 1990's, Capacity Spectrum Method (ATC-40, 1996) was recommended by ATC-40 (1996) as a displacement-based design and assessment tool for structures. It was originally developed as a rapid evaluation procedure for a pilot seismic risk project of the Puget Sound Naval Shipyard of the U.S. Navy (Freeman et al., 1975). Detailed explanations of three versions of procedure, which are called Procedure A, B and C can be found in ATC-40

(1996) documents. Firstly, proposed method requires force-displacement curve of MDOF system which presents the capacity of the structure and response spectrum of earthquake or a design spectrum. Then, that curve compares with estimated demand response spectrum. Both of them are converted in Acceleration-Displacement Response Spectrum (ADRS) that the spectral accelerations are plotted against spectral displacements with radial lines that represent the period. The demand is obtained by reducing elastic response spectrum with spectral reduction factors which depend on effective damping. All spectral reduction factors are functions of some parameters such as, structural behaviour type which is about hysteretic properties of structure and ground motion shaking duration. On the other hand, selection of these parameters is the hardest part of this procedure and approximations involved in the determination of these characteristics are the main weaknesses of the method.

Displacement Coefficient Method is the primary nonlinear static procedure presented in FEMA-273 (1997) and FEMA-356 (2000). This approach modifies the linear elastic response of the equivalent SDOF system by multiplying it by a series of coefficients C_0 through C_3 to generate an estimate of the maximum global displacement (elastic and inelastic), which is called the target displacement. The process begins with an idealized force-deformation curve relating base shear to roof displacement. An effective period, T_e, is generated from the initial period, T_i, by a graphical procedure that accounts for some loss of stiffness in the transition from elastic to inelastic behavior. The effective period represents the linear stiffness of the equivalent SDOF system. When plotted on an elastic response spectrum representing the seismic ground motion as peak acceleration, Sa, versus period, T, the effective period identifies a maximum acceleration response for the oscillator. Recently, various studies have proposed simplified expressions especially for C_1 modification coefficient by Aydinoglu and Kacmaz (2002); Ramirez et al.(2003), Ruiz-Garcia and Miranda (2003); Chopra and Chintanapakdee (2004).

Miranda and Ruiz-Garcia (2002) conducted a study to evaluate the accuracy of six approximate methods that are proposed some researchers such as Rosenblueth and Herrera (1964), Gülkan and Sözen (1974), Newmark and Hall (1982) and Miranda (2000). SDOF systems that were used Elasto-plastic, modified Clough stiffness degrading (Clough and Johnston, 1996) and Takeda hysteretic models (Takeda et al , 1970) with periods between 0.05 and 3.0 sec. were considered when subjected to264 ground motions recorded on firm sites in California. For each method, mean ratios of approximate to exact displacement and dispersion of relative errors were computed as a function of vibration period and displacement ductility ratio. It is observed that approximate procedures can lead to significant errors in estimation of maximum displacement demand when applied to individual ground motion records.

Chopra and Goel (1999) have proposed an improved capacity-demand diagram method described in ATC 40 (1996). This procedure uses constant ductility demand spectrum to estimate seismic deformation of equivalent inelastic SDOF systems that represents of MDOF systems.

1.2.2 Pushover Analysis

1.2.2.1 Conventional Pushover Analysis

The purpose of pushover analysis is to evaluate the expected performance of a structural system by estimating its strength and deformation demands in design earthquakes by means of a static inelastic analysis, and comparing these demands to available capacities at the performance levels of interest. However, pushover analysis has no rigorous theoretical foundation. It is based on the response of an equivalent SDOF system. This means that the response is controlled by a single mode, and that mode shape remains constant throughout the time history response (Krawinkler and Seneviratna, 1998).

However, these assumptions are incorrect. For this reason, researchers investigated various aspects of pushover analysis to identify the limitations and weaknesses of the procedure and proposed improved pushover procedures that consider the effects of lateral load patterns, higher modes, failure mechanisms, etc.

Krawinkler and Seneviratna (1998) conducted a detailed study that discusses the advantages, disadvantages and the applicability of pushover analysis. In this study, basic concepts and main assumptions of the nonlinear static response were identified. The accuracy of pushover predictions were evaluated on a four-story steel perimeter frame damaged in the 1994 Northridge earthquake. The frame was subjected to nine ground motion records. Local and global seismic demands were calculated from pushover analysis results at the target displacement for each individual record. Results showed that for regular low-rise structures in which higher mode effects are not very important and in which inelasticity is distributed uniformly over the height, the analysis provides very good predictions of seismic demands. Nonlinear static procedure also exposes the design weaknesses, which are story mechanisms, excessive deformation demands, strength irregularities and overloads on potentially brittle elements such as columns and connections that may remain hidden in elastic analysis. On the other hand, author also recommended implementing pushover analysis with caution and judgment considering its many limitations since the method is approximate in nature and contains many unresolved issues that need to be investigated.

Gupta (1999) analyzed the recorded responses of eight buildings that experienced ground accelerations in the excess of 0.25g during the 1994 Northridge earthquake to understand the behaviour of actual structures and to evaluate the acceptability of pushover analysis. The selected buildings were 5, 7, 10, 13, 14, 17, 19- and 20-story structures having moment resisting frames, shear walls as lateral force resisting systems. In addition, these buildings were instrumented at the time of the earthquake. The recorded story displacement, inter-story drift, story inertia force and story shear profiles at various instants of time were evaluated. It was observed that the responses of buildings were significantly affected by higher modes with the exception of low-rise structures. Furthermore, these effects were better understood by analyzing the inertia force and story drift profiles rather than story displacements..

Mwafy and Elnashai (2001) performed a series of pushover analyses and incremental dynamic collapse analyses to investigate the validity and the applicability of pushover analysis. Twenty reinforced concrete buildings, four eight-story irregular frames, four twelve-story regular frames and four eight-story dual frame-walls, with different base shear coefficients, 0.15 and 0.30 and with three different design ductility levels, low, medium and high, were analyzed. For nonlinear time-history analysis, four natural and four artificial earthquake records scaled to peak ground accelerations of 0.15g and 0.30g were applied on detailed 2-D models of structures. By using the results of earthquake records, pushover-like load-displacement curves obtained by using upper and lower response envelopes as well as the best fit were prepared for each structure cases with the help of regression analyses. In addition, pushover analyses were conducted with uniform, triangular and multimodal load patterns to compare and check validity of the results. The results showed that the triangular load pattern outcomes were in good correlation with the dynamic analysis results leading to conservative prediction of capacity and a reasonable estimation of deformation. In addition, results showed that pushover analysis is more appropriate for low-rise and short period structures and triangular loading is adequate to predict the response of such structures. On the other hand, uniform load distribution provides a conservative prediction of seismic demands in the range before first collapse. It also yields an acceptable estimation of shear demands at the collapse limit state. Furthermore, the fundamental period elongation varies in the range of 60% to 100%. For this reason, elastic period formulations in seismic codes do not provide uniform levels of safety for different structural systems. Finally, further developments on accounting the inelasticity of lateral load patterns are suggested. This would make analysis more accurate for high-rise and highly irregular structures.

1.2.2.2 Adaptive Pushover Analysis Procedures

Conventional pushover analysis consists in the application and monotonic increase of a predefined lateral load pattern, kept constant throughout the analysis. However, such a procedure exhibits a number of limitations, mainly related to its inability to account for the progressive stiffness degradation, the change of modal characteristics and the period elongation of structure to monotonic loading. As a result, recent years many researchers have introduced adaptive pushover methods to overcome such limitations.

Bracci, Kunnath and Reinhorn (1997) were the first to introduce a procedure that utilizes fully adaptive patterns. Proposed procedure developed for evaluating the seismic performance and retrofit of existing low-to-midrise reinforced concrete (RC) buildings. The procedure was derived from the well-known capacity spectrum method and was intended to provide practicing engineers with a methodology for estimating the margin of safety against structural failure. A series of seismic story demand curves was established from modal superposition analyses wherein changes in the dynamic characteristics of the structure at various response phases ranging from elastic to full failure mechanism were considered. These demands were compared to the lateral story capacities as determined from an independent inelastic pushover analysis. The distributions of lateral forces used in the progressive pushover analysis were based on stiffness dependent incremental story shear demands and forms a critical aspect of the methodology. The proposed technique was applied to a one-third scale model, three-story reinforced concrete frame building that was subjected to repeated shaking table excitations, and that was later retrofitted and tested again at the same intensities. This study indicated that the procedure could provide reliable estimates of story demands versus capacities for use in seismic performance and retrofit evaluation of structures.

A different adaptive methodology, which accounts for the effects of higher modes and limitations of traditional pushover analysis, was proposed by Gupta and Kunnath (2000). The proposed method was identical to response spectrum analysis. At any step, load pattern was constantly updated, depending on the instantaneous dynamic characteristics of the structure, and a site-specific spectrum or a design spectrum was used to define the applied load. According to the method, eigenvalue analysis was carried out before each load increment, accounting for the current structural stiffness state. The number of modes of interest that are considered was predefined and the storey forces for each mode are estimated as the product between the modal participation factor, mass-normalized mode shape, weight of the storey and spectral amplification of the mode being considered. Then, a static analysis is carried out for each mode independently and the calculated action effects for each mode are combined with SRSS and added to the corresponding values from the previous step. 4, 8, 12, 16, and 20-story structures having moment resisting frames, frames with soft and weak story and shear walls were analyzed for evaluating the accuracy and applicability of method. The results of method were compared with the nonlinear time history results that were obtained by analyzing the same frames with fifteen earthquake data from the SAC ground motion records from Los Angles area. Mainly global structure behaviour, interstory drift distributions and plastic hinge locations were compared. According to observations, while traditional pushover analysis failed to capture the effects of higher modes, the results of proposed adaptive methodology were in very good correlation with nonlinear dynamic analysis.. The procedure was also validated using an existing multistory building for which instrumented data was available.

Elnashai (2001) proposed an adaptive pushover scheme within a single-analysis pushover algorithm. This single-run procedure was fully adaptive and multi-modal and accounts for system degradation and period elongation by updating the force distribution at every step or at predefined steps of the analysis. The dynamic properties of the structure are determined by means of eigenvalue analyses that consider the instantaneous structural stiffness state, at each analysis step. Site specific or ground motion specific spectral shapes can also be considered in the scaling of forces, to account for the dynamic amplification that expected ground motion might have on the different vibration modes of the structure. Accuracy of proposed algorithm was tested by Antoniou and Pinho (2004). Observations indicated that further research work was required before this adaptive pushover algorithm can be valid alternative to nonlinear time history analysis.

Vamvatsikos and Cornell (2002) developed Incremental Dynamic Analysis (IDA) method. Actually, IDA was the dynamic equivalent to a familiar static pushover analysis. In this method, for a given structure and a ground motion, IDA was done by conducting a series of nonlinear time-history analyses. The intensity of the ground motion, measured using an intensity measure (IM), was incrementally increased in each analysis. Finally A plot of intensity measure (IM) of ground motion versus damage measure (DM) of structural response under scaled ground motion, which was known as an IDA curve, obtained. Vamvatsikos and Cornell (2002) demonstrated the utility of this procedure by considering a 9-story steel moment resisting frame. This building was analyzed for different levels of seismic intensity. The output was in the form of demands such as peak roof drift, or maximum base shear for a given hazard level. This data enables the engineer to proceed with the design of the structure such that members have enough capacity to sustain the demands imposed by an earthquake corresponding to the pre-determined hazard level.

1.2.2.3 Pushover Procedures Considering Higher-Mode Effects.

One of the first attempts to consider higher-mode effects was made by Paret, Sasaki and Freeman (1996) who introduced "Modal Criticality Index" (MCI). MCI was used to identify the vibration mode most likely to cause building failure. The procedure comprises several pushover analyses under forcing vectors representing the various modes. The individual pushover curves are then converted to ADRS format, after which the Capacity Spectrum method (Freeman,1975) is utilized to compare the structural capacity with the earthquake demand. MCIs are calculated by dividing earthquake demand to structure's capacity. According the procedure, the largest MCI value identifies the critical mode (Figure 1.1). Then, Sasaki, Freeman and Paret (1998) extended the idea of MCI to develop Multi-Mode Pushover (MMP) procedure. Aim of method is to identify failure mechanisms due to higher modes of vibration. MMP was used load patterns whose shapes are based on the elastic mode shapes of the structure while obtaining capacity curves. Method uses Capacity Spectrum Method (ATC-40, 1996) to compare the pushover curve to the earthquake demand graphically. A seventeen-story steel frame damaged by 1994 Northridge earthquake and a 12-story steel frame damaged by 1989 Loma Prieta earthquake were evaluated using MMP. For both frames, pushover analysis based only on first mode load pattern was inadequate to identify the actual damage. However, pushover results of combined effect of first mode and higher modes matched more closely to the actual damage distribution. Obtained results showed that, MMP, which is a simple extension of the current pushover procedures; results in more closely match of actual damage than nonlinear static procedures based on first mode load patterns for the structures with significant higher order modal response. On the other hand, this procedure developed for identifying failure mechanisms due to higher modes.

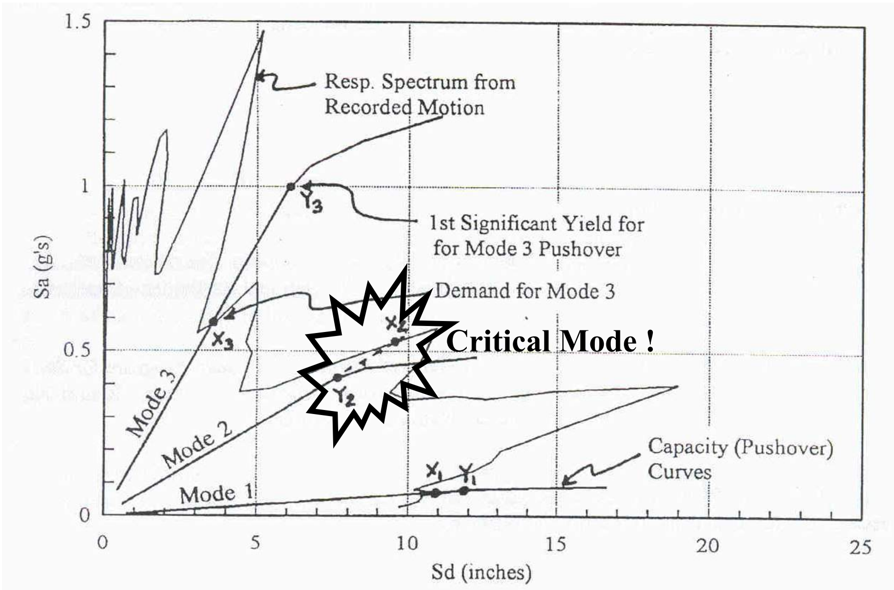

Figure 1.1 : Capacity and demand curves of seventeen story steel building frame (Paret, Sasaki and Freeman, 1996))

Aydinoglu (2003) described a multi-modal incremental response-spectrum analysis method (IRSA). Main objective of study was to develop a new pushover analysis method, which was able to consider multi-mode effects in a practical and theoretical consistent manner. The proposed procedure was based on development of modal capacity diagrams, which were defined as the backbone curves of modal hysteresis curves. These diagrams were used for estimation of the instantaneous modal inelastic spectral displacements in a piecewise linear process called pushover-history analysis. A generic frame model of the nine-story SAC building with neglecting gravity loads and P-Δ effects was analyzed for evaluating the accuracy and applicability of method. The results of method, which were mainly story drift ratios, plastic hinge rotations, story shears and overturning moments, were compared with the nonlinear time history results of 1940 El Centro (N-S) record. In addition, a practical version of the procedure was developed which was based on the code-specific smooth response spectrum and equal displacement rule.

Chopra and Goel (2001) developed an improved pushover analysis procedure named as Modal Pushover Analysis (MPA). Main objective of the study to develop an improved pushover analysis procedure based on structural dynamics theory, which retains the conceptual simplicity and computational attractiveness of current procedures with invariant force distribution now common in structural engineering practice. Firstly, the procedure was applied to linearly elastic buildings and it was shown that the procedure is equivalent to the well-known response spectrum analysis. Then, the procedure was extended to estimate the seismic demands of inelastic systems by describing the assumptions and approximations involved. Earthquake induced demands for a 9-story SAC building were determined by MPA, nonlinear dynamic analysis and pushover analysis using uniform, code and multi-modal load patterns. The comparison of results indicated that pushover analysis for all load patterns greatly underestimates the story drift demands and lead to large errors in plastic hinge rotations. MPA was more accurate than all pushover analyses in estimating floor displacements, story drifts, plastic hinge rotations and plastic hinge locations. MPA results were also shown to be weakly dependent on ground motion intensity, based on the results obtained from El Centro ground motion scaled by factors varying from 0.25 to 3.0. It was concluded that by including the contributions of a sufficient number of modes, usually three, the height wise distribution of responses estimated by MPA is generally similar to the 'exact' results from nonlinear time history analysis. Then Goel and Chopra (2005) extended the procedure for computing the member forces. Because, previous investigations showed that proposed version of method was not applicable to estimating the member forces. Because forces computed by this procedure may exceed the actual member capacity. Therefore, member forces were recomputed from member deformations that are determined from MPA. With the help of this modification, procedure was able to capture strain-hardening or softening effects in forces in members deformed beyond elastic limit. Accuracy of improvement was tested by using 9 and 20 storey six SAC buildings and by applying 20 ground motions. Results showed that extended procedure provided good estimates of member forces for five of six SAC buildings. The bias in forces was generally less than that in story drifts.

İnel, Tjhin and Aschheim (2003) conducted a study to evaluate the accuracy of five lateral load patterns, which were namely the first mode, inverted triangular, rectangular, "code", and adaptive lateral load patterns in current pushover analysis procedures such as capacity spectrum method (ATC-40, 1996) and displacement coefficient method (FEMA-356, 2000). These patterns were applied to 3 and 9 storey regular steel moment resisting frames that were designed as a part of the SAC joint venture (FEMA-2000) and their modified versions with a weak first story. In addition, modal pushover analysis (MPA) (Chopra and Goel, 2001) was studied. To compare the pushover results, also nonlinear time history analyses were performed using eleven ground motion records selected from Pacific Earthquake Research Center (PEER) strong motion database. Maximum response of story displacement, interstory drift, story shear and overturning moments obtained from pushover analyses at different values of peak roof drifts were compared with the nonlinear time history analyses. Approximate upper bounds of error for each lateral load pattern with respect to mean dynamic response were reported to show the accuracy of load patterns. According to results, current pushover analysis procedures were found to provide very good estimates of peak displacement response for both regular and weak-story buildings on selected ground motion set, when first mode, triangular and code load patterns were used for obtaining capacity curve.

Another simplified pushover analysis procedure, which takes into account higher mode effects for nonlinear seismic evaluation of planar building frames, referred as the upper bound method was proposed by Jan, Liu and Kao (2004). In this procedure, five designed buildings according to seismic code of Taiwan, which were 2, 5, 10, 20- and 30-story moment resisting frames of strong column-weak beam systems were analyzed. In addition, thirteen horizontal records from Chi-Chi earthquake in Taiwan were used, while obtaining the elastic displacement-response contribution ratios of higher modes with respect to fundamental mode. From the envelope curves of the contribution ratios demonstrated that first two modes dominated displacement response and other higher modes could be ignored. Then using the dynamic parameters of first two modes and response spectrum of earthquakes, structure and earthquake specific load patterns were obtained for each case. The accuracy of the procedure was evaluated by comparing the results obtained from pushover analysis with triangular loading, modal pushover analysis and nonlinear dynamic analysis. Results showed that seismic predictions of pushover analysis with triangular loading and modal pushover analysis were in good correlation with nonlinear dynamic analysis for frames not taller than 10 stories while only the proposed procedure could predict the seismic demands of 20- and 30-story buildings.

1.2.3 Characterization of Near Fault Ground Motions and Equivalent Pulses

In literature, several researchers such as Sommervile(1997, 1998), Alavi and Krawinkler (2001, 2004) and Rodrigez-Marek (2000) stated that, near-fault ground motions are different from ordinary ground motions in that they often contain strong coherent dynamic long period pulses and permanent ground displacements. For this reason, since mid 20th century, dynamic responses of structures under near-fault ground motion excitation have been examined extensively.

In 1960's, Biggs (1964) evaluated the response of elastic and inelastic SDOF systems to one sided force pulses of various shapes, i.e. triangular, rectangular and ramp like pulses. He observed that for each pulse shape, the maximum elastic response is a function of the pulse intensity and the td/T ratio, where td is the duration of the pulse and T is the natural period of the system. For undamped elastic systems subjected to one-sided force pulses, the displacement response factor, which is the maximum dynamic normalized displacement, does not exceed 2.0 for elasto-plastic systems. He further noted the dependence of the ductility demand on the td/T ratio and strength of the system relative to the intensity of the input pulse.

In the past, evaluating dynamic response was time consuming and computationally expensive. In addition, there were not enough ground motion records. For this reason, simple pulse shapes were used to represent earthquake ground motions. Veletsos et al (1965) presented elastic response spectra for half and full cycle sinusoidal pulses of ground velocity. His works showed that largest effect of damping is obtained in the medium period range. He also evaluated inelastic strength demand spectra for various target ductility ratios and an undamped elasto-plastic system subjected to a half cycle ground velocity pulse. Finally, the full cycle velocity pulse was used in their study to represent the Eureka ground motion, recorded in California earthquake on December 21, 1954.

The response of elastic SDOF systems to a half-cycle sinusoidal force pulse was discussed in Chopra (1995). Chopra showed that the effect of damping on maximum response to pulse type forces is not significant, if system is not highly damped. The reason is that the energy dissipation of damping is small if system is subjected to pulse type excitations with short duration. For the sinusoidal pulse, the displacement response factor is more sensitive to the damping ratio when pulse duration is shorter than natural period of the system.

Somerville (1997) conducted a study to develop an improved parameterization for the engineering specification of near fault ground motions. In addition to response spectrum, he tried to include time domain parameters of near-fault ground motion pulse to earthquake magnitude and distance. By using the analysis results of specially selected fifteen time histories recorded in the distance range 0.0 to 10 km from earthquakes in the magnitude range of 6.2 to 7.3 and twelve simulated time histories that span range of 3.0 to 10 km and magnitude distribution of 6.5 to 7.5, time domain parameters of model was obtained with the help of regression analysis. His formulations showed that period of near-fault fault normal forward directivity pulse is a function of moment magnitude. Moreover, approximate relationship of peak ground velocity near-fault fault normal forward directivity pulse is proportional with again moment magnitude and recorded distance.

In 2000, a similar study was conducted by Alavi and Krawinkler (2001). A set of fifteen near-fault ground motion records with forward directivity is used to evaluate elastic and inelastic demands of SDOF and MDOF systems. These records were recorded on stiff soil. In addition, these motions cover a moment magnitude range from 6.2 to 7.3 and rapture distance range from 0.0 to 8.9. In addition, a small set of simulated record set was used which was generated for a project sponsored by CDMG Strong Ground Motion Instrumentation program [Somerville, 1998]. They cover systematic ranges of moment magnitude 6.5, 7.0 and 7.5 and rapture distance 3, 5, 10 km for two stations, f6 and f8, in forward direction of a strike slip fault. As a result of these investigations, similar formulations were obtained to Somerville (1998). According to findings, ground motion time domain parameters were assigned to basic pull shapes: Half pulse P1, Full pulse P2 and multiple pulses P3 to compare the results of equivalent pulse and original record results, both record were applied to MDOF systems with a fundamental period of T=0.5 sec. and T=2.0 sec and with base shear coefficients of γ=0.4 and γ=0.15 which represent relatively strong and weak structures, respectively. The most important observation was that for most of the records, if the structure is weak, maximum storey ductility demand occurs at the base stories. On the other hand, for stronger structure, maximum storey ductility demand occurs at upper stories.

1.3 Objective and Scope

A procedure which is called dynamic pull analysis is proposed in this study for MDOF systems which employs simple inelastic dynamic analysis for calculating the seismic capacity and a generalized SDOF system for calculating the seismic demand. The procedure was applied on a six-story reinforced concrete frame and a twelve-story reinforced concrete frame that are designed according to the regulations of TS-500 (2000) and TEC (1997).

The results obtained from the proposed procedure are compared with the results of nonlinear static procedures and nonlinear time history results obtained under several near-fault ground motion records that have significant velocity and acceleration pulses. Mainly, the deformation demand, interstory drift profiles, base shear capacity, plastic hinge mechanisms and plastic rotations are compared. Estimated plastic rotations, displacement profiles and interstory drifts are used for deciding on procedure acceptability. The consistency of the decisions on the procedure acceptability according to the results obtained from the proposed procedure is controlled with the decisions according to the results obtained from nonlinear time history analysis. All nonlinear static analyses and time history analyses are conducted by using the software Drain-2DX (Allahabadi, 1987).

The main objective of the study was to develop an appropriate procedure for estimating the seismic response of multi degree of freedom (MDOF) systems.

This thesis is composed of five main chapters and two appendices. Brief contents are given as follows:

Chapter 1 Statement of the problem and literature survey on analysis procedures and assessment methods.

Chapter 2 Brief information about the methods used for comparing the results of the proposed procedure.

Chapter 3 Explanation of the proposed procedure in detail.

Chapter 4 Presentation of case studies. Results obtained from a six-story building frame and twelve-story building by using the proposed procedure. Comparison of results with those obtained by the other methods that are summariesed in chapter two

Chapter 5 A brief summary, discussion and conclusions.

Appendix A Bilinearization process of FEMA-273

Appendix B Inelastic modelling features and plastic hinge calculation procedure in Drain-2DX.

Appendix C Deriving an equation obtaining dynamic response of linear SDOF systems to dynamic pull record

.

CHAPTER 2

METHODS FOR ESTIMATING SEISMIC RESPONSE

2.1 Introduction

Target displacement, which is the inelastic displacement demand of a system, represents the probable maximum global displacement demand of structure when subjected to design earthquake. Accurate estimation of target displacement is important, because all comparisons of internal force and deformation demands with available capacities are carried out at the target displacement for a performance check.

Main purpose of this chapter is to introduce the methods that are used for estimating seismic response for comparison purposes throughout the thesis study. Firstly theoretical background of linear and nonlinear time history analysis are explained. Then advantages, limitations, weakness and accuracy of pushover analysis which are widely used for design and seismic performance evaluation purposes are discussed briefly. After that, two commonly known approximate procedures, Displacement Coefficient Method (FEMA-356, 2000) and Constant Ductility Spectrum Method (Chopra and Goel, 1999), which make use of pushover curve of the structure for estimating seismic demand are summariesed. Finally, steps of an improved version of pushover analysis, named Modal Pushover Analysis (MPA) (Chopra and Goel, 2001), are explained.

2.2 Time History Analysis

2.2.1 Linear Time History Analysis (LTHA)

The differential equations governing the linear response of a multistory building to horizontal earthquake ground motion $\ddot{u}_g(t)$ are as follows,

$$m \cdot \ddot{u} + c \cdot \dot{u} + k \cdot u = -m \cdot \iota \cdot \ddot{u}_g(t) \tag{2.1}$$

where

u is u is the vector of N lateral floor displacements relative to the ground

m is mass matrix

c is classical damping matrix

k is stiffness matrix

ı is peak influence matrix which is equal to unity; i.e., [1]

Distribution of these effective earthquake forces over the system is defined by a vector which can be expanded as a summation of modal inertia force distribution, s_n (Chopra, 2001: Section 13.12)

$$p_{eff}(t) = -m \cdot \iota \cdot \ddot{u}_g(t) = -s \cdot \ddot{u}_g(t) \tag{2.2}$$

$$s = m \cdot \iota \cdot = \sum_{n=1}^{N} s_n = \sum_{n=1}^{N} \Gamma_n \cdot m \cdot \phi_n \tag{2.3}$$

$$L_n = \phi_n^T \cdot m \cdot \iota \tag{2.4}$$

$$M_n = \phi_n^T \cdot m \cdot \phi_n \tag{2.5}$$

$$\Gamma_n = \frac{L_n}{\Gamma_n} \tag{2.6}$$

where

Φ_n is the n^{th} natural vibration mode of system.

By utilizing the orthogonality property of modes, it is demonstrated that none of the modes other than the nth mode contributes to the response. Then floor displacements are,

$$u_n(t) = \phi_n \cdot q_n(t) \tag{2.7}$$

where

q_n is the modal coordinate defined by

$$q_n(t) = \Gamma_n \cdot D_n(t) \tag{2.8}$$

Here, D_n is the deformation of the nth mode SDOF system

Then, inserting Eq.(2.7) and Eq.(2.8) into Eq.(2.1), equation of motion becomes,

$$\ddot{D}_n + 2 \cdot \zeta_n \cdot \omega_n \cdot \dot{D}_n + \omega_n^2 \cdot D_n = -\ddot{u}_g(t) \tag{2.9}$$

Comparing Eq.(2.1) and Eq.(2.9) gives the modal floor displacements

$$u_n = \Gamma_n \cdot \phi_n \cdot D_n(t) \tag{2.10}$$

Any response quantity r(t) story drifts, internal element forces, etc, can be expressed by

$$r_n = r_n^{st} \cdot A_n(t) \tag{2.11}$$

where

r_n^{st} is the static response, the static value of r due to external forces, and

$$A_n(t) = \omega_n^2 \cdot D_n(t) \tag{2.12}$$

A_n is the pseudo acceleration response of n^{th} mode SDOF system (Chopra, 2001; Section 12.1).

Therefore, the response of the system to the total excitation becomes,

$$u(t) = \sum_{n=1}^{N} u_n(t) = \sum_{n=1}^{N} \Gamma_n \cdot \phi_n \cdot D_n(t) \tag{2.13}$$

$$r(t) = \sum_{n=1}^{N} r_n(t) = \sum_{n=1}^{N} r_n^{st} \cdot A_n(t) \tag{2.14}$$

More detailed derivation of this linear time history analysis which is called classical modal response history analysis can be found in textbooks (Chopra, 2001: Sections 12.4 and 13.1.3)

2.2.2 Nonlinear Time History Analysis (NLTHA)

For each structural element of a building, the initial force-deformation curve is idealized as bilinear, and the unloading and reloading curves differ from the initial loading branch. Thus, the relations between lateral forces f_s at the N floor levels and the lateral displacements u are not single valued, but depend on the history of the displacements:

$$f_s = f_s(u, \mathrm{sign}(\dot{u})) \tag{2.15}$$

With this generalization for inelastic systems, Eq. (2.1) becomes

$$m \cdot \ddot{u} + c \cdot \dot{u} + f_s(u, \mathrm{sign}(\dot{u})) = -m \cdot \iota \cdot \ddot{u}_g(t) \tag{2.16}$$

The standard approach is to solve directly this equation of motion by appropriate integration method such as Newmark integration method (1959), Wilson-θ method (Wilson, Farhomad and Bathe; 1973), etc. NLTHA results for the case studies, which are shown in chapter four, are assumed to be “exact“ for this thesis study, in evaluating the results of other methods.

2.3. Simplified Nonlinear Analysis Procedures

2.3.1 Conventional Pushover Analysis

Pushover analysis is an iterative incremental solution of the static equilibrium equations in which the structure is subjected to monotonically increasing lateral forces with a height wise invariant distribution until a target displacement is reached.

Pushover analysis consists of a series of analyses, to obtain a force-displacement curve of the overall structure. A two or three-dimensional model which includes nonlinear load-deformation diagrams of all lateral force resisting elements is first created and gravity loads are applied initially. A predefined lateral load pattern that is distributed along the building height is then applied. Lateral loads are homogenously increased at each step. After a certain step, some of the members start to yield. Then structural model is modified according to nonlinear load deformation diagrams of members that results in a reduced global stiffness of the overall structure. Procedure is repeated until a control displacement at the top of building reaches a target level of deformation or structure becomes unstable. The roof displacement is plotted with base shear to obtain the global capacity curve; i.e., Pushover curves (Figure 2.1).

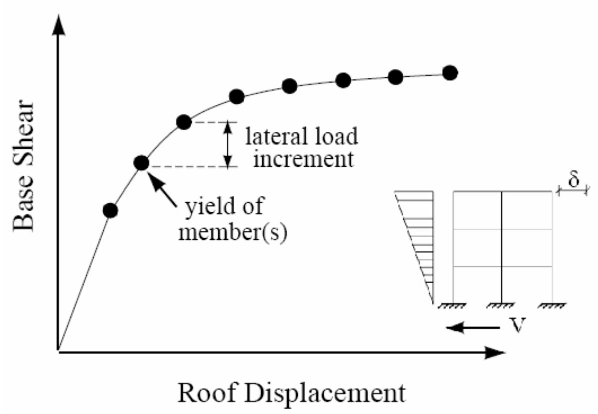

Figure 2.1 : Typical pushover curve of a structure

In literature, two types of pushover analysis exist which are force controlled and displacement controlled. Force controlled pushover procedure should be used when the load is known such as gravity loading. On the other hand, pushover analysis is performed as displacement-controlled proposed by Allahabadi (1987). The magnitude of load combination is increased until control displacement reaches a specified value. All internal forces and deformations are computed at the target displacement level.

Krawinkler and Seneviratna (1998) state that the pushover analysis is expected to provide information on many response characteristics that can not be obtained from an elastic static or dynamic analysis. These are:

- The realistic force demands on potentially brittle elements, such as axial force demands on columns, force demands on brace connections, moment demands on beam-to-column connections, shear force demands in deep reinforced concrete spandrel beams, shear force demands in unreinforced masonry walls etc.
- Estimates of the deformation demands for elements that have to deform inelastically in order to dissipate the energy imparted to the structure by ground motions.
- Consequences of the strength deterioration of individual elements on the behaviour of the structural system.
- Identification of strength discontinuities in plan or elevation that will lead to changes in the dynamic characteristics in the inelastic range.
- Verification of the completeness and adequacy of load path, considering all the elements of structural system, all the connections, the stiff nonstructural elements of significant strength, and the foundation system.

Pushover analysis also exposes design weaknesses that may remain hidden in an elastic analysis. These are story mechanisms, excessive deformation demands, strength irregularities and overloads on potentially brittle members.

Although pushover analysis has several advantages over elastic analysis procedures, procedure has some limitations that affect the accuracy of results such as estimate of target displacement, selection of lateral load patterns and identification of failure mechanisms due to higher modes of vibration

In the pushover analysis, target displacement can be estimated as the displacement demand for the corresponding equivalent SDOF domain through the use of a shape vector and equation (Lawson et al 1994). The roof displacement at mass center of the structure is used as target displacement. The theoretical background for the determination of basic properties of equivalent SDOF system is explained following sections in this chapter. Moreover, hysteretic characteristics of MDOF systems should be incorporated into the equivalent SDOF model if displacement demand is affected from stiffness degradation or pinching, strength deterioration and P-Δ effects. Foundation uplift, torsional effects and semi-rigid diaphragms are also expected to effect the target displacement [Krawinkler and Seneviratna, 1998].

Lateral loads represent the likely distribution of inertia forces imposed on structure during an earthquake. On the other hand, in pushover analysis, generally a constant lateral load pattern is used, assuming that the distribution of inertia forces is same during earthquake and the deformed configuration of structure under the action of constant lateral load pattern is expected to be similar to that experienced in design earthquake. On the other hand, Mwayf and Elnashai (2001) showed that the capacity curve is very sensitive to the choice of lateral load pattern. In other words, different constant load patterns reveal different capacity curves. For this reason, selection of lateral load pattern is more critical than the accurate estimation of target displacement (Figure 2.2).

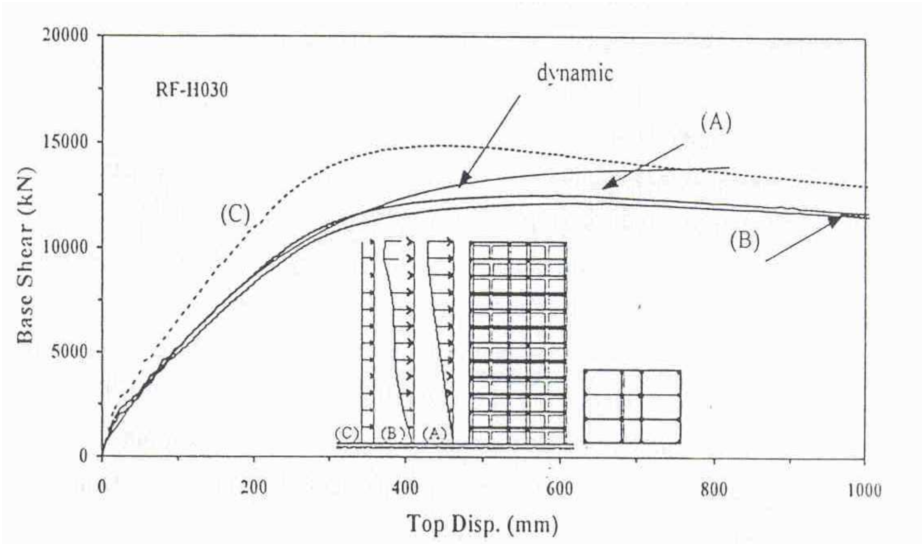

Figure 2.2 : Comparison of dynamic and static pushover curves that are obtained from different load patterns (Mwayf and Elnashai, 2001)

The lateral load patterns used in pushover analysis are proportional to product of story mass and displacement associated with a shape vector at the story under consideration. Commonly used lateral force patterns are uniform, elastic first mode, equivalent lateral "code" distributions and a single concentrated horizontal force at the top of structure. Multi-modal load pattern derived from Square Root of Sum of Squares (SRSS) story shears is also used to consider at least elastic higher mode effects approximately for long period structures. However, in this study FEMA-356 lateral load pattern is used. The lateral load pattern defined in FEMA-356 (2000) is given by the following formula that is used to calculate the internal force at any story,

$$F_i = \frac{m_i \cdot h_i^k}{\sum m_i \cdot h_i^k} \tag{2.17}$$

where

h is height of the i-th story above the base k is a factor to account for the higher mode effects (k=1 for $T1 \leq 0.5$ sec and k=2 for $T1 > 2.5$ sec., and varies linearly)

Pushover analysis is performed as force-controlled for gravity loading and displacement controlled for lateral loading for FEMA-356 lateral load pattern. A displacement-controlled pushover analysis is composed of the following steps:

1. Mathematical model that represents the overall structural behavior is created.
2. Nonlinear load deformation relationships for structural members are defined.
3. Gravity loads and percentage of live loads are initially applied to system.
4. A predefined lateral load pattern, which is distributed along the building height, is then applied.
5. Lateral loads are increased until some member(s) yield under the combined effects of gravity and lateral loads.
6. The structural model is modified to account for the reduced stiffness of yielded members.
7. Lateral loads are increased homogenously until the roof displacement reaches a certain level of deformation, or the structure becomes unstable.
8. Finally, the roof displacement versus base shear is obtained to get the global capacity (pushover) curve of the structure

2.3.2 Seismic Demand Calculation

2.3.2.1 Displacement Coefficient Method

The coefficient method of FEMA-356 (2000) is used for the calculation of target displacement, δt. According to the coefficient method;

$$\delta_t = C_0 \cdot C_1 \cdot C_2 \cdot C_3 \cdot Sa \cdot \frac{T_e^2}{4 \cdot \pi^2} \cdot g \tag{2.18}$$

In Equation 2.21, δ_t is the estimated maximum inelastic displacement of the control node. $Sa \cdot \frac{T_e^2}{4 \cdot \pi^2} \cdot g$ is the elastic spectral displacement corresponding to the period T_e for the considered ground motion. For the calculation of the effective period T_e, cracked concrete section stiffnesses are used in this study.

$$T_e = T_i \cdot \sqrt{\frac{K_i}{K_e}} \tag{2.19}$$

where,

T_e is the effective fundamental period (sec.)

T_i is the elastic fundamental period (sec.) in the direction under consideration

K_i is the elastic lateral stiffness of the structure in the direction under consideration

K_e is the effective lateral stiffness of the structure in the direction under consideration

C_0, C_1, C_2 and C_3 are the coefficients that modify the elastic spectral displacement. These coefficients are explained below.

C_0 : Modification factor to relate spectral displacement to the MDOF system control node displacement. Multiplication of first mode participation factor with the amplitude of the first mode vector at the control node level is used as C_0.

C_1 : Modification factor to relate expected maximum inelastic displacements to displacements calculated from linear elastic spectral response.

$$C_1 = (1.0 \quad for \quad T_e \geq T_s) \tag{2.20}$$

$$C_1 = \frac{1.0 + \dfrac{(R-1)\cdot T_s}{T_e}}{R} \quad \text{for} \quad T_e < T_s \tag{2.21}$$

$$R = \frac{Sa}{(\dfrac{Vy}{W})} \cdot Cm \tag{2.22}$$

where,

Sa is response spectrum acceleration, at the effective fundamental period and damping ratio of the system in the direction under consideration,

R is ratio of elastic strength demand to calculated yield strength ,

T_s is the characteristic period of the response spectrum, defined as the period associated with the transition from the constant acceleration segment to constant velocity segment of spectrum,

Vy is the yield strength calculated using results of the nonlinear static procedure for idealized nonlinear force- deformation curve for system

Cm is the effective modal mass calculated for fundamental mode using eigenvalues analysis.

W is the weight of structure.

C_2 : Modification factor to represent the effect of pinched hysteretic shape, stiffness degradation and strength degradation on maximum displacement response. In this study, target displacements for each ground motion record were calculated for immediate occupancy performance level; i.e, C_2 is taken as 1.0

C_3 : Modification factor to represent increased displacements due to P-Δ effects. C_3 is accepted as 1 in this study, since P-Δ effects are not considered.

$$C_3 = 1.0 + \frac{|\alpha| \cdot (R-1)^{1.5}}{T_e} \tag{2.23}$$

where

α is ratio of post yield stiffness to effective elastic stiffness, where the nonlinear force displacement relation shall be characterized by a bilinear relation (Figure 2.3).

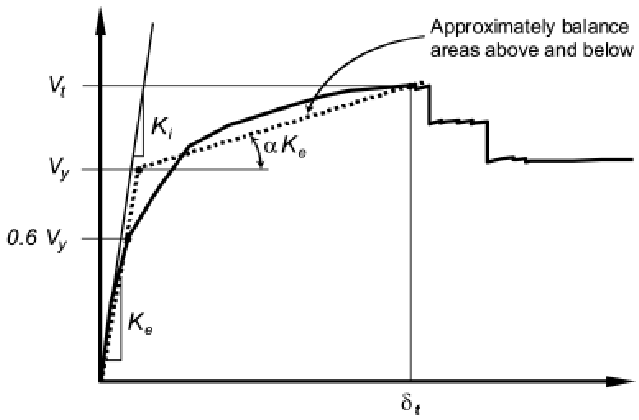

Figure 2.3: Idealization of pushover curve (FEMA-356)

2.3.2.2 Constant Ductility Spectrum Method

Constant ductility spectrum procedure is proposed by Chopra and Goel in 1999. Design spectrum is established by reducing the elastic design spectrum by appropriate ductility-dependent factors that depend on T_n. The earliest recommendation for the reduction factor, Ry, starts with the work of Velestos and Newmark (1965), which is the basis for the inelastic design spectra developed by Newmark and Hall (NH) (1982). Starting with the elastic design spectrum of Figure 2.4 and these Ry-μ−T relations for acceleration, velocity, and displacement-sensitive spectral regions, the inelastic design spectrum constructed by the procedure described in Chopra (1995, Section 7.10) is shown in Figure 2.4

In recent years, several recommendations for the reduction factor have been developed (Krawinkler and Nassar (KN), 1992); Vidic, Fajfar, and Fischinger (VFF), 1994). The inelastic design spectra based on two of these recommendations, are shown in Figure 2.5, Figure 2.6 and Figure 2.7. For a fixed $\mu = 4$, the inelastic spectra from NH is compared with in KN and VFF. The three spectra are very similar in the velocity-sensitive region of the spectrum, but differ in the acceleration-sensitive region.

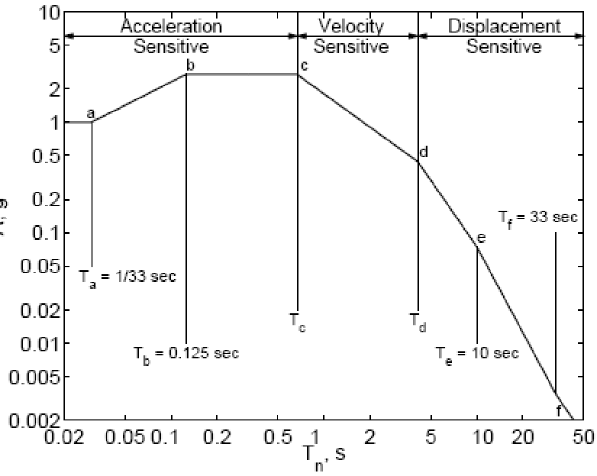

Figure 2.4: Newmark-Hall elastic design spectrum

SeismoSignal (2002) is used in this thesis work for developing elastic and inelastic response spectra of the selected earthquakes, instead of using the developed inelastic design spectrum reduction factor recommendations.

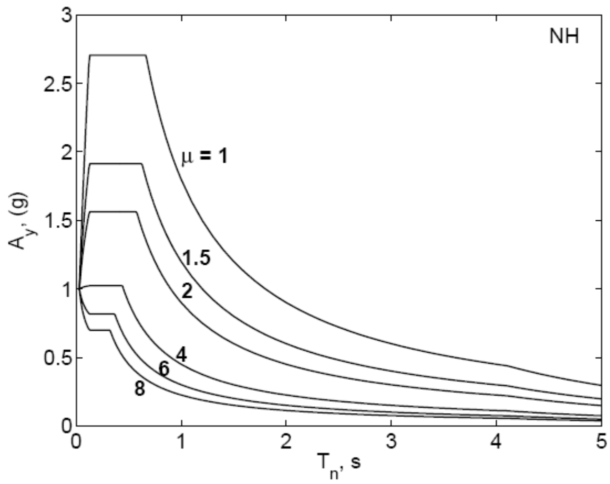

Figure 2.5: Inelastic design spectra: Newmark and Hall (1982) (NH)

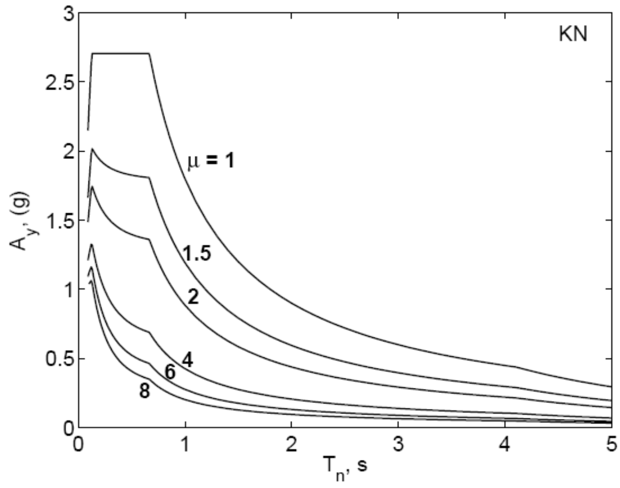

Figure 2.6: Inelastic design spectra: Krawinkler and Nassar (1992) (KN)

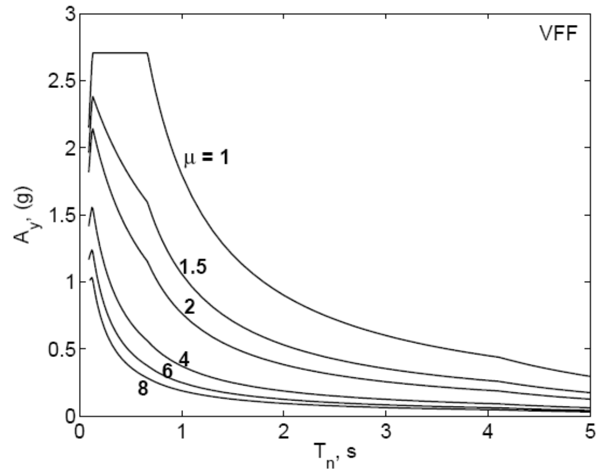

Figure 2.7: Inelastic design spectra: Vidic, Fajfar and Fischinger(1994) (VFF)

Proposed procedure consists of following steps:

1. Obtain pushover curve for MDOF system
2. Idealize the capacity curve as a bilinear curve using FEMA-273 procedure (Appendix A)
3. Convert the idealized curve to acceleration displacement response spectrum (ADRS) format, obtain the capacity diagram (Figure 2.8), by using following formulation.

$$Sa = \frac{(\frac{V}{W})}{\alpha_1} \tag{2.24}$$

$$Sd = \frac{u_r}{\Gamma_1 \cdot \phi_{r1}} \tag{2.25}$$

where

Sa is spectral acceleration (m/s^2)

Sd is spectral displacement (m)

Φ_{r1} is first mode shape function roof level amplitude value

Γ_1 is fundamental mode modal amplification factor.

W is weight of building

V is base shear (kN)

u_r is roof displacement (mt.)

α_1 is modal mass participation ratio for first mode

4. Obtain elastic and inelastic response spectra for 5% damping and various ductility levels in ADRS format. Then plot on the same graph bilinear capacity and demand curves.

5. Compute the ductility value at each intersection point on capacity and demand curves. When the calculated ductility is equal to ductility of inelastic demand curve, that intersection point is selected as inelastic displacement demand of equivalent SDOF system.

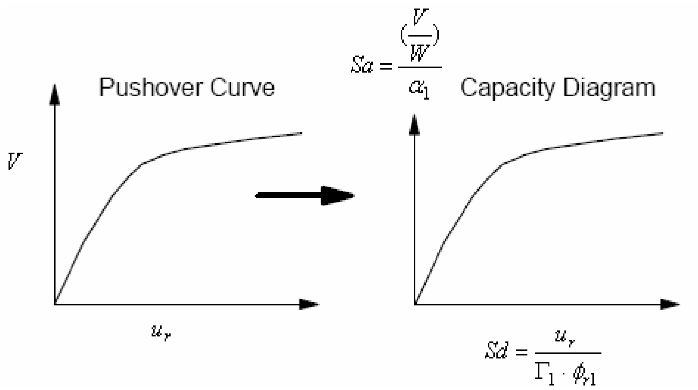

Figure 2.8: Obtaining capacity diagram

6. Convert the inelastic displacement demand of equivalent SDOF system to response of MDOF system by following equation:

$$u_r = Sd \cdot \Gamma_1 \cdot \phi_{r1} \quad (2.26)$$

7. Take the results of MDOF responses from pushover database

2.3.2.3 Modal Pushover Analysis (MPA)

This procedure which is called Modal Pushover Analysis (MPA) was proposed by Chopra and Goel in 2001. Their principle objective was to develop an improved analysis procedure based on structural dynamics theory that has conceptual and computational simplicity with constant load pattern. On the other hand, method has three main limitations. These are neglecting coupling among modal co-ordinates due to yielding of the system, superposition of modal responses, which is strictly valid only for elastic system, and estimating the total response by combining the peak modal responses using an appropriate modal combination rule, like SRSS and CQC rule.

The MPA procedure is summarized in a sequence of following steps:

1. Compute the natural frequencies, ω_n, and modes, Φ_n, for linearly elastic vibration of the building.
2. For the n^{th} mode, develop the base shear roof-displacement (V_{bn}–u_{rn}) pushover curve for the force distribution,

$$s_n^* = m \cdot \phi_n^i \tag{2.27}$$

where

m is the mass matrix.

Φ^i_n is the mode shape of i^{th} mode.

3. Apply force distribution s_n^* incrementally and record the base shears and associated roof displacements. System should push beyond the target roof displacement in the selected mode.
4. Idealize the capacity curve as a bilinear curve using FEMA-273 procedure (Appendix A).
5. Develop the F_{sn} / L_n-D_n relation by scaling the horizontal al axis by $\Gamma_n\Phi_n$ and by scaling the vertical axis by M_n^* which is equal to $L_n\,\Gamma_n$ (Figure 2.10).

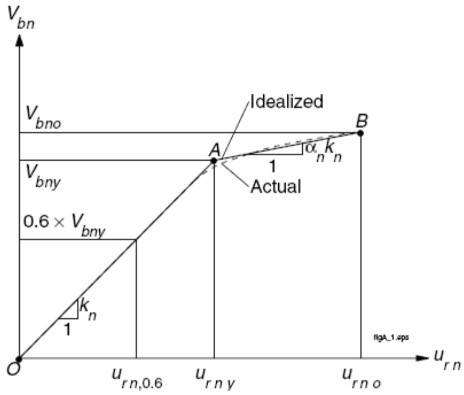

Figure 2.9: Idealization of pushover curve (Chopra and Goel, 2001)

6. Calculate the peak deformation of nth mode inelastic representative SDOF system (Figure 2.10) under selected ground motion excitation, D_n.

7. Convert SDOF system result to MDOF from

$$u_{rno} = \Gamma_n \cdot \phi^i_{rn} \cdot D_n \tag{2.28}$$

where

Γ_n is modal amplification factor for nth mode.

Φ_{rn} is shape factor at roof level.

D_n is peak response of representative SDOF system.

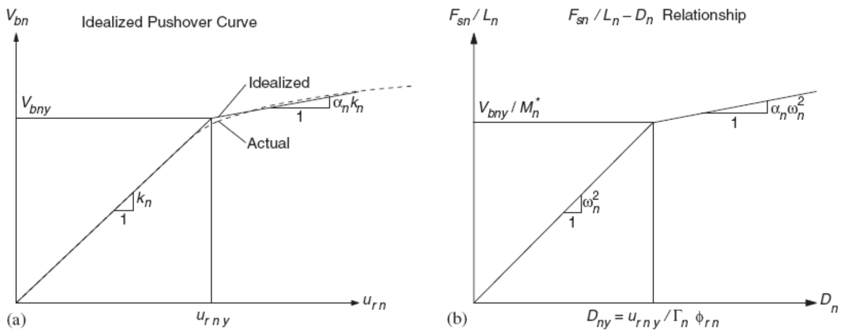

Figure 2.10: (a) Pushover curve and (b) SDF-system curve.

(Chopra and Goel, 2001)

8. Take the results of MDOF responses from pushover database (Figure 2.11).
9. Repeat the procedure from step 2 to 8 for other modes. Usually first three modes are enough for obtaining required accuracy.
10. Determine the total response by combining the peak modal responses by using usually SRSS (square root of sum of squares) or Complete Quadratic Combination (CQC) rule.

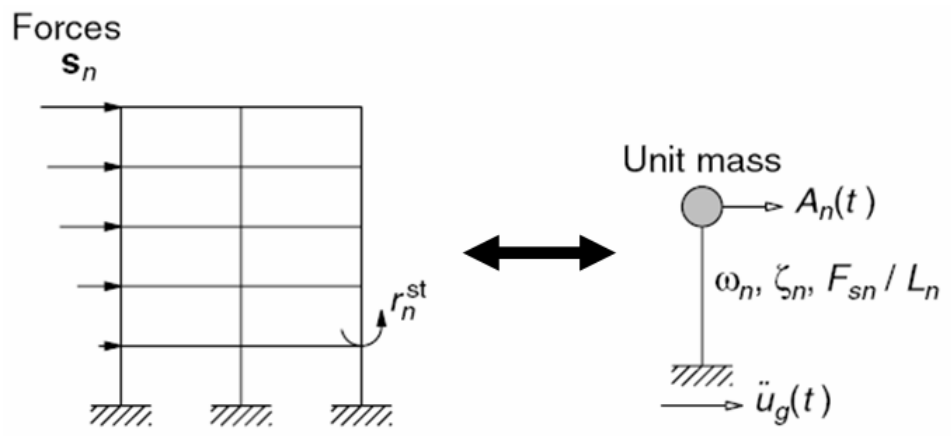

Figure 2.11: Conceptual explanation of MPA of inelastic MDOF systems

(Chopra and Goel, 2001)

This procedure is referred to as Procedure A by developers. In this study only the result of procedure A of MPA are used for case studies. For this reason, other two simple methods that are Procedure B and C are not explained in the text of thesis.

CHAPTER 3

DYNAMIC PULL ANALYSIS (DPA)

3.1 Introduction

The main objective of this chapter is to introduce a procedure, called "Dynamic Pull Analysis" (DPA) for multi degree of freedom (MDOF) systems. The proposed procedure employs a simple inelastic dynamic analysis procedure for calculating the seismic capacity and a generalized SDOF system for calculating the seismic demand under ground excitation. Principles and basic parameters of DPA are introduced on linear single degree of freedom (SDOF) systems, nonlinear SDOF systems and linear MDOF systems. Finally, DPA procedure is extended to nonlinear MDOF systems where the underlying assumptions and approximations are defined.

3.2 Linear Single Degree of Freedom Systems

An idealized linear single degree of freedom system consists of a mass, m, along the degree of freedom, a massless column which gives the stiffness of system, k, and a linear viscous damper with damping coefficient, c (Figure 3.1). In a general way of explaining the proposed method, solution of a system under

"Dynamic Pull Record" (DPR) for estimating seismic performance is called "Dynamic Pull Analysis" (DPA).

DPR has two variables. The first one is "A" which is the slope of the pull and the second is t_d which is the pull duration (Figure 3.1).

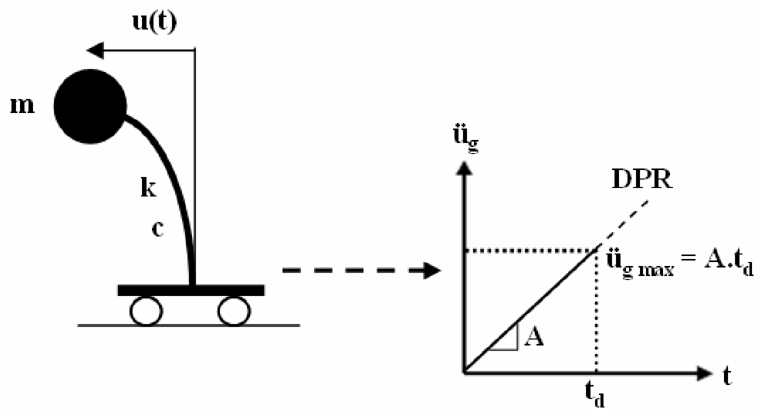

Figure 3.1 : DPA under DPR

Response of a SDOF system under dynamic pull record can be obtained analytically by solving the equation of motion.

$$m \cdot \ddot{u} + c \cdot \dot{u} + k \cdot u = -m \cdot \iota \cdot \ddot{u}_g(t) \tag{3.1}$$

subjected to the initial conditions;

$$u(0) = 0 \qquad \dot{u}(0) = 0 \tag{3.2}$$

According to Figure 3.1, we can insert $(A \cdot t)$ instead of $\ddot{u}_g(t)$, where $t \leq t_d$.

Detailed solution of equation of motion can be found in Appendix C. However, results of steady state, $u_s(t)$, and transient, $u_t(t)$, parts are presented separately below. Total displacement is equal to the sum of $u_t(t)$ and $u_s(t)$.

$$u_t(t) = \frac{A}{\omega_n^2} \cdot e^{(-\zeta \cdot \omega_n \cdot t)} \cdot \left(\cdot (\frac{(1 - 2 \cdot \zeta^2)}{\omega_D}) \cdot \sin(\omega_D \cdot t) - \frac{2 \cdot \zeta}{\omega_n} \cdot \cos(\omega_D \cdot t) \right) \quad ; \quad t \le t_d \tag{3.3}$$

$$u_s(t) = \left(-\frac{A \cdot t}{\omega_n^2} \right) + \left(\frac{2 \cdot \zeta \cdot A}{\omega_n^3} \right) \quad ; \quad t < t_d \tag{3.4}$$

$$u(t) = u_t(t) + u_s(t) \quad ; \quad t < t_d \tag{3.5}$$

When the effect of steady state and transient response of SDOF system is compared, the ratio between $u_t(t)$ to $u_s(t)$ decreases with increasing damping and increasing cycles. Accordingly, with increasing cycle number, steady state part of the response dominates the response of SDOF system (Figure 3.2).

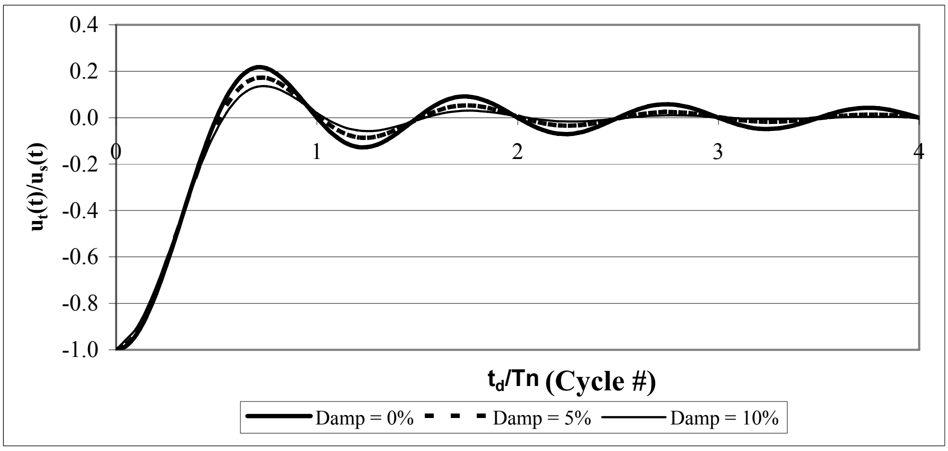

Figure 3.2 : $u_t(t)/u_s(t)$ vs.t_d/T(cycle #) for ζ = 0%, 5%, 10%

Figure 3.3 shows the graphical representation of Equations (3.3), (3.4) and (3.5). This figure demonstrates that the amplitude of transient cyclic displacement decreases with increasing damping values. The total displacement, u(t), has always a monotonically increasing trend in the negative direction. In addition, Figure 3.3 demonstrates that the peak displacement value of the linear SDOF system increases in excitation time of DPR, t_d.

The time where the response of a linear SDOF under DPR is equal to absolute maximum displacement response of the same system under an earthquake excitation is called the target time of DPA, t_d. During the analysis, t_d should be sufficiently long such that the linear SDOF system reaches the seismic displacement demand under an earthquake excitation.

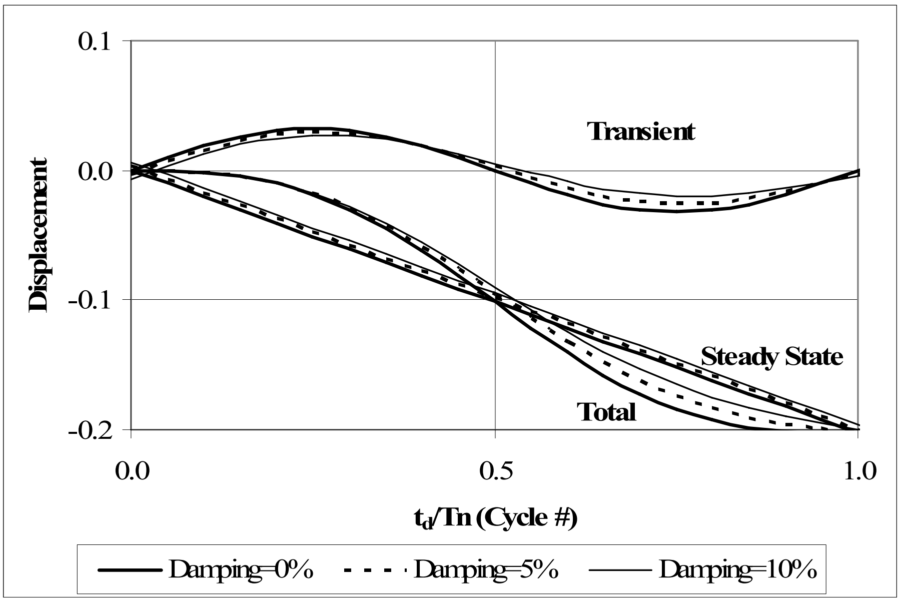

Figure 3.3 : u(t) vs. t_d/T_n (cycle #) graph for ζ = 0%, 5%, 10%; A= 1

3.2.1 Linear Elastic Dynamic Pull Spectrum

Response spectrum provides a convenient means to summarize the peak response of all possible linear SDOF systems to a particular component of ground motion. It also provides a practical approach to apply the knowledge of structural dynamics to the design of structures and development of lateral force requirements in building codes. By the help of the derived equation for response of linear SDOF system, response spectra of DPR for different damping ratios can be calculated easily from following equation when t is equal to t_d. Derivation of acceleration response spectrum of DPR can be found in Appendix C.

$$Sa(\omega_n) = \left| A \cdot t \cdot (1 - (e^{(-\varsigma \cdot \omega_n \cdot t)} \cdot \frac{\sin \omega_D \cdot t}{\omega_D \cdot t}) \right| \quad \text{where} \quad t = t_d \qquad (3.6)$$

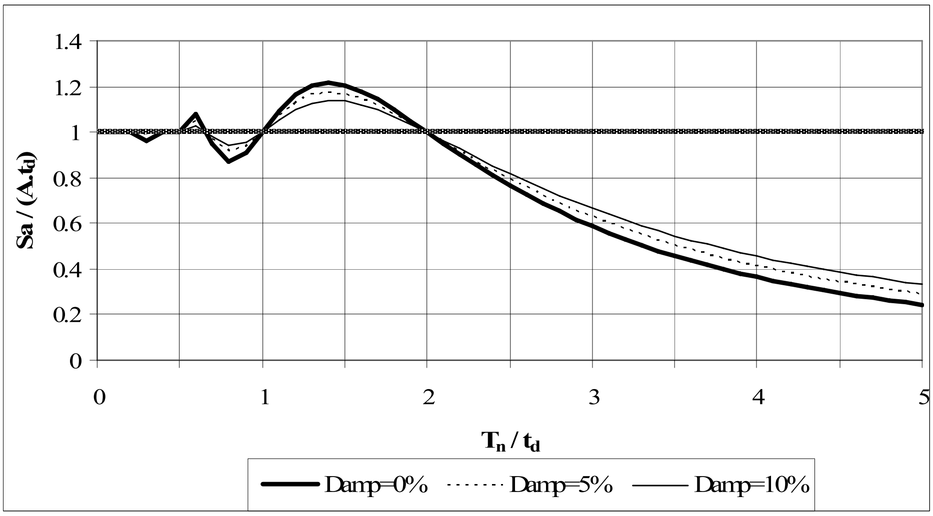

Figure 3.4 : Normalized response spectra of DPR for ζ = 0%, 5%, 10%

Figure 3.4 shows the graphical representation of acceleration response spectra for different damping ratios. According to this figure, the following observations can be made.

- When period is lower than $0.5t_d$, $(T_n/t_d < 0.5)$, acceleration response spectrum almost follows the $(Sa/A \cdot t_d = 1)$ flat spectrum line. This is also equal to equivalent static displacement.
- When the period is equal to 1 or 2, response acceleration is equal to 1, $(Sa/A \cdot t_d = 1)$.

- When the period is longer than $2t_d$, $T_n/t_d > 2.0$, response acceleration is lower than 1, ($Sa/A \cdot t_d < 1$). This means that the duration of pulse is too short to drive the linear SDOF system into larger accelerations or the equivalent static displacement, $(Sd)_{static} = (m \cdot A \cdot t_d)/k$.
- The maximum response acceleration, which is about 1.2, (for 5% damping ratio) is obtained, when $T_n/t_d \cong 1.5$

3.2.2 Linear Elastic Seismic Demand

The slope of the force-deformation relation of a linear SDOF system is its stiffness. The force-deformation relationship of a linear elastic SDOF system follows this line under any excitation. Figure 3.5 shows the dynamic response of the same linear SDOF system under Erzincan earthquake EW component excitation and DPR. Resultant plot indicates that both procedures result in the same linear stiffness.

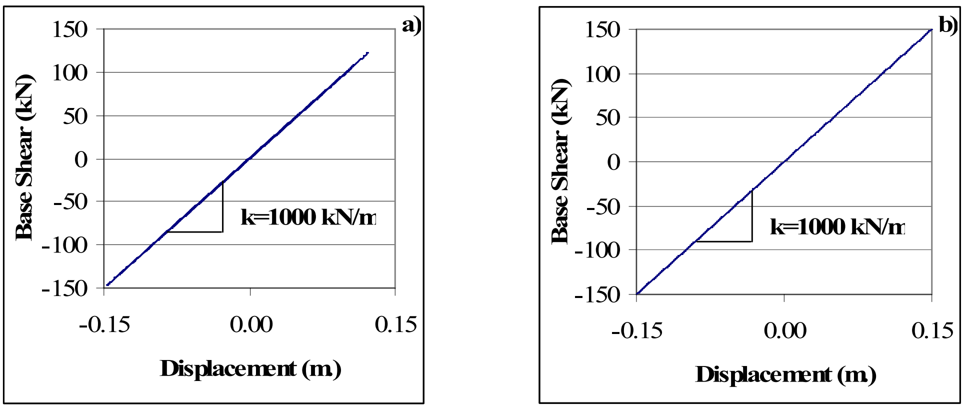

Figure 3.5 : Linear stiffness obtained from a) Erzincan earthquake EW component b) DPR.

In converting the linear elastic response to Acceleration Response Spectrum (ADRS) format, dividing the force component to weight of the system, W, is sufficient to calculate the spectral acceleration, Sa. On the other hand, displacement component is equal to the spectral displacement, Sd (Figure 3.6). Therefore, the following relations can be used for obtaining the linear elastic response in the ADRS format.

$$Sa = \frac{V}{W} \quad ; \quad Sd = u_o \tag{3.7}$$

where

Sa is spectral acceleration (m/s^2)

Sd is spectral displacement (m)

W is the weight of system

f_o is base shear (kN)

u_o is relative displacement (mt.)

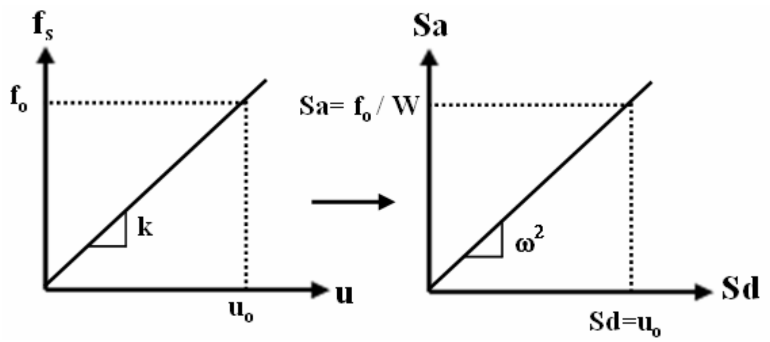

Figure 3.6 : Converting the linear elastic response into ADRS format where $t = t_d$

The demand of an earthquake ground motion can be represented by acceleration response spectrum. Acceleration response spectrum has traditionally been plotted with Sa, spectral acceleration, vs T, period. In order to illustrate the relation between accelerations and displacements more visually, the Sa vs T coordinate system for response spectrum is converted to a set of coordinates defined by Sa and Sd, spectral displacement. When the spectral values are plotted in ADRS format, the period can be represented by lines radiating from origin (Mahaney et al., 1993). An example of demand spectrum is shown in Figure 3.7.

Demand curve of a strong ground motion can be obtained by converting 5% elastic response spectrum to ADRS format by using the following equations.

$$Sd = \frac{Sa \cdot T^2}{4 \cdot \pi^2} \tag{3.8}$$

where

T is the period of the SDOF system (sec.)

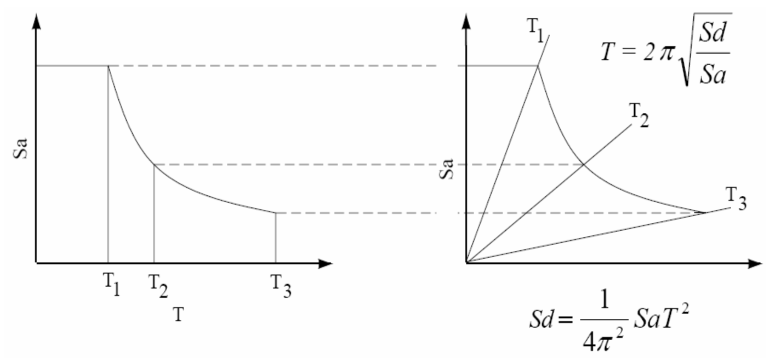

Figure 3.7 : Converting response spectrum into ADRS format (Mahaney et al., 1993)

Intersection of the linear elastic response curve with the demand spectrum represents the seismic demand of the system, which can be defined as target displacement. After finding target displacement, pull duration, t_d, can be found easily by searching the analysis database for obtaining the time step when the desired displacement value is reached (Figure 3.8). Another way is to solve Equation (3.5) for obtaining t_d.

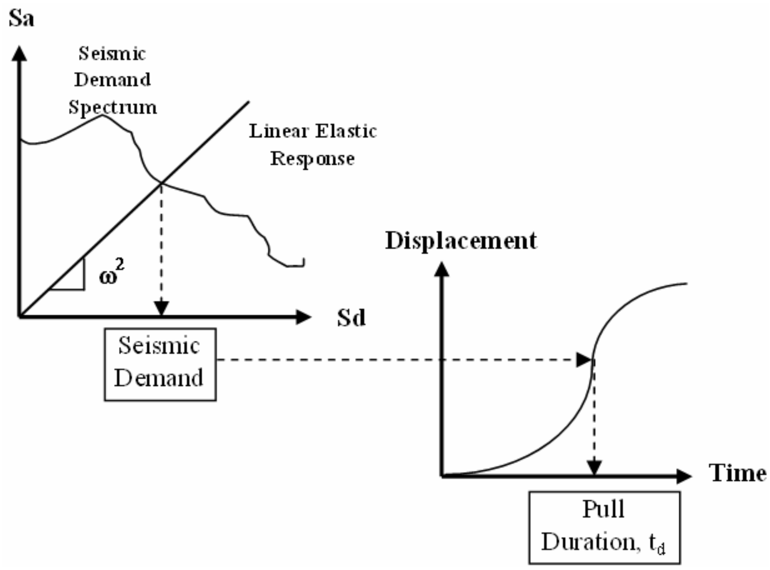

Figure 3.8 : Graphical explanation of calculating pull duration, t_d

3.2.3 Numerical Examples

The parameters of linear SDOF systems that are used in numerical study are presented in Table 3.1. In this table, results of the explained procedure, DPA, and results of linear time history analysis (LTHA) are listed. For all cases of DPA, A, which is the slope of DPR, is selected as 1 m/s^3 and Erzincan earthquake EW component is used for calculating the response of linear SDOF systems. Figure 3.9 shows the DPA spectra, which are plotted according to A, and t_d results of cases and Erzincan earthquake EW component acceleration response spectrum on the same graph. Following items can be observed from the presented information.

Table 3.1 : Parameters of linear SDOF systems and results obtained from DPA and linear time history analysis (A is 1 m/s^3)

Case #	K (kN/mt)	M (ton)	T_n (sec.)	ζ (%)	u_m (mt.) DPA	u_m (mt.) LTHA	t_d (sec)
1	1579.14	10.00	0.5	5	**0.054**	**0.054**	8.48
2	701.839	10.00	0.75	5	**0.124**	**0.124**	8.68
3	394.784	10.00	1	5	**0.146**	**0.147**	5.78
4	175.46	10.00	1.5	5	**0.192**	**0.192**	3.54
5	98.696	10.00	2	5	**0.373**	**0.374**	3.53

- Both method give exactly same peak absolute acceleration displacement.
- Decrease in the stiffness, k, decreases pull duration, t_d,
- Each spectrum of DPA intersects the acceleration response spectrum of earthquake at the period of the associated linear SDOF systems (Figure 3.9).

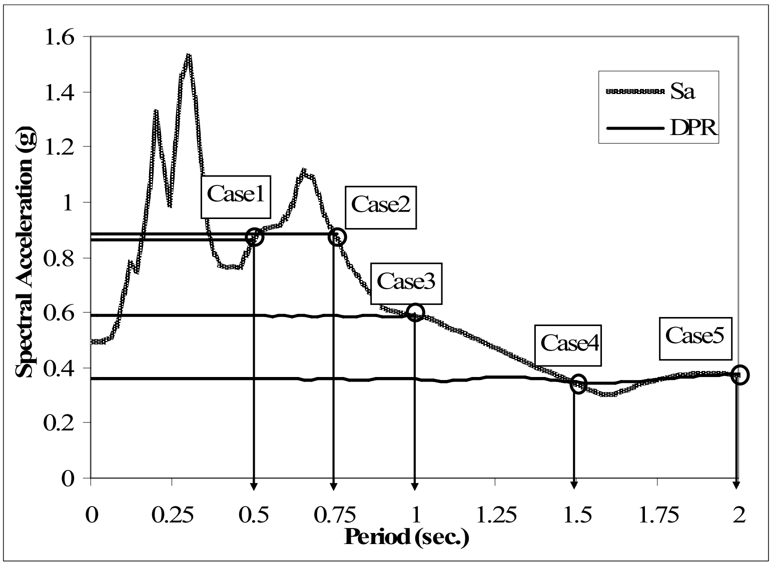

Figure 3.9 : Comparison of earthquake and DPR spectra

3.3 Nonlinear Single Degree of Freedom Systems

The response of structures deforming into their inelastic range during intense ground shaking is important in earthquake engineering. Since 1960s hundreds of laboratory tests have been conducted to determine the force-displacement behaviour of structures for earthquake conditions. Results of these experiments show that the cyclic force-deformation behaviour of a structure depends on the structural material and structural system (Chopra, 1995). In addition to laboratory tests, many computer simulation studies have focused on the earthquake response of SDOF systems with their force-deformation behaviour defined by idealized versions of experimental curves. In this study, the simplest of such idealized force-deformation behaviour, which is called the elastoplastic force-deformation relation is chosen.

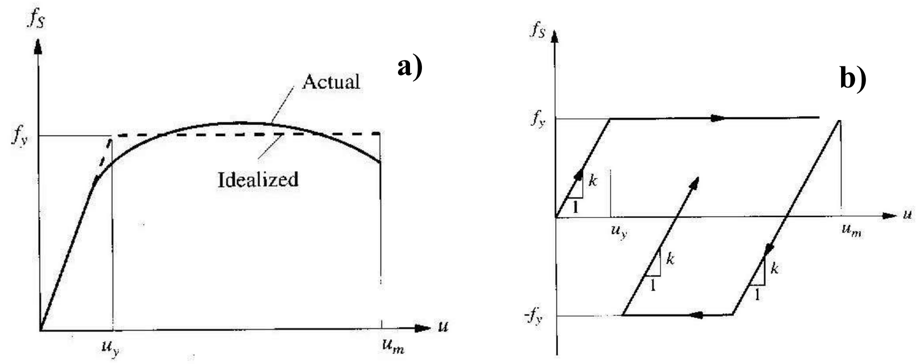

Figure 3.10 : a) Force-deformation curve during initial loading b) Elastoplastic force-deformation relation (Chopra, 1995)

Elastoplastic approximation to the actual force-deformation curve is shown in Figure 3.10.a. While idealizing the actual curve, area under two curves must be equal at the selected value of the maximum displacement, u_m. On initial loading, this idealized system is linearly elastic with stiffness, k, as long as the force does not go beyond f_y, the yield strength. When force reaches f_y, yielding begins. Therefore, u_y becomes yield deformation. Figure 3.10.b shows a typical cycle of loading, unloading and reloading for an elastoplastic system. This type of system can be defined by using the vibration parameters of elastic SDOF system. Therefore, natural period of corresponding linear system is the same as the period of elastoplastic one undergoing small oscillations (i.e., $u<u_y$). On the other hand, at larger oscillations, the natural vibration period is not defined for elastoplastic systems (Figure 3.11).

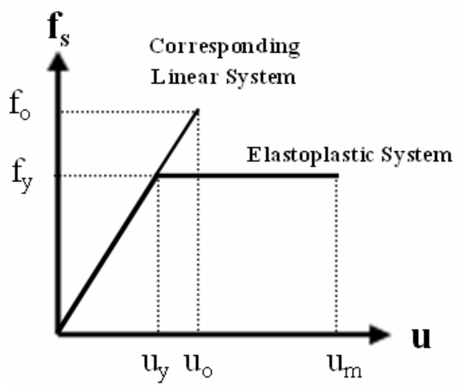

Figure 3.11 : Elastoplastic system and its corresponding linear system

Figure 3.12 is obtained by plotting force-deformation relation of earthquake excitation and DPR on the same graph. It is observed that the capacity curve of DPA for nonlinear SDOF system envelopes the obtained under earthquake response. Capacity curve of DPA also represents ideal force-deformation curve during initial loading (Figure 3.10.a).

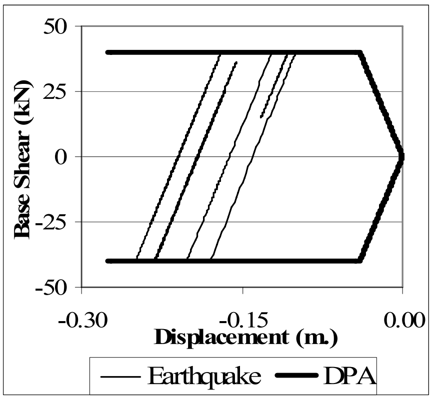

Figure 3.12 : Capacity curves obtained from Erzincan earthquake EW component and DPA.

3.3.1 Response Reduction Due to Nonlinearity

The component of the strength reduction factor due to nonlinear hysteretic behavior, R, is defined as the ratio of the elastic strength demand, f_o, to the inelastic strength demand, f_y (Figure 3.11).

$$R = \frac{f_o}{f_y} = \frac{u_o}{u_y} \tag{3.9}$$

In addition, relation between u_m and u_o can be written as,

$$\mu = \frac{u_m}{u_y} = R \cdot \frac{u_m}{u_o} \tag{3.10}$$

where,

μ is the ductility factor.

In general, for SDOF systems allowed to respond nonlinearly during ground motions, inelastic deformations increase as the lateral yielding strength of the system, f_y, decreases. For a given ground motion and a strength reduction factor, the problem is to compute the ductility level

For a given ground acceleration time history, a R-μ-T spectrum can be constructed by plotting the strength reduction factors of a family of SDOF systems (with different periods of vibrations) undergoing different levels of inelastic deformation, i.e., ductility factors when subjected to the same ground motion.

While obtaining the R-μ-T relation for earthquakes, the following methodology can be used.

1. Define the ground motion, $\ddot{u}_g(t)$.
2. Select and fix damping ratio, ζ.
3. Select and fix mass, m.
4. Select a value of ductility factor, μ.
5. Determine the natural period, T_n.
6. Determine the elastic response of corresponding linear SDOF system, u_o.
7. Calculate the peak seismic force of corresponding linear system, $f_o = k \cdot u_o$.
8. Select a strength reduction factor, R, then calculate yield strength, $f_y = R \cdot f_o$.
9. Solve the equation of motion and calculate peak deformation, u_m. According to this deformation response, calculate new ductility factor, μ_{new}.
10. If μ_{new} is not equal to μ, change R and repeat steps 8 to 10.

    Otherwise, go to step11.

11. Repeat steps 5 to 11 for a range of T_n resulting in the spectrum valid for the μ value chosen in step 4.

12. Repeat steps 4 to 12 for several values of μ.

A typical R-μ-T spectra is shown in Figure 3.13 below.

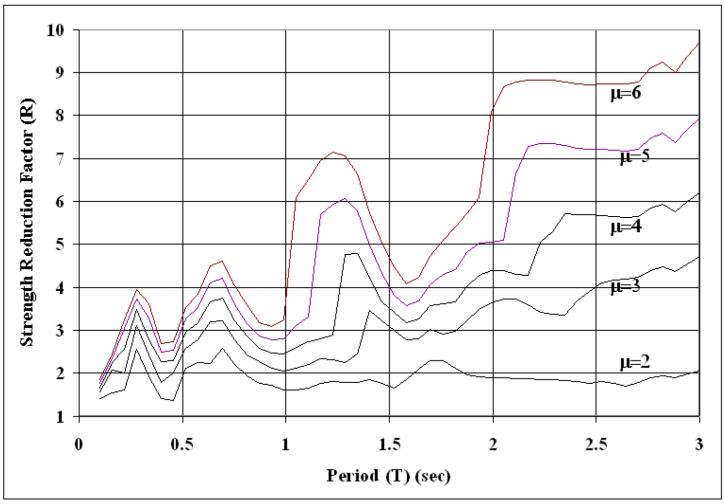

Figure 3.14 : R-μ-T spectra for Erzincan Earthquake, EW component

3.3.3 Calculating Seismic Demand of a Nonlinear SDOF System

The maximum inelastic displacement of an elastoplastic system under a specific strong ground motion record can be calculated by using the R-μ-T spectra of the earthquake ground motion. In other words, for a known period, T_n, and strength reduction factor, R, ductility factor, μ, can be calculated. Then by multiplying calculated ductility factor, μ, with yield displacement, u_y, maximum inelastic response, u_m, can be obtained.

$$u_m = \mu \cdot u_y \tag{3.11}$$

3.3.4 Numerical Examples

Figure 3.15 shows a comparison between inelastic spectrum of Erzincan earthquake EW component and nonlinear spectra of DPR for T_n=2 sec, A=1 m/s^3 and t_d=1.63 sec. It is observed from this figure that first contact of capacity curve with nonlinear pull spectra is obtained when μ of pull spectrum is equal to 5.40 Multiplying the obtained with u_y=0.063 m leads to u_m=0.339m. This is exactly equal to the inelastic displacement demand obtained from response history analysis under Erzincan EW ground excitation.

This simple example demonstrates that R-μ-T relation of earthquakes can be safely used for estimating the peak response of nonlinear SDOF systems accurately.

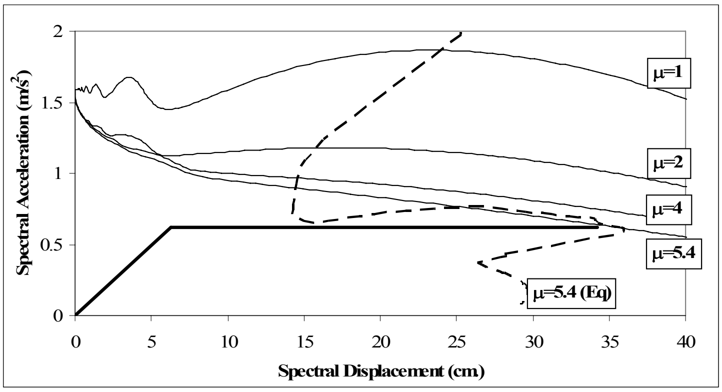

Figure 3.15 : Intersection of capacity spectrum with nonlinear DPA spectra

3.4 Linear Multi Degree of Freedom Systems

Linear response curve, which is used as a term for defining force-deformation relations of linear MDOF systems in DPA, can be obtained by extracting relevant response quantities from analysis database of simple linear time history analysis under pull excitation. This obtained curve represents the overall stiffness of the system since effects of all dynamic modes are included simultaneously during the dynamic pull analysis (Section 2.2.1). Therefore, linear response curve of MDOF system becomes a resultant curve of dynamic analysis at each time increment. However, since modal contributions under pull and earthquake excitations are not equal, different displacement shapes are obtained at equal control node displacements. This issue is discussed in the following sections.

3.4.1 Numerical Examples

Compared in this section of thesis are the earthquake-induced responses for the twelve storey-building frames determined by two linear analyses: Response Spectrum Analysis (RSA) and Dynamic Pull Analysis (DPA). Drain-2DX (Allahabadi, 1987) is used for analyzing elastic case study frame. Detailed definition of twelve-storey frame can be found in Chapter 4, and dynamic properties of frame are listed in Table 4.4.

DPA and linear time history analysis (LTHA) may be compared at equal maximum roof displacement. For simulating this situation, DPA demand target displacement is obtained from spectral modal analysis, same as the maximum displacement demand obtained from Erzincan earthquake EW component. This situation allows us to compare the modal contributions of each method. Figure 3.16 presents the response histories of roof displacement.

As suggested by Equation (2.10), the modal floor displacements are proportional to the mode shapes since the system remains elastic. Figure 3.17 and Figure 3.18 illustrate the variation of floor displacement and storey drift ratios from LTHA and DPA for first three modal responses and all modes responses separately. According to these figures, it is observed that DPA overestimates the first mode response. In addition, storey displacement profiles of second and third mode are different from exact response. Therefore, we can conclude that in DPA errors arise from not capturing the modal contributions accurately.

In conclusion, the accuracy of predictions of DPA depends on ground motion characteristics and structural properties as well as the inherent limitations of procedure like using generalized SDOF system approximation for MDOF systems. Larger difference in storey displacement profile and storey drift ratio profile show that the DPA would be less reliable in estimating the seismic demand of elastic MDOF systems. For this reason, it is suggested for linear elastic MDOF systems to use RSA for estimating absolute peak displacement response.

3.5 Nonlinear Multi Degree of Freedom Systems

Dynamic Pull Analysis (DPA) consists of nonlinear time history analysis (NLTHA) to obtain the force-deformation relation of the MDOF system. Two or three-dimensional mathematical model which includes nonlinear load deformation diagrams of all force resisting elements is first created and gravity loads are applied initially. A predefined artificial acceleration time history record, DPR, is then applied to the model as ground acceleration. A major property of DPR is that at each time step acceleration component of record increases homogenously. After a certain time step, some of the members start to yield. Then structural model is modified according to nonlinear load deformation diagrams of members that results in a reduced global stiffness of the structure. Procedure continues until a control displacement at the top of the building reaches a target level or structure becomes unstable. The roof displacement is plotted with base shear to obtain the global capacity curve of the structure. Therefore, seismic demand can be estimated with the methodology introduced for nonlinear SDOF systems in Section 3.3 by using the idealized or bilinear capacity curve of the equivalent SDOF system.

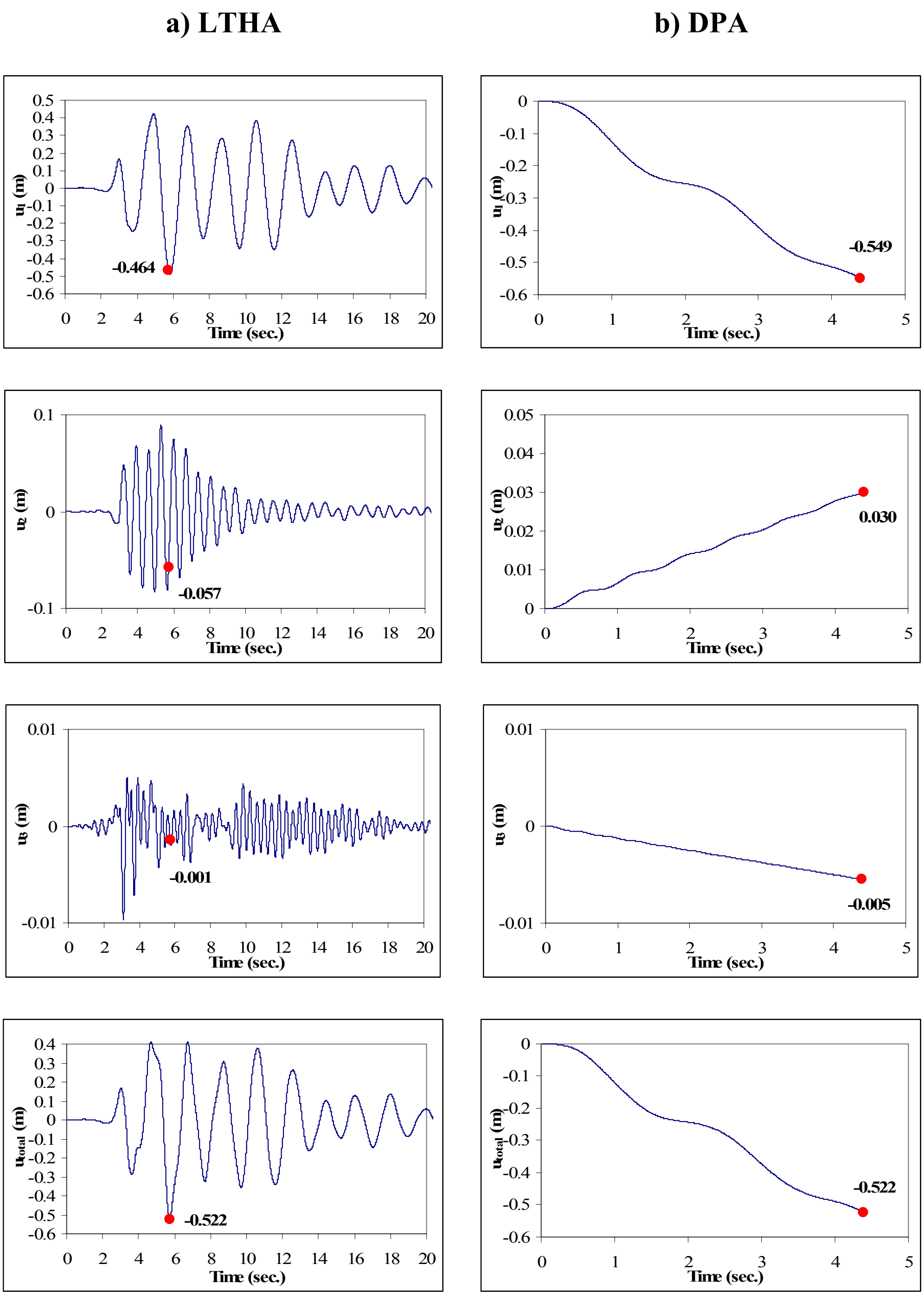

Figure 3.16 : Response histories of roof displacements from LTHA (Erzincan EQ EW component) and DPA: First three modal responses and total (all modes) responses.

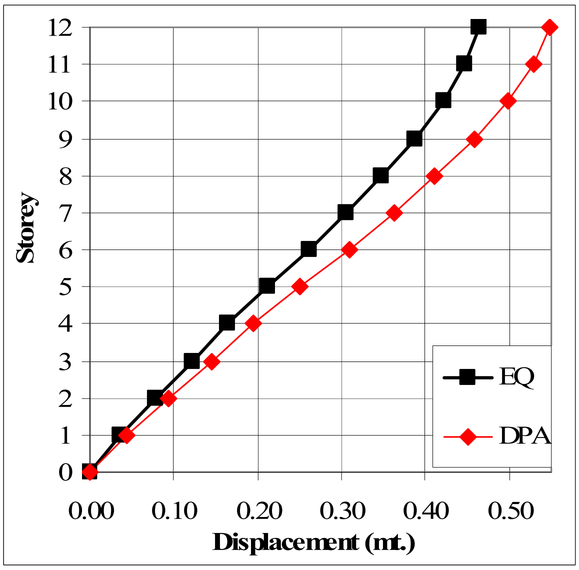

a) Mode 1

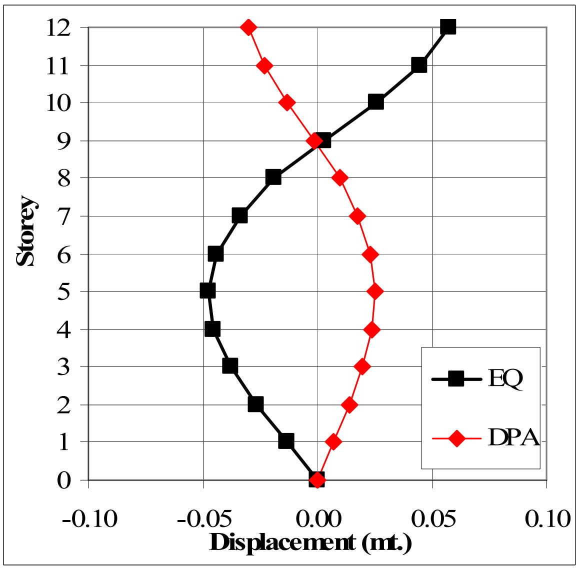

b) Mode2

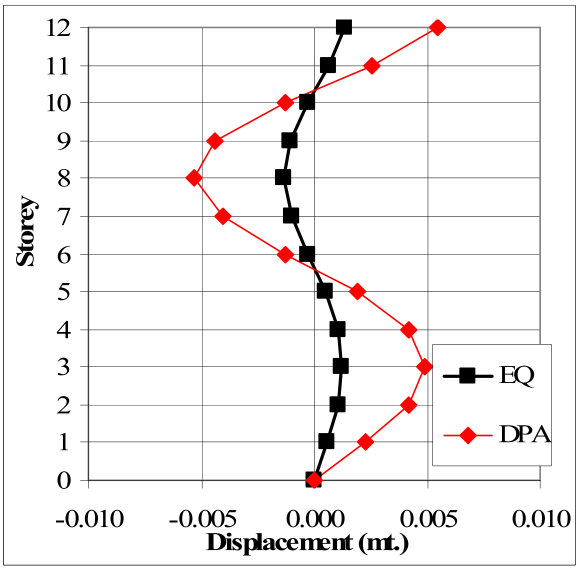

c) Mode 3

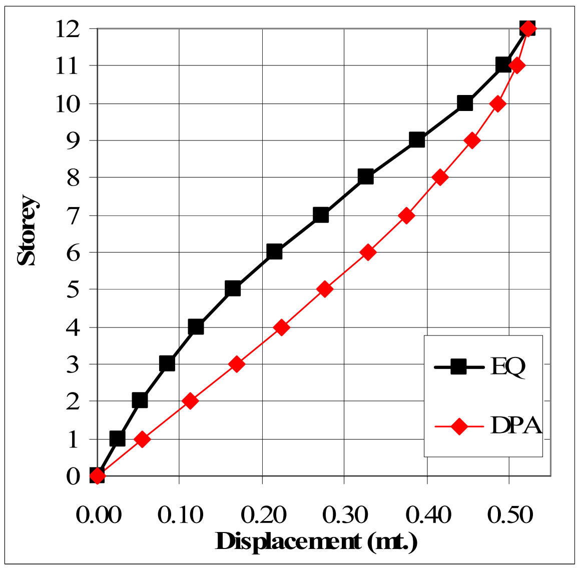

d) All Modes

Figure 3.17 : Variation of floor displacements from LTHA (Erzincan earthquake EW component) and DPA

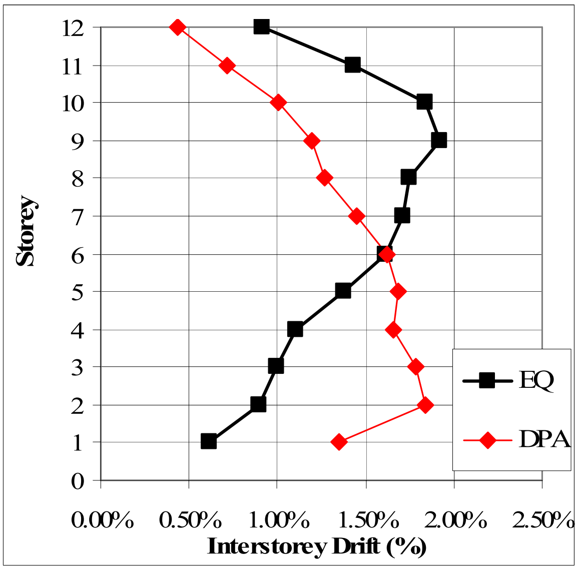

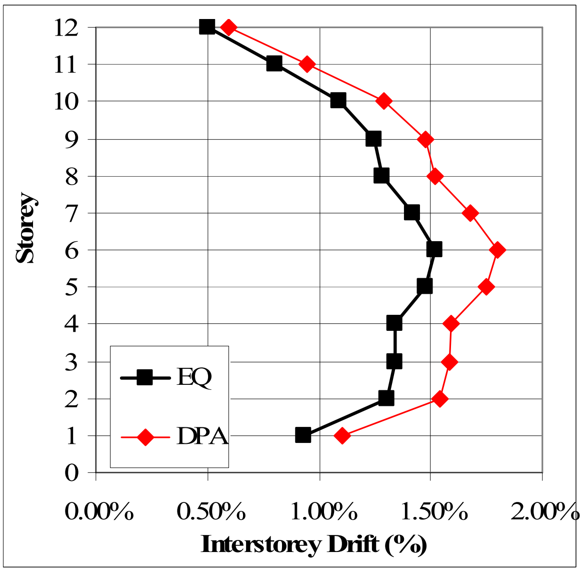

a) Mode 1

b) Mode2

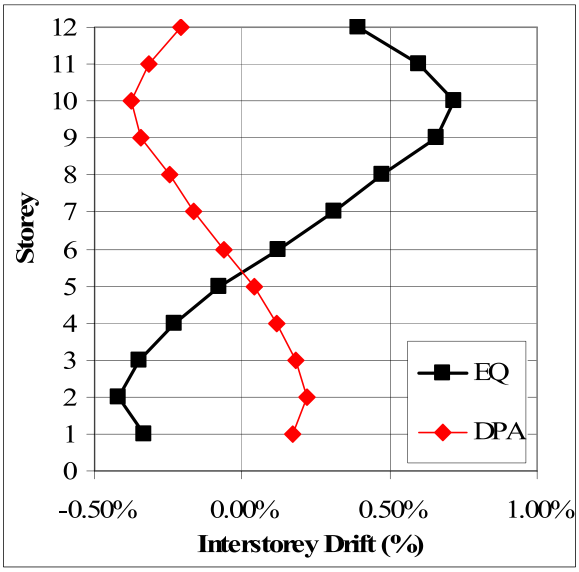

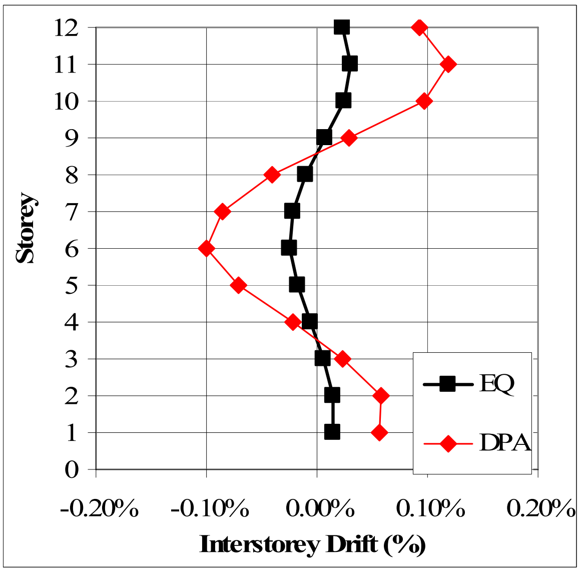

c) Mode 3

d) All Modes

Figure 3.18 : Variation of storey drift ratios from LTHA (Erzincan earthquake EW component) and DPA

Bilinearization procedure that is explained in FEMA-356 (2000) is used for obtaining the generalized SDOF system representations of MDOF systems. According to this procedure, the nonlinear force displacement relationship between base shear and displacement of the control node shall be replaced with an idealized bilinear relationship to calculate stiffness, k_g, and yield strength, V_{by}, of generalized SDOF system. This relationship shall be bilinear, with initial slope k_g and post-yield slope α_g. Line segments on the idealized force displacement curve shall be located by using an iterative graphical procedure that approximately balances the area above and below the curve. The effective lateral stiffness, k_g, shall be taken as the secant stiffness calculated at a base shear force equal to 60% of the effective yield strength of the structure. The post-yield slope, α_g, shall be determined by a line segment that passes through the actual curve at the calculated target displacement. The yield strength shall not be taken as greater than the maximum base shear force at any point along the actual curve (Figure 3.19). An algorithm which is also used in thesis study can be found in Appendix A for obtaining accurate SDOF representations of MDOF systems.

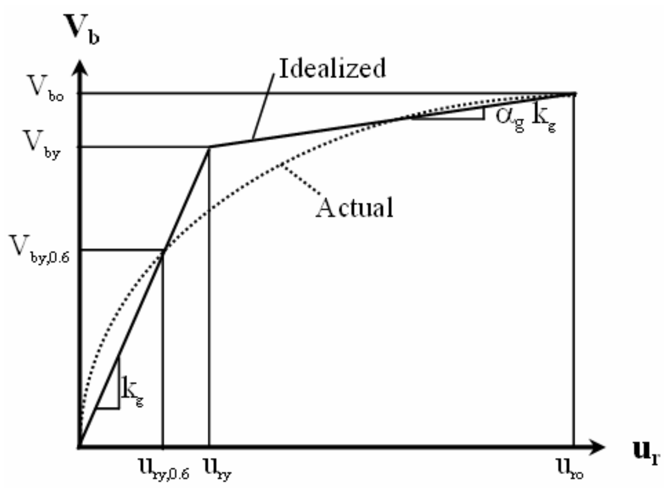

Figure 3.19 : Idealization of pushover curve

Therefore, the nonlinear MDOF systems can be described with generalized nonlinear SDOF systems with the following parameters: T_g (elastic period), ζ_g (damping), either of M_g (mass) or k_g (initial stiffness of bilinear curve) and α_g (the post-yield slope). The bilinear capacity curves of generalized SDOF systems can be converted into ADRS format by using the equations below.

$$Sa = \frac{V_b}{W} \quad ; \quad Sd = u_r \tag{3.12}$$

where,

W is the total weight of the system.

3.5.1 Influencing Parameters

The accuracy of DPA depends strongly on how well various structural aspects of the MDOF systems are represented by corresponding generalized SDOF systems. However, preliminary evaluations of DPA show that generalized SDOF system approximation is affected by two problems which are the selection of target displacement while obtaining idealized curve and selection of A, the slope of DPR.

Figure 3.20 shows how the selection of target displacement affects the generalized SDOF system parameters of the same MDOF system. We can observe from this figure that selection of target displacement affects the parameters of generalized SDOF system significantly. Now the problem is to identify which one is more representative than the others. To solve this uncertainty, an iterative solution strategy is introduced while calculating the target displacement with DPA. Steps of iterative implementation are explained below.

1. Assume a trial target displacement so that area under the capacity curve can be calculated.
2. Obtain bilinear curve that satisfies the FEMA-356 bilinearization criteria.
3. Compute target displacement by using DPA.
4. Repeat steps 2 to 4 until the target displacement is equal to the value in the previous iteration.

This iterative process indicates that all generalized SDOF systems of nonlinear MDOF systems are also ground motion dependent. In other words, same nonlinear MDOF system may have different representative generalized SDOF systems for different ground motions.

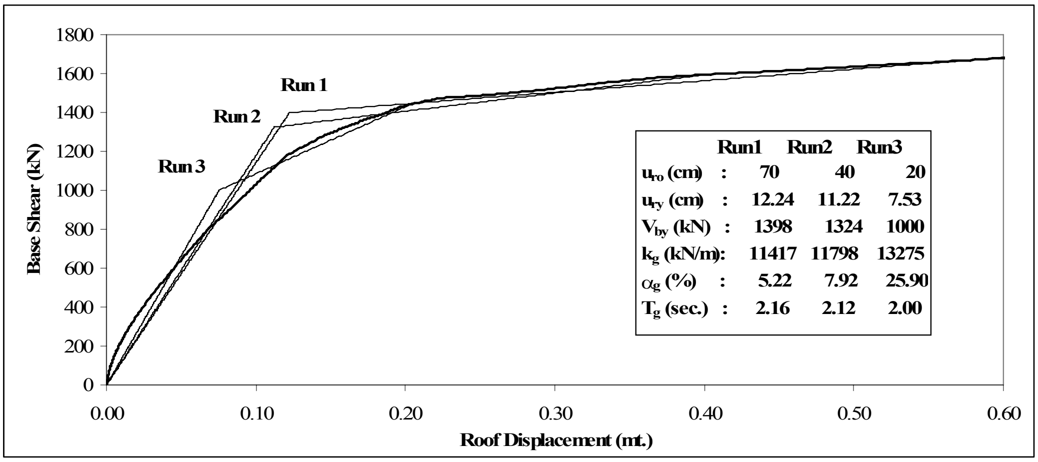

Figure 3.20 : Generalized SDOF system curves with different target displacements of same MDOF system.

Selection of A, the slope of DPR, is another observed problem affecting the accuracy of DPA. Because A changes the shape of capacity curve of MDOF systems. Figure 3.21 shows the capacity curves of case study frames which are obtained from DPA based on different A values. It is observed from Figure 3.21 that for selecting values of A smaller or equal to 0.1, $A \le 0.1$, capacity curves overlap each other for both frames; i.e., effect of A on the capacity curve of MDOF system is not significant. Causes of this situation can be explained by the help of acceleration, velocity and displacement response spectra in a numerical example. In this numerical example, peak acceleration, $\ddot{u}_{g\,max}$, of DPR is fixed to 10 m/s^2 and four different A values (0.01, 0.1, 1 and 10 m/s^3) are selected to demonstrate the effect of A on elastic 5% damped response spectra. According to Figure 3.22 which shows the response spectra results of different DPRs on same graph, when A has a value smaller than 1, all spectra of DPRs yield approximately same results. We can conclude that, responses of same systems become identical if A is less than or equal to 0.1. For this reason, it is suggested to use $A \leq 0.1$ for DPA to eliminate the effect of A on MDOF system to obtain more consistent results.

a)

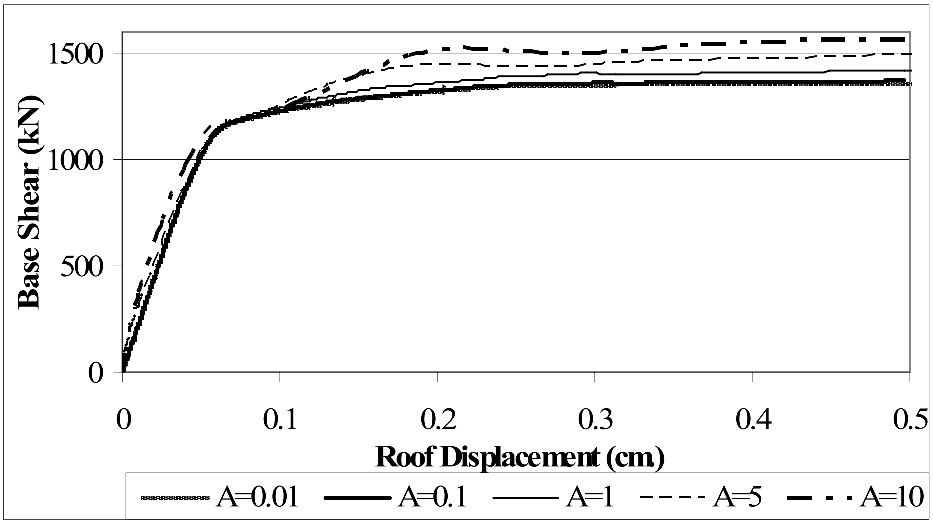

b)

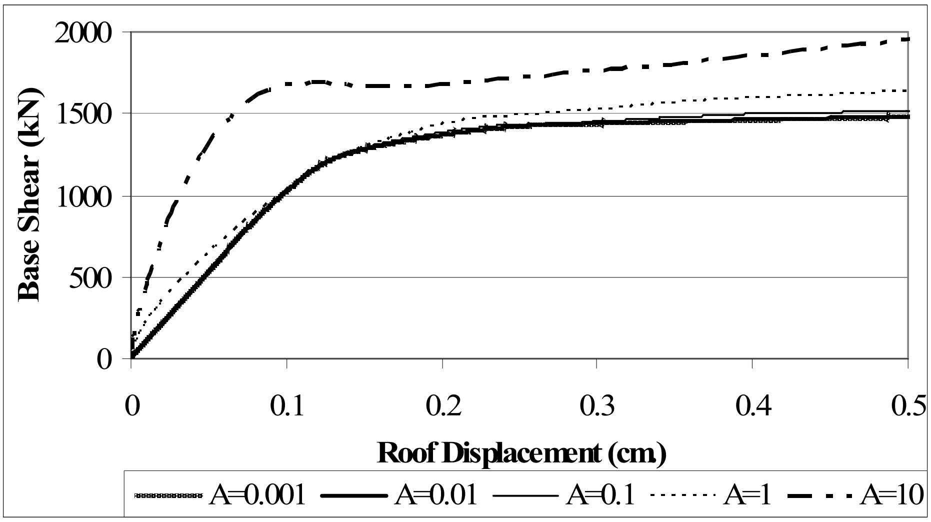

Figure 3.21 : Obtained capacity curves of case study frames with different A values a) Six storey building frame b) Twelve storey building frame

a)

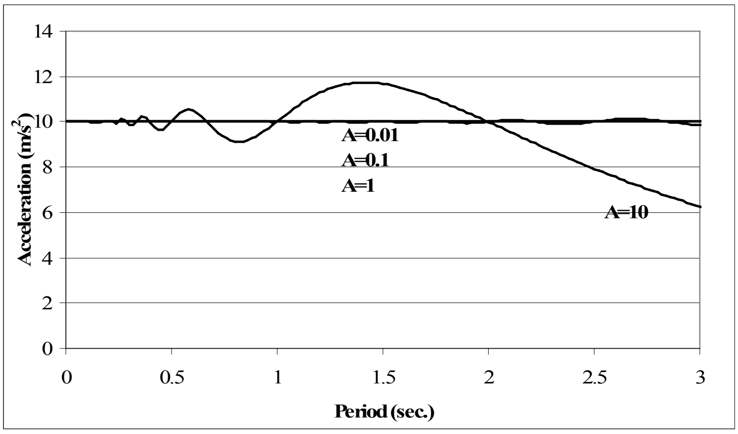

b)

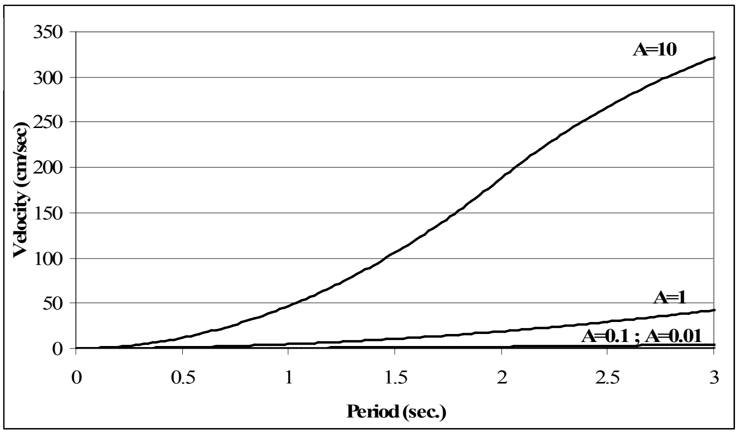

c)

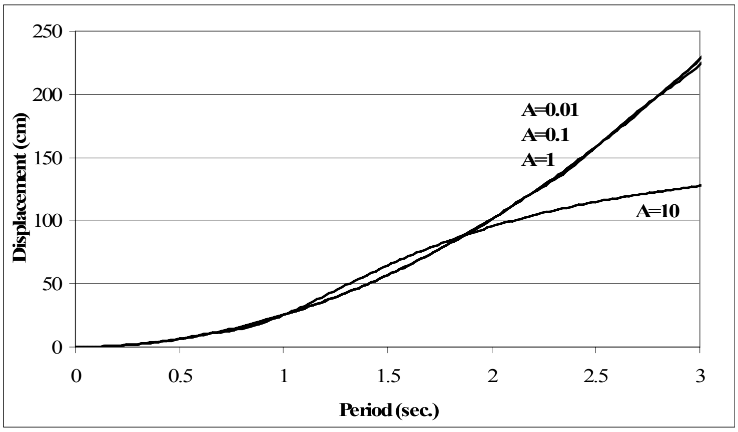

Figure 3.22 : a) Acceleration b) Velocity c) Displacement response spectra of DPRs for $\ddot{u}_{g\,max}$=10 m/s^2 and A= 0.01, 0.1, 1 and 10 m/s^3

3.5.2 Calculating the Seismic Demand of a Nonlinear MDOF System with DPA

The absolute peak inelastic displacement response of nonlinear MDOF systems to earthquake excitation can be estimated by employing a generalized SDOF system which is summarized next as a sequence of steps. Results of numerical examples and discussion of results are presented in Chapter 4.

1. Model the structure by accounting for cracked section stiffnesses for concrete members (Appendix B).
2. Apply "Dynamic Pull Record" (DPR) with selecting ($A \leq 0.1$).
3. Develop capacity curve from the results of DPR.
4. Construct a bilinear representation of capacity curve by using an initial guess for target displacement (Appendix A).
5. Convert the bilinear capacity curve and 5% damped elastic earthquake spectrum into ADRS format, and calculate yield strength reduction factor, R (Figure 3.23), where.

$$R = \frac{Sa_{demand}}{Sa_{yields}} \tag{3.13}$$

In Equation (3.13), Sa_{yield} is the spectral acceleration value of capacity curve at yielding, and Sa_{demand} is spectral acceleration value of the intersection of both linear elastic stiffness spectrum and demand spectrum of earthquake in the ADRS format.

6. Calculate natural vibration period, T_g, and post yielding strain hardening ratio, α_g, of generalized SDOF system (Figure 3.19).

$$T_g = \frac{2 \cdot \pi}{\sqrt{\left[\frac{\left(V_{by} / u_{ry} \right)}{M_g} \right]}} \tag{3.14}$$

$$\alpha_g = \frac{(V_{bo} - V_{by})}{(u_{ro} - u_{ry})} \tag{3.15}$$

where

T_g is the period of generalized SDOF system (sec).

α_g is post yielding strain hardening ratio of the generalized SDOF system (kN/mt.).

V_{by} is estimated yield base shear of MDOF system (kN).

V_{bo} is the estimated linear elastic base shear demand of MDOF system at target displacement (kN).

u_{ry} is the yield displacement value of bilinear capacity curve (m.)

u_{ro} is the target displacement value of bilinear capacity curve (m.)

M_g is the total mass of building (ton).

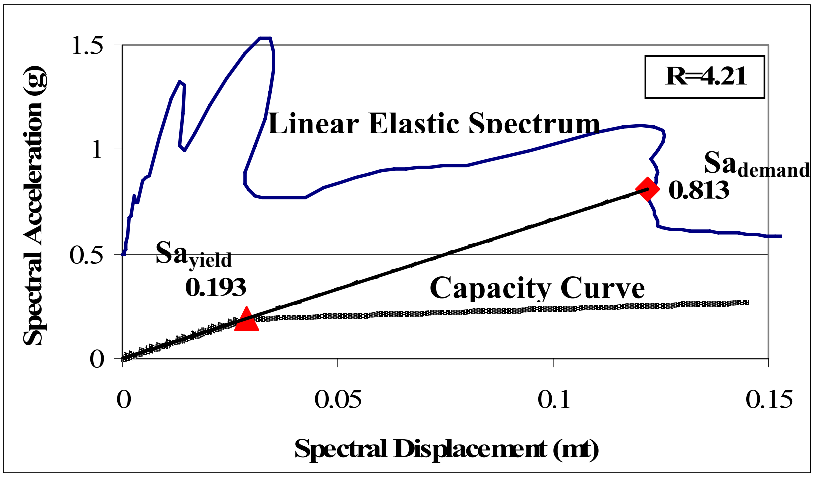

Figure 3.23 : Calculation of yield strength reduction factor, R

7. Develop earthquake specific R-μ-T relation by including the effect of post yielding strain hardening ratio, α.

8. Obtain the ductility level, μ, by using earthquake specific R-μ-T relation.

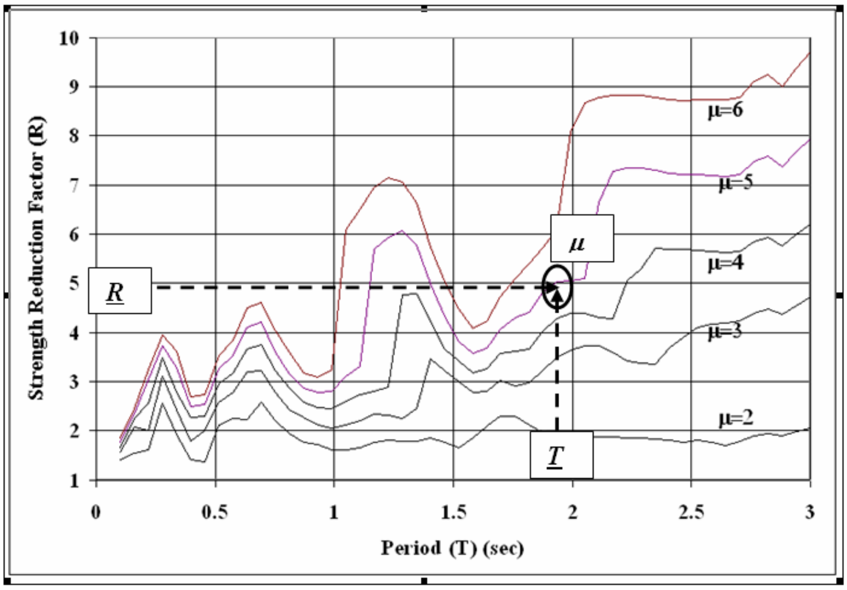

Figure 3.24 : Obtaining the ductility factor for generalized SDOF system

9. Calculate the maximum response of MDOF system from following formula.

   $$u_{ro} = \mu \cdot u_{ry} \quad (3.16)$$

   where

   μ is the calculated ductility demand from earthquake specific R-μ-T spectra.

10. If calculated response of MDOF system is not equal to initial guess of target displacement, repeat the steps 4 to 10 by updating the initial guess of target displacement with the displacement value that is calculated at step 9.

11. Obtain the desired results of MDOF responses from dynamic pull analysis database at calculated seismic response.

CHAPTER 4

CASE STUDIES

4.1 Introduction

In this section, "Dynamic Pull Analysis" is applied to a six-story and a twelve-story reinforced concrete frames that are designed according to the regulations of TS-500 (2000) and TEC (1997). The results of DPA are compared with the results of several nonlinear static procedures, which are modal pushover analysis (Chopra and Goel, 2001), constant ductility spectrum method (Chopra and Goel, 1999), displacement coefficient method (FEMA-356, 2000), and nonlinear time history analysis. The last method is assumed to be exact through the study, and used as a reference to test the accuracy of the other methods. Several near-fault ground motion records that have significant velocity and acceleration pulses have been used to test the validity of the proposed method in the nonlinear response range.

4.2 Description of Buildings

4.2.1 Six Story Building

Six-story structure is designed as a residential building according to the regulations of TS-500 (2000) and TEC (1997). The building is designed for a strength reduction factor of 4 and it is located in seismic zone 1 with local site class Z3 according to TEC (1997) (Figure 4.1).

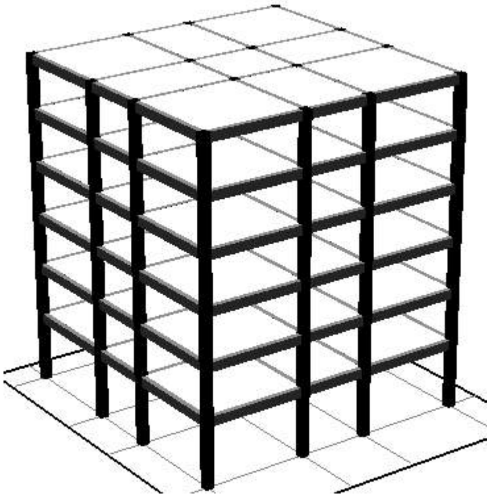

Figure 4.1 : 3- D view o six-story building

Concrete C25 and steel S420 are used in the design. No shearwall are employed in the framing system. Slabs thicknesses are 14 cm in all the floors. Total mass of building is 1200 tons. All column and beam dimensions are presented in Table 4.1. Height of the first story is 4 m., others are 3 mt (Figure 4.3). The floor plan of the building is shown in Figure 4.2. As can be seen from this figure, the building is symmetrical about both orthogonal axes. The anticipated failure mechanism is a beam mechanism according to the regulations of TEC (1997).

Table 4.1 : Section and mass properties of six-storey building

Story	**Beam**		**Column**		**Mass (t)**
	Depth (cm)	**Width (cm)**	**Depth (cm)**	**Width (cm)**	
1-5	55	30	50	50	202.4
6	55	30	50	50	188.0

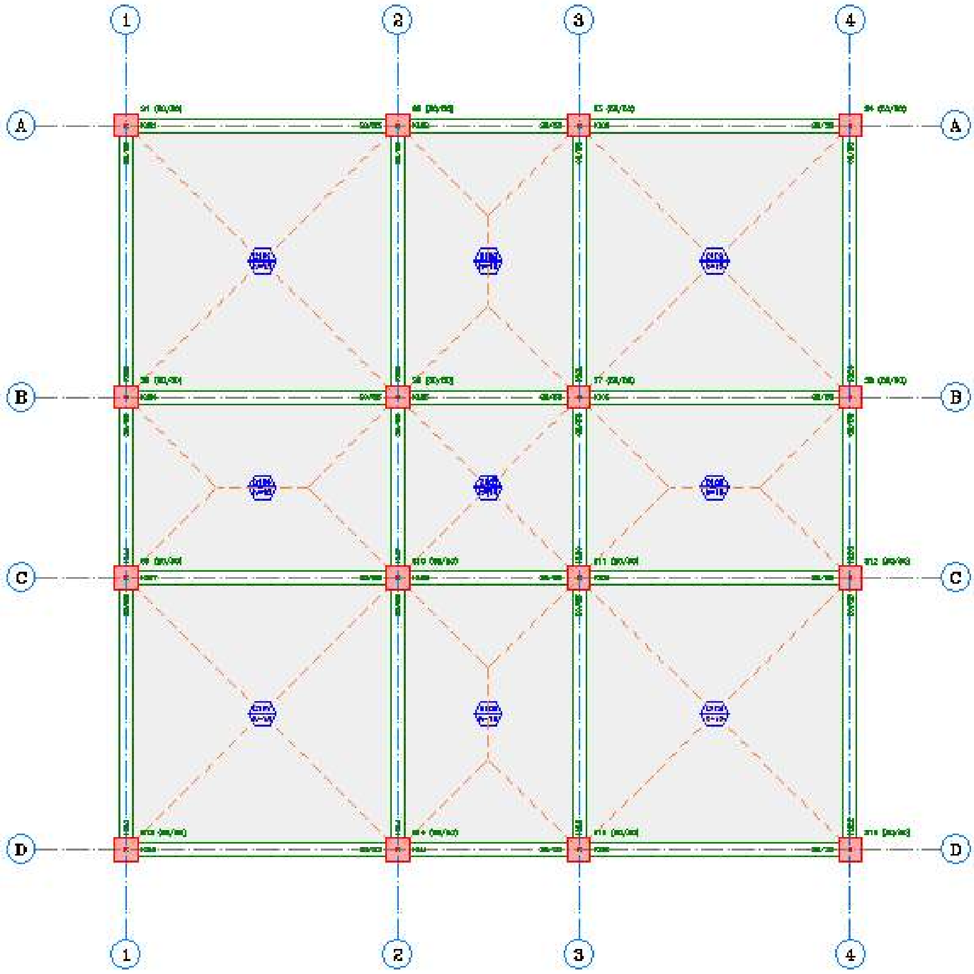

Figure 4.2 : Structural plan view of the six story building

The building is modeled in 2-D using the frame axes C and D (Figure 4.2) due to symmetry in both directions. 2-D model of the building is shown in Figure 4.3. Second order effects are not considered in both linear and nonlinear analyses. For all nonlinear analysis, moment curvature diagrams of all members are considered as elasto-plastic (a small strain hardening is used in the post elastic range). Rigid floor diaphragms are assigned at each storey level and seismic mass of the frames are lumped at the mass center of each storey. Detailed explanation about modelling with Drain-2DX (Allahabadi, 1987) and calculating moment curvature relations of members can be found in Appendix B.

Rayleigh damping ratio of 5% is set for the first and fourth mode. Dynamic properties of the frame are listed in Table 4.2.

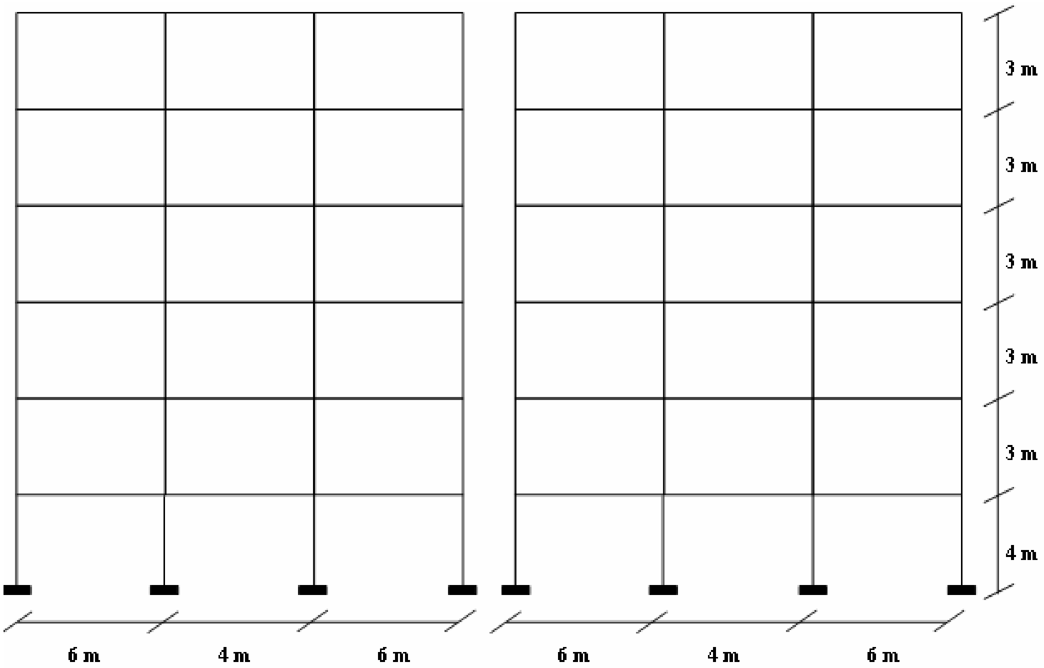

Figure 4.3 : 2-D model of six-story building

Table 4.2 : Modal periods and mode shapes of the six storey frame

Modal Properties		Mode		
		1	2	3
Period (sec.)		0.94	0.29	0.16
Modal Participation Factor		1.26	-0.38	0.18
Modal Mass Factor (%)		89.32	8.46	2.22
Damping (%)		5.00	2.93	3.60
Mode Shape Amplitude	1	0.28	0.73	-0.98
	2	0.49	1.00	-0.60
	3	0.68	0.78	0.51
	4	0.83	0.20	1.00
	5	0.94	-0.49	0.25
	Roof	1.00	-1.00	-0.91

4.2.1 Twelve Story Building

This twelve-story structure is designed as a residential building according to the regulations of TS-500 (2000) and TEC (1997). The building is designed for a strength reduction factor 4, structure located in seismic zone 1 with local site class Z3 according to TEC (1997) (Figure 4.4).

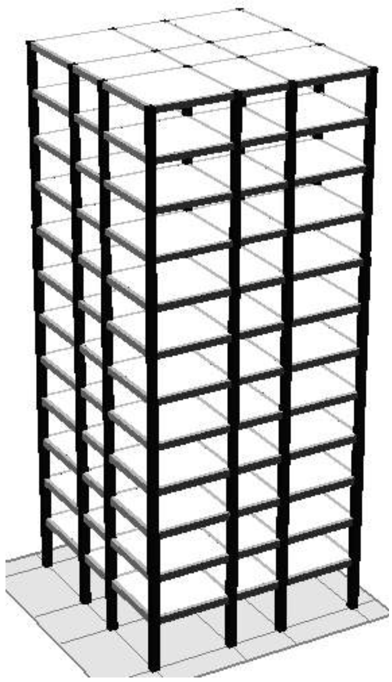

Figure 4.4 : 3- D view of the twelve-story building

Concrete C25 and steel S420 are used in the design. No shearwall are employed in the framing system. Slabs thicknesses are 14 cm at all floors. Total mass of the building is 2696.84 tons. All column and beam dimensions are given in Table 4.3. Height of the first story is 4 m and other stories are 3.2 m (Figure 4.5).

Table 4.3 : Section and mass properties of twelve storey building

Story	Beam		Column		Mass (t)
	Depth (cm)	Width (cm)	Depth (cm)	Width (cm)	
1-4	55	30	60	60	237.34
5-8	50	30	55	55	225.78
9-11	45	30	50	50	214.84
12	45	30	50	50	199.84

The floor plan of the building is shown in Figure 4.2. Structural floor plan is same as the six storey frame. For this reason same modeling assumptions for 2-D modelling are also valid for this system. The anticipated failure mechanism is a beam mechanism according to the regulations of TEC (1997). 2-D model of the frame system is illustrated in Figure 4.5. Rayleigh damping ratio of 5% is set for the first and fifth mode. Dynamic properties of the frame are listed in Table 4.4.

Table 4.4 : Periods and mode shapes of twelve story frame

Modal Properties		Mode			
		1	2	3	4
Period (sec.)		1.95	0.70	0.40	0.26
Modal Participation Factor		1.36	-0.56	0.31	-0.20
Modal Mass Factor (%)		77.75	12.54	4.49	1.95
Damping (%)		5.00	2.86	3.09	3.92
Mode Shape Amplitude	1	-0.08	-0.23	-0.42	0.56
	2	-0.17	-0.47	-0.76	0.85
	3	-0.26	-0.66	-0.89	0.66
	4	-0.36	-0.79	-0.76	0.07
	5	-0.46	-0.83	-0.35	-0.64
	6	-0.56	-0.76	0.23	-0.95
	7	-0.66	-0.59	0.73	-0.58
	8	-0.75	-0.32	0.97	0.22
	9	-0.83	0.04	0.80	0.95
	10	-0.91	0.45	0.23	0.88
	11	-0.97	0.78	-0.46	0.01
	Roof	-1.00	1.00	-1.00	-1.00

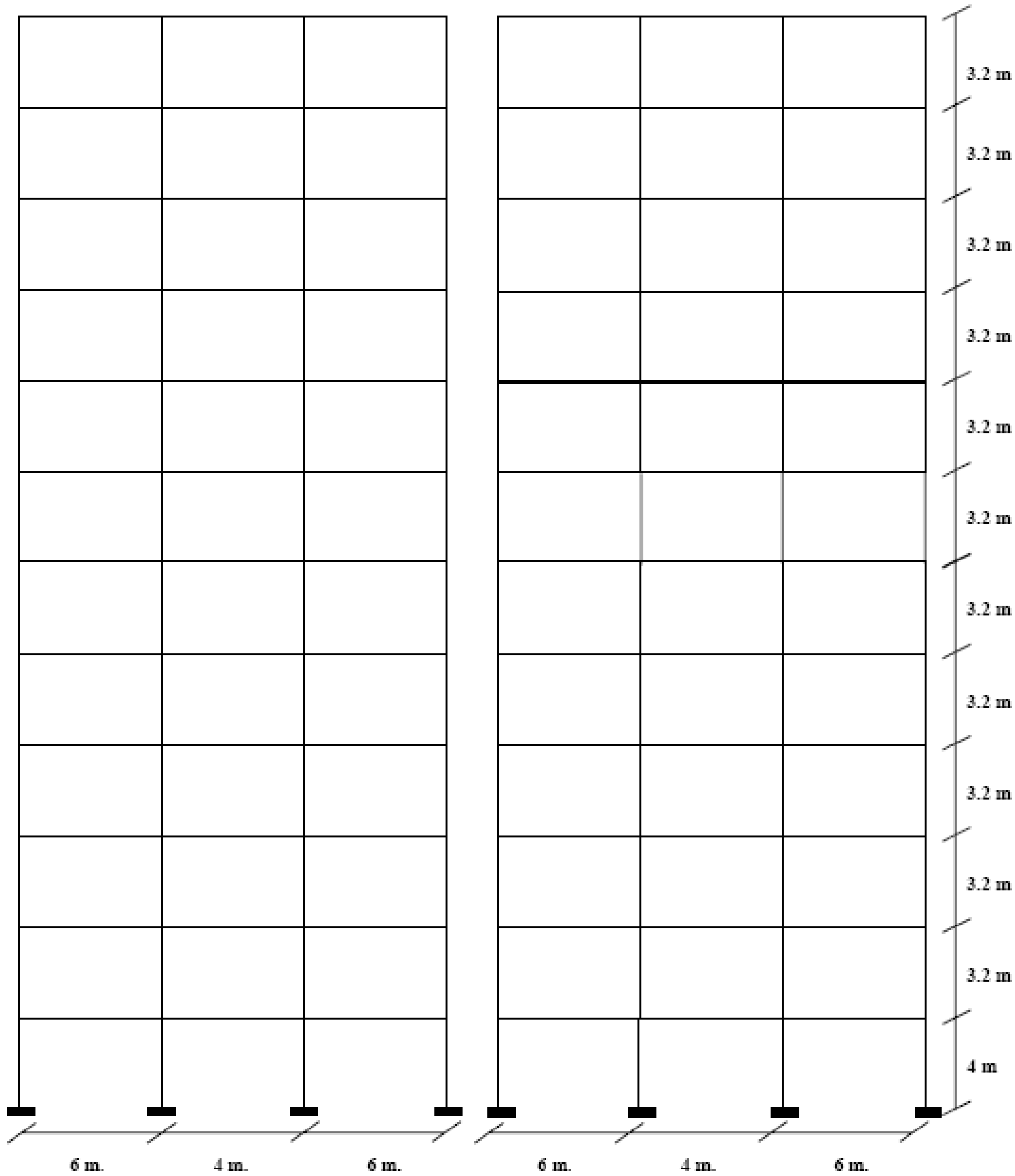

Figure 4.5 : 2-D model of twelve-story building

4.3 Earthquake Ground Motions

Ground motions recorded close to a ruptured fault can be significantly different from those observed further away from the seismic source. The near-fault zone is typically assumed to be restricted to within a distance of about 20 km from the ruptured fault. In the near fault zone, ground motions at a particular site are significantly influenced by the rapture mechanism and slip direction relative to the site and permanent ground displacement at the site resulting from tectonic movement (Rodrigez-Marek, 2000).

In this study, the seismic excitation is defined by a set of three near fault strong motion records listed in Table 4.5. These ground motions were obtained from PEER earthquake database (2005) recorded at distances of 12 to 21 km on NEHRP soil class D. The ground acceleration, velocity and displacement time histories of the near fault records are shown in Figure 4.6 to Figure 4.8, respectively. The constant-ductility pseudo-acceleration and yield-deformation spectra for each of these ground motions for ductility factor μ =1 (elastic), 2, 4, and 6 are shown in Figure 4.6c to Figure 4.8c. These inelastic spectra were developed for bilinear SDOF systems with zero post-yield stiffness.

Table 4.5 : Earthquake ground motion employed in the study

Earthquake Name	**Station Name**	**Comp.**	**Date**	**Mechanism**	**R (km)**	**PGA (m/sec^2)**	**PGV (cm/sec)**
Erzincan	Erzincan	EW	13.3.92	Strike-Slip	12.71	5.05	83.95
Northridge	Rinaldi	228^o	17.1.94	Reverse	20.62	8.09	160.10
Northridge	Sylmar	52^o	17.1.94	Reverse	21.87	6.01	117.42

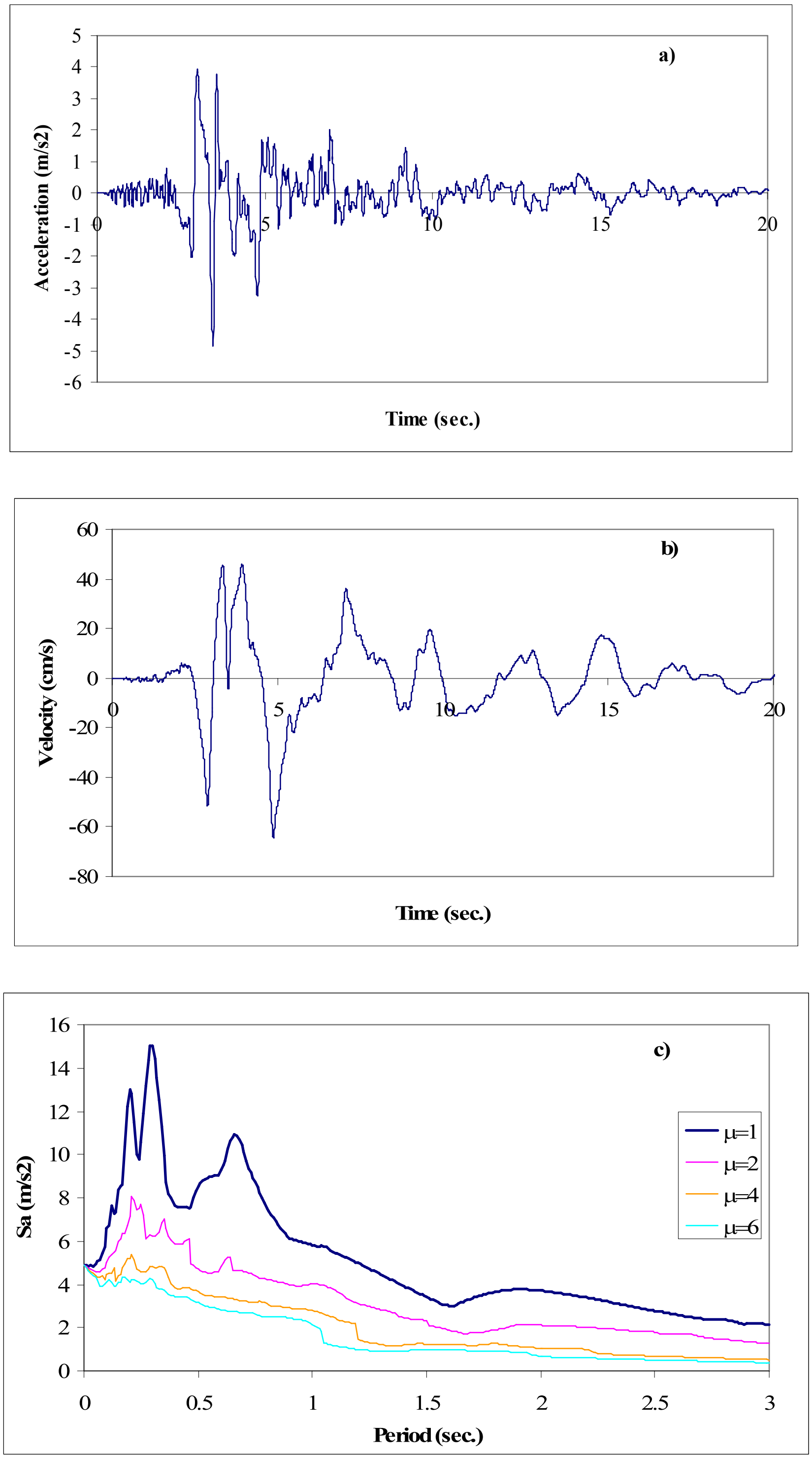

Figure 4.6 : a) Acceleration time history b) Velocity time history c) Elastic and inelastic spectra of Erzincan EW component

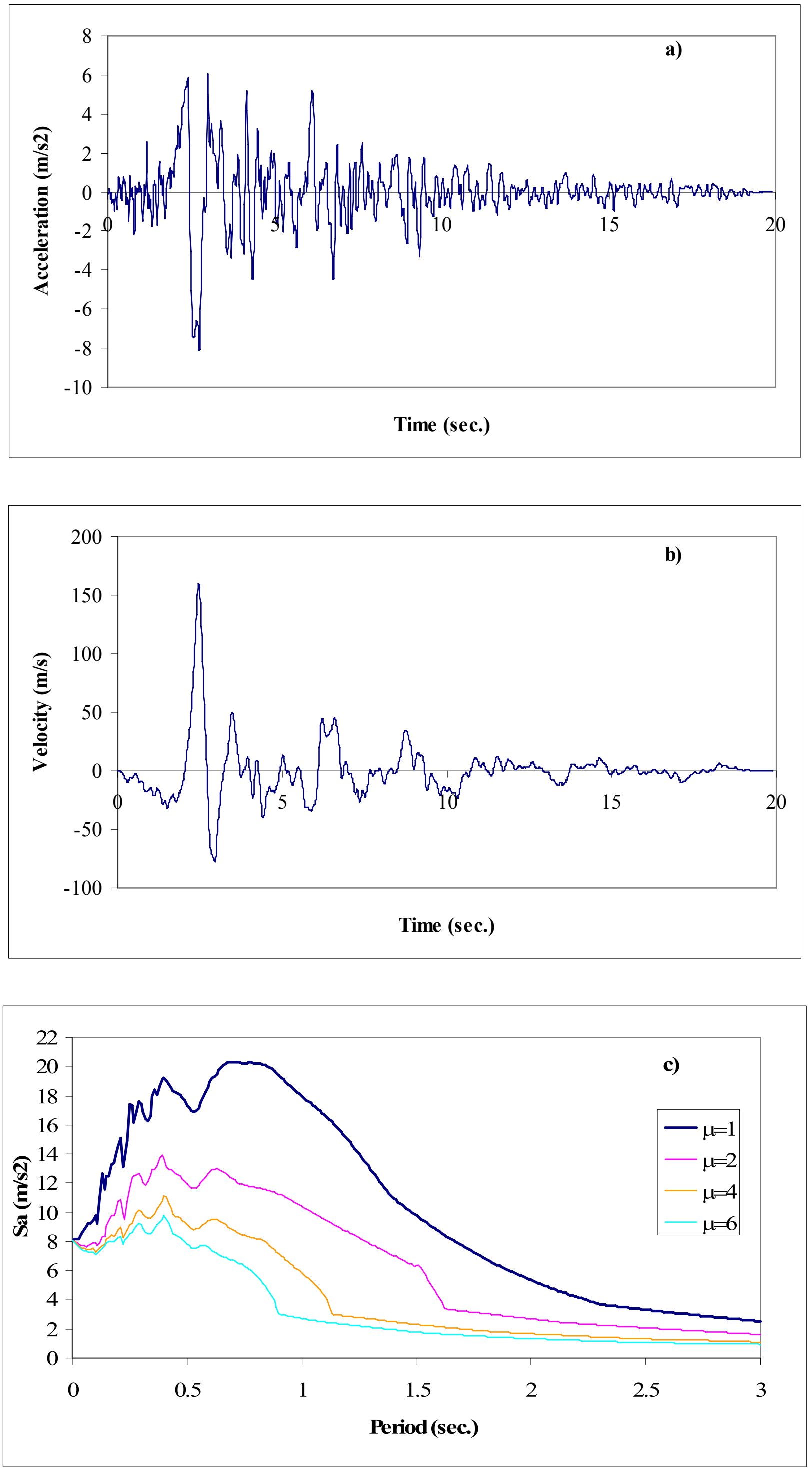

Figure 4.7 : a) Acceleration time history b) Velocity time history c) Elastic and inelastic spectra of Rinaldi 228^{o} component

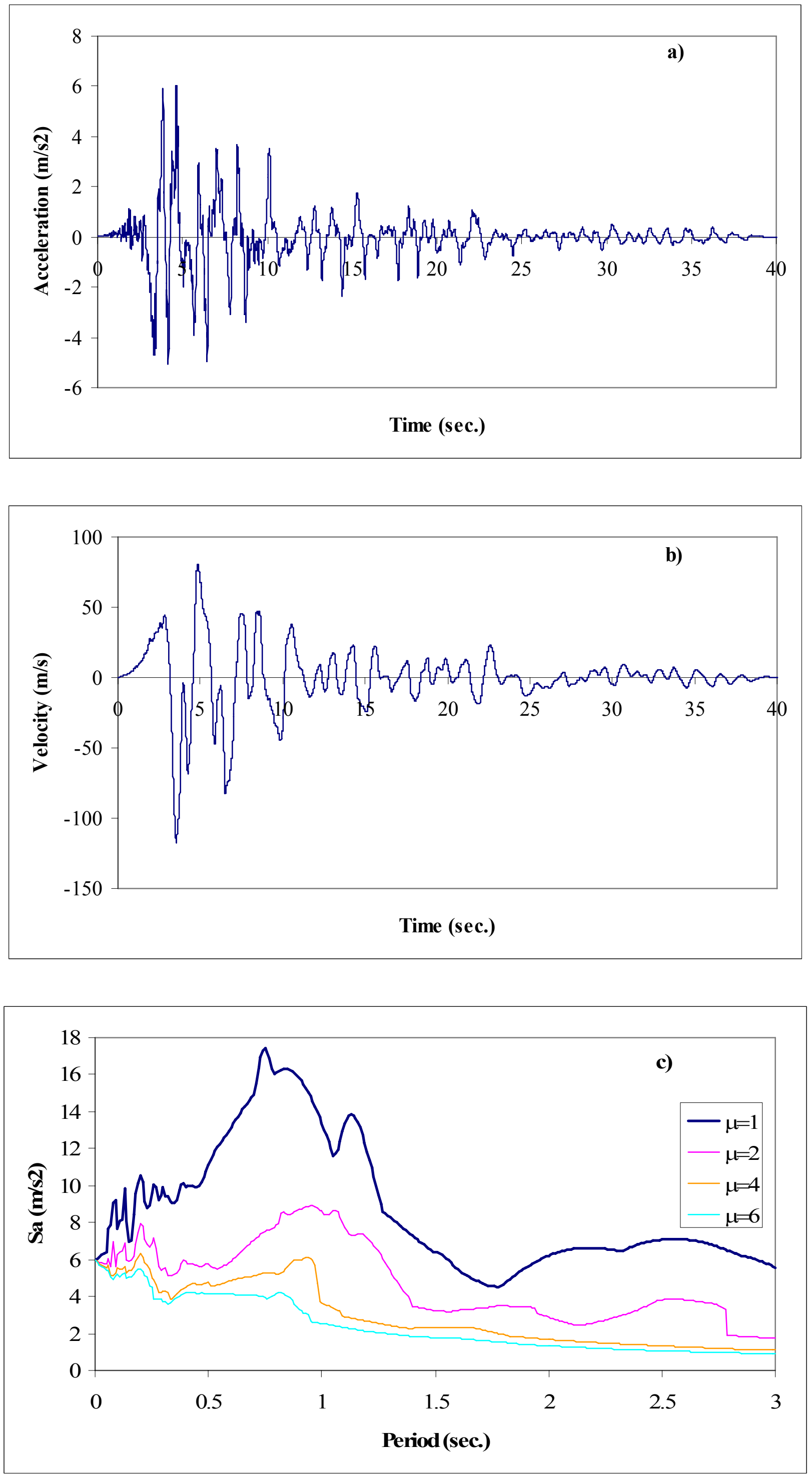

Figure 4.8 : a) Acceleration time history b) Velocity time history c) Elastic and inelastic spectra of Sylmar 52^{o} component

4.4 Comparative Evaluation of Nonlinear MDOF Systems

Compared in this section of thesis are the earthquake-induced demands for the six- storey and twelve storey-building frames determined by five different procedures: displacement coefficient method (FEMA-356, 2000), constant ductility spectra method (Chopra and Goel, 1999), modal pushover analysis (Chopra and Goel, 2001), dynamic pull analysis and nonlinear time history analysis. Gravity load effects were included in all analyses. Capacity curves were obtained by performing pushover analyses and nonlinear time history analyses using Drain-2DX (Allahabadi, 1987). At target displacement, storey displacement, inter-storey drift ratio, capacity curves and plastic hinge rotation demands for all methods were extracted from the analysis database and compared with the results of nonlinear time history analysis which was assumed as exact. Errors involved in response quantities from each method were calculated with respect to exact demands to check the accuracy of predictions.

4.4.1 Comparison of Displacement Demands

Target displacement represents the estimated maximum displacement demand of MDOF system when subjected to the strong ground motion. Accurate estimation of target displacement is important, because all force and deformation demands at the target value are compared with available capacities of system for controlling the condition of structure.

Target displacement results of known approximate procedures, constant ductility spectra method (CDS), displacement coefficient method (FEMA), modal pushover analysis (MPA), the proposed method which is called dynamic pull analysis (DPA) and nonlinear time history analysis (NLTHA), which is assumed to be the exact reference, are presented in Table

4.6 and Table 4.7. In addition, error profiles of calculated target displacements with reference to NLTHA results are illustrated in Figure 4.9 and Figure 4.10.

Table 4.6 : Target displacement results from each method for six-storey building frame (All results are in m.)

EQ	Station	Records	NLTH	FEMA	CDS	MPA	DPA
Erzincan	Erzincan	E-W	0.234	0.170	0.303	0.274	0.254
Northridge	Rinaldi	228	0.294	0.541	0.417	0.346	0.341
Northridge	Sylmar	52	0.326	0.428	0.480	0.342	0.340

Table 4.7 : Target displacement results from each method for twelve-storey building frame (All results are in m.)

EQ	Station	Records	NLTH	FEMA	CDS	MPA	DPA
Erzincan	Erzincan	E-W	0.271	0.495	0.450	0.413	0.274
Northridge	Rinaldi	228	0.577	0.751	0.873	0.724	0.677
Northridge	Sylmar	52	0.663	0.782	0.887	0.768	0.572

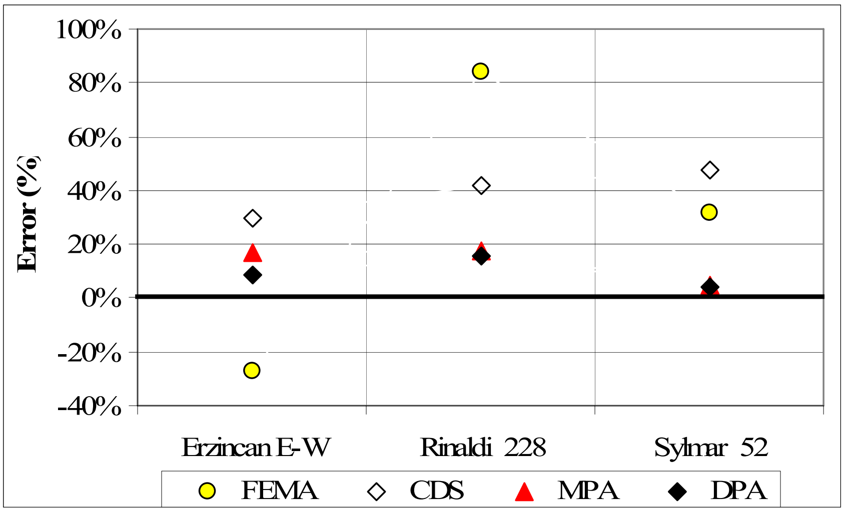

Figure 4.9 : Error profiles of target displacements for six storey building frame

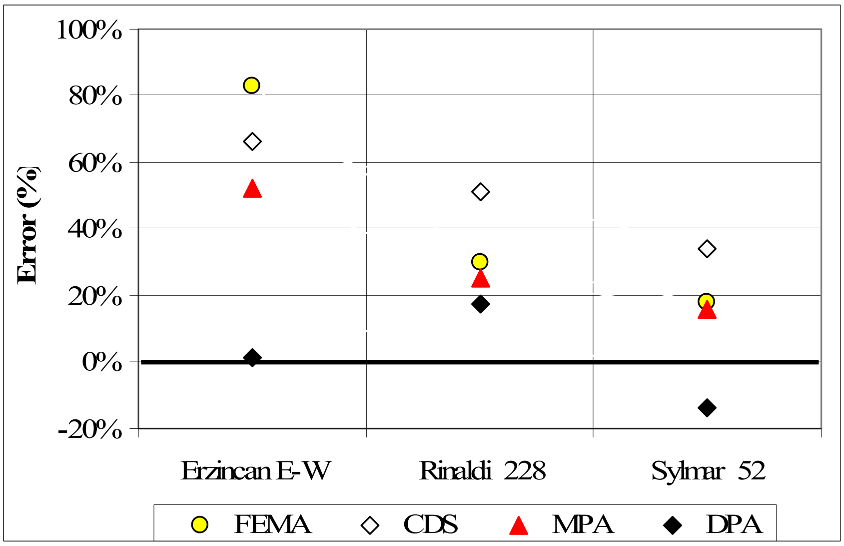

Figure 4.10 : Error profiles of target displacements for twelve storey building frame

The following observations can be made from the target displacement predictions.

- Results of comparison of target displacements with nonlinear time history analysis indicate that MPA and DPA give more accurate probable maximum roof displacement results than other nonlinear static procedures.
- Displacement coefficient method and constant ductility spectrum method results in overestimation of target displacement in inelastic range for most of the cases.

4.4.2 Comparison of Capacity Curves

Capacity curve which is expressed as the base shear versus roof displacement relation for MDOF systems represents the global nonlinear response of a structure. Capacity curves for each method are obtained from the analyses database. The dynamic capacity curves for each ground motion are also included in the figures to make comparison of dynamic capacity curves with ones obtained from other methods (Figure 4.11 and Figure 4.12).

In the actual methodology of modal pushover analysis (Chopra and Goel, 2001), there is no need to represent the capacity curve of structure. However, to make an appropriate comparison, capacity curve of the method is developed. In obtaining the capacity curve for MPA, each strong ground motion record was multiplied with ten equally divided scale factors which vary from 0.1 to 1.0. By using the displacement response of MPA obtained from scaled earthquakes, base shear capacities were extracted from pushover database. Finally all results of selected modes were combined by SRSS to develop an overall capacity curve for each earthquake response and each case study frames.

In all cases, roof displacement is normalized with respect to total height of the frame and base shear is normalized with respect to the total seismic weight of frames.

Following observations can be made from obtained capacity curves.

- In most of the cases of twelve storey-building frames, capacity curve of MPA yielded higher base shear capacity.
- In all of the cases of both six storey and twelve storey-building frames, capacity curve of DPA yielded higher initial stiffness.
- In all of the cases of both frames, capacity curve of FEMA-356 underestimates the base shear capacity of frames.
- Capacity curve of DPA which is also a dynamic capacity curve covers the dynamic capacity curve of earthquakes in most of the cases.

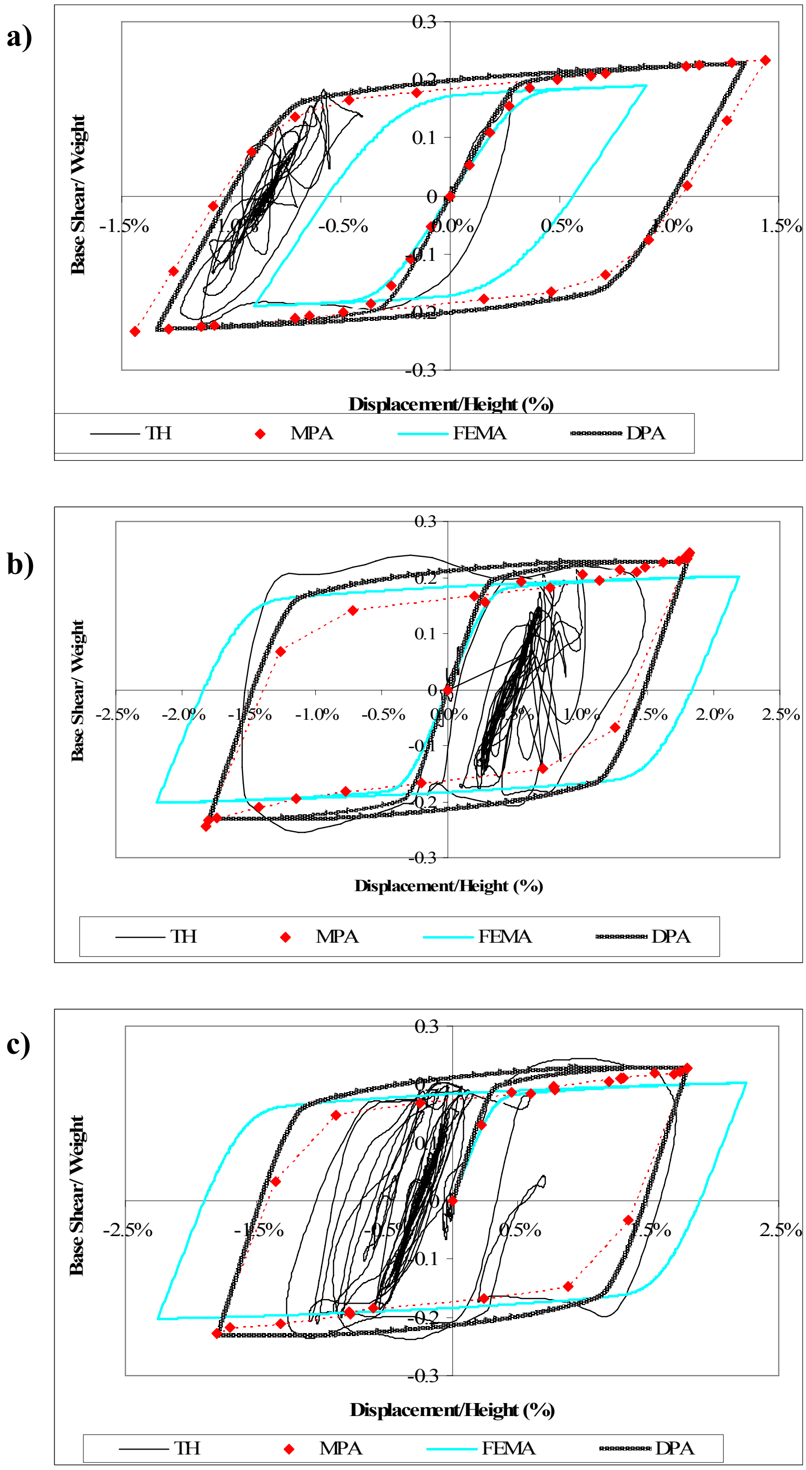

Figure 4.11 : Capacity curves for the six-storey frame. a) Erzincan-EW b) Rinaldi-228° c) Sylmar-52°

a)

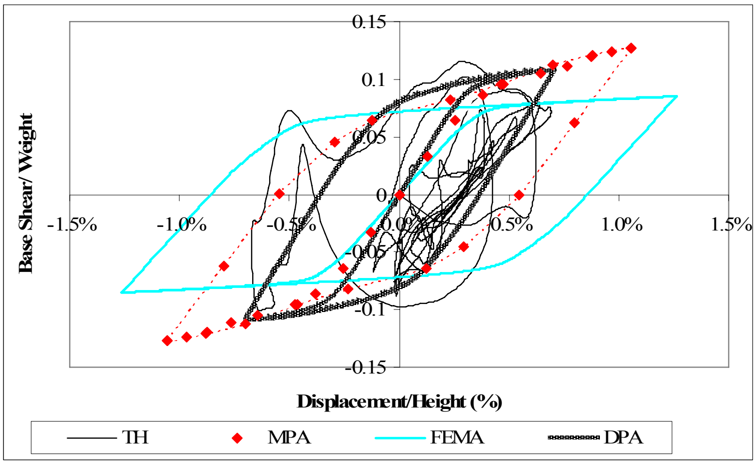

b)

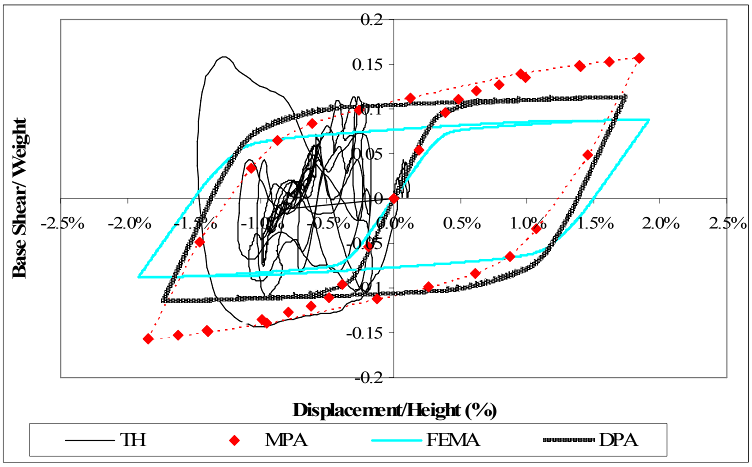

c)

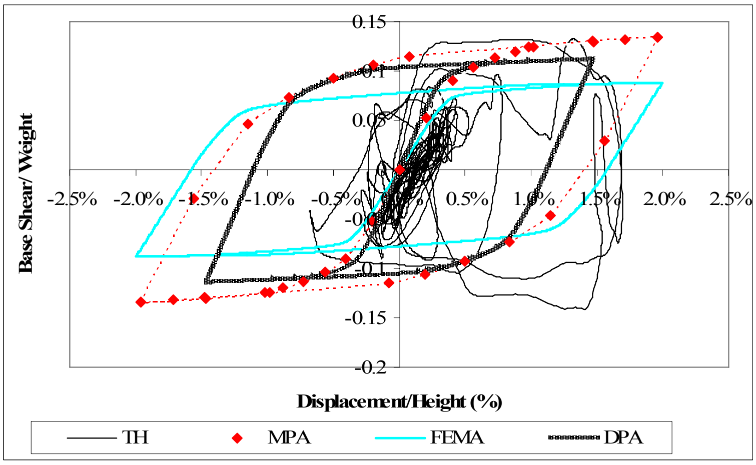

Figure 4.12 : Capacity curves for the twelve-storey frame. a) Erzincan-EW b) Rinaldi-228^{o} c) Sylmar-52^{o}

4.4.3 Comparison of Storey Displacement Profiles and Interstorey Drift Ratios

In this section, storey displacements and interstory drift ratios from different methods are compared with the exact dynamic behaviour at maximum displacement response. All storey displacement and interstory drift profiles were obtained from analyses database at the associated target displacement of each method.

Story displacement profiles and interstory drift ratio distributions of frames are presented in Figure 4.13 to Figure 4.16.

According to the results obtained from case studies, the following observations can be made.

- For the six storey building frame, MPA and DPA capture exact storey displacement more accurately than the displacement coefficient method and constant ductility spectrum method.
- For the twelve storey building frame, DPA captures exact storey displacements more accurately than the nonlinear static procedures.
- Error in storey displacement profile estimations under any earthquake increases in all methods when the number of stories increases.
- For the twelve storey building frame, the proposed procedure generally overestimates the interstory drift ratios in the first two floors.
- In the comparison of nonlinear static procedures, MPA gives more accurate results than the displacement coefficient method

and constant ductility spectrum method because of including higher mode effects.

- First mode alone, which is the basis for pushover analyses procedures currently used in performance based earthquake engineering practice, does not adequately estimate the seismic demand.
- For the six storey frame, interstory drift ratios and its distribution over the frame for all strong ground motions are very similar. In contrary, no clear trend was observed for the twelve storey building frame. The difference in due to dominance of first mode in the six storey frame.

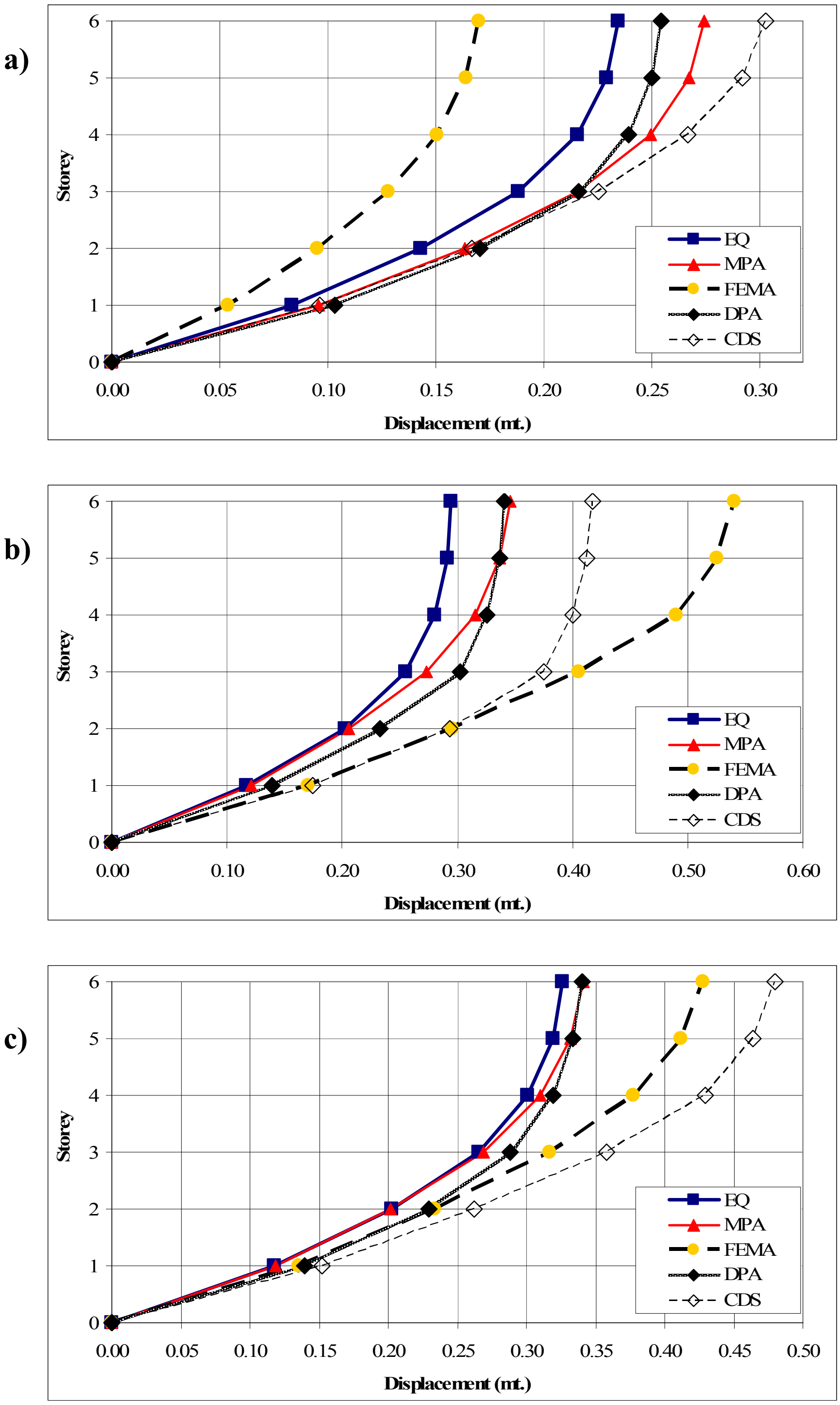

Figure 4.13 : Storey displacement of six-storey frame at the associated target displacements for different methods a) Erzincan-EW b) Rinaldi-228° c) Sylmar-52°

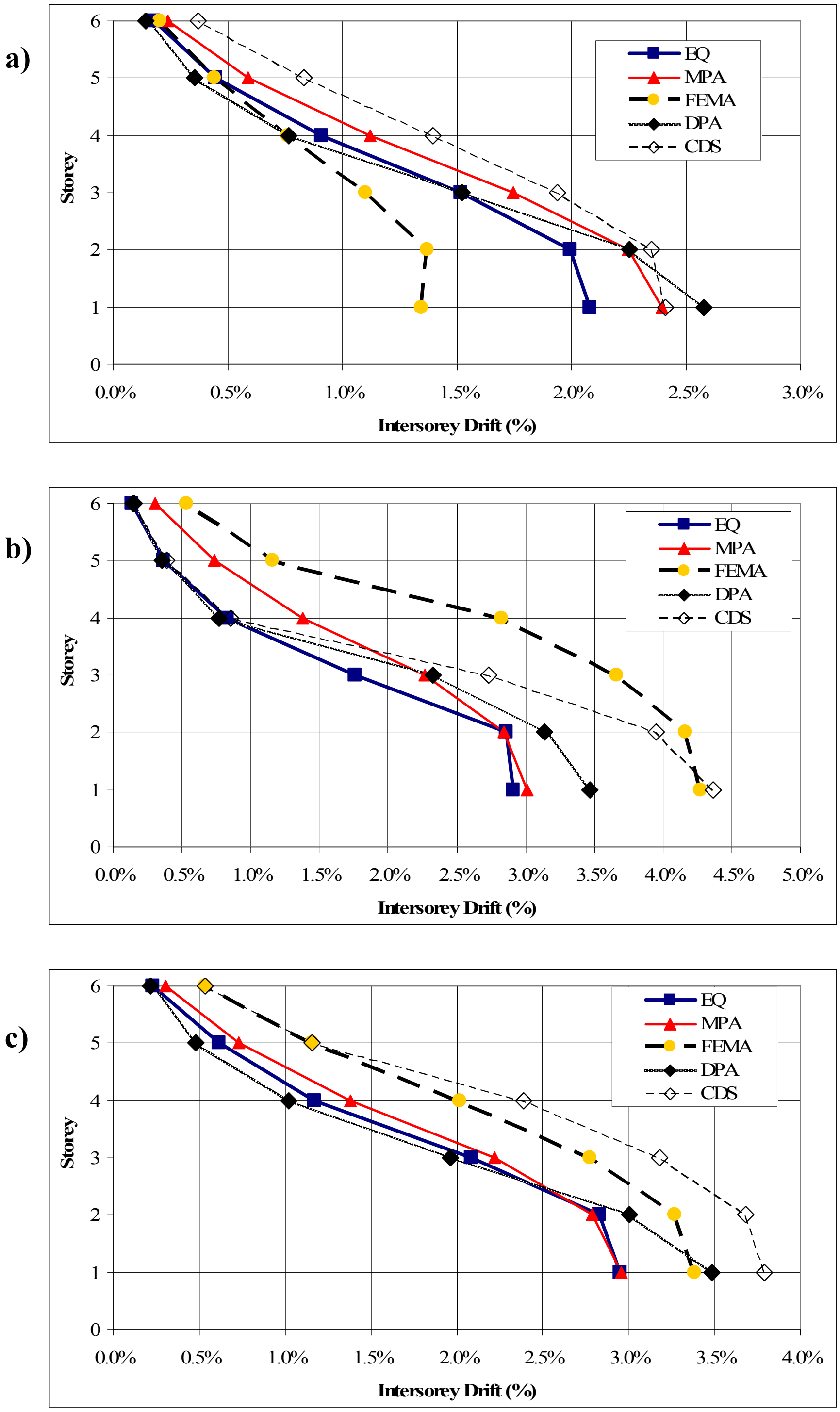

Figure 4.14 : Storey drift ratio profiles of six-storey frame at the associated target displacements for different methods a) Erzincan-EW b) Rinaldi-228^{o} c) Sylmar-52^{o}

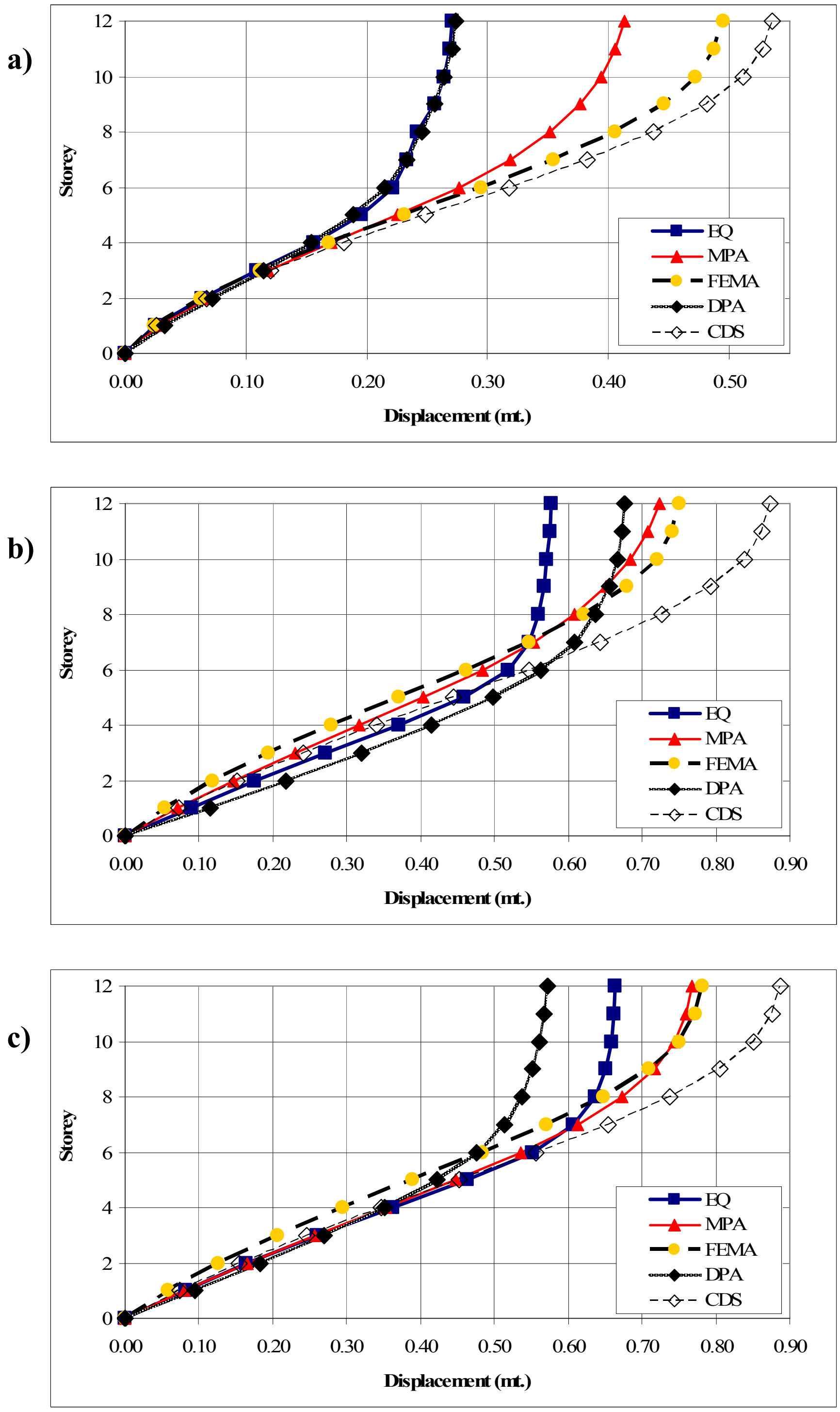

Figure 4.15 : Storey displacement of twelve-storey frame at the associated target displacements for different methods a) Erzincan-EW b) Rinaldi-228° c) Sylmar-52°

a)

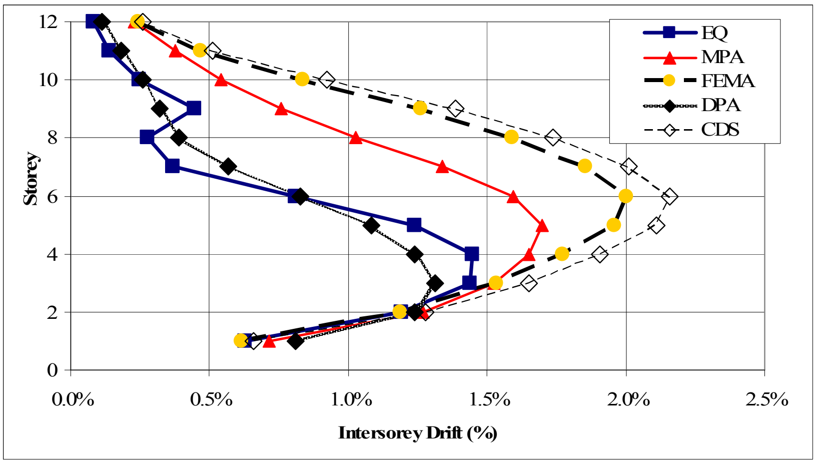

b)

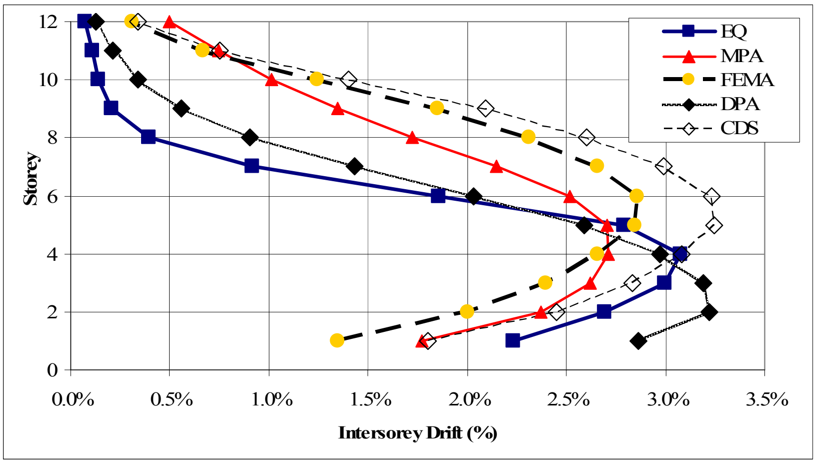

c)

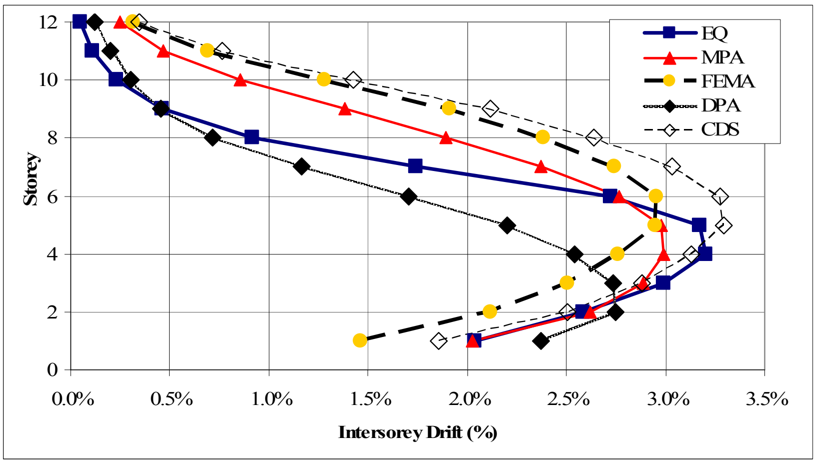

Figure 4.16 : Storey drift ratio profiles of twelve-storey frame at the associated target displacements for different methods a) Erzincan-EW b) Rinaldi-228° c) Sylmar-52°

4.4.4 Comparison of Plastic Hinge Patterns and Rotations

Observing the plastic hinge distribution patterns in the structure is important. Because each hinge location shows the weakness of members and failure potential that the system would experience under earthquake excitation. In this section, plastic hinge distributions obtained from each method at the associated target displacement are illustrated in Figure 4.17 to Figure 4.25. In addition, mean values of storey plastic hinge rotations obtained from each method for each earthquake response are also illustrated in Figure 4.26 to Figure 4.29. These figures are plotted for the storey mean values obtained in beams and columns separately.

The guidelines for the assessment of the structures published by the Applied Technology Council (ATC-40, 1996) and Federal Emergency Management Agency (FEMA-356, 2000) have similar detailed vulnerability assessment procedures. These procedures propose similar plastic rotation limits for the three limit states, namely "Immediate Occupancy" (IO), "Life Safety" (LS), "Collapse Prevention" (CP) (Structural stability, SS, in case of ATC-40). The maximum plastic rotation attained by a member under given ground motion is compared with these plastic rotation limits and performance of that member end under each earthquake ground motion is assessed. The plastic rotation limits differ according to type, predominant failure mode and ductility characteristics of the member. The calculated plastic rotation limits according to FEMA-356 (2000) criteria for the case study frames are presented in Table 4.8. According to these limits, different hinge symbols which are also listed in Table 4.8 are used in the displaying the plastic hinge pattern.

Table 4.8 : Plastic hinge rotation limits for reinforced columns and beams in case study frames (All values are in rad.)

	Immediate Occupancy IO (Null)	**Immediate Occupancy IO (+)**	**Life Safety LS (O)**	**Collapse Prevention CP (●)**	**Failure F (X)**
Column	<0	<0.005	0.015	0.020	>0.020
Beam	<0	<0.010	0.020	0.025	>0.025

Following observations can be made from plastic hinge location distributions;

- For the six storey-building frame, DPA captures the exact plastic hinge patterns more accurately than modal pushover analysis, displacement coefficient method and constant ductility method.
- For the six storey building frame columns, DPA and MPA estimate the mean values of storey plastic hinge more accurately than the other two nonlinear static procedures.
- For the six storey and the twelve storey building frame beams, only DPA estimates are close enough to exact response. The other procedures overestimate the plastic hinge rotations.
- For the twelve storey building frame, only the plastic hinge pattern of DPA resembles the plastic hinge pattern of NLTHA. The other procedures foresee more plastic hinges especially at upper floors.
- For the twelve storey building frame columns, DPA generally overestimates the mean value of plastic rotation in the first storey whereas the other methods significantly underestimate the first storey column plastic rotations. However, in the upper stories, all methods have similar plastic hinge rotation predictions since plastic column rotations are very small in upper stories.

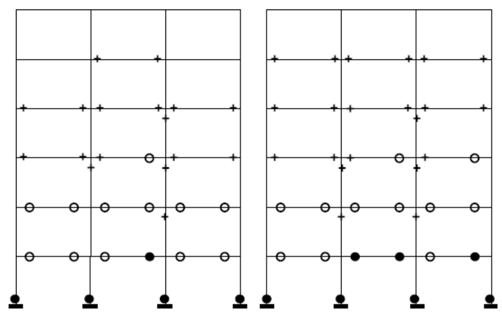

a) Nonlinear Time History

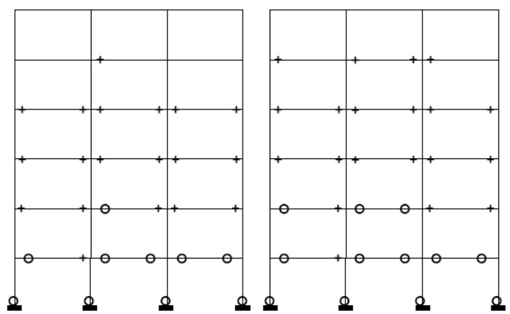

b) FEMA-356

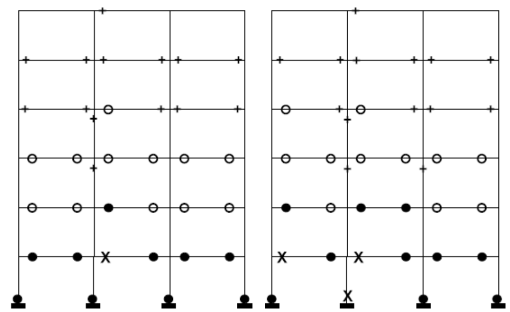

c) Constant Ductility Spectrum

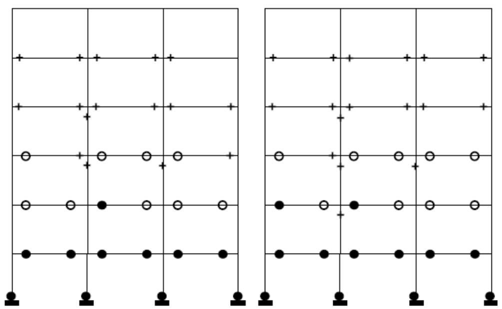

d) Modal Pushover Analysis

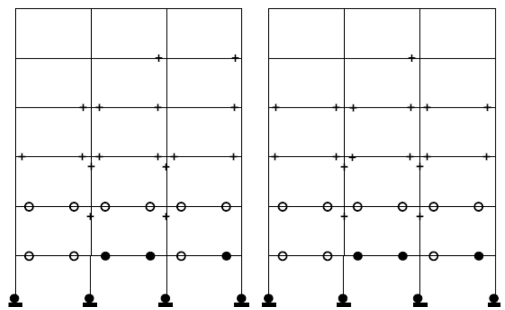

e) Dynamic Pull Analysis

Figure 4.17 : Plastic hinge distribution in the six storey frame under Erzincan-EW ground motion

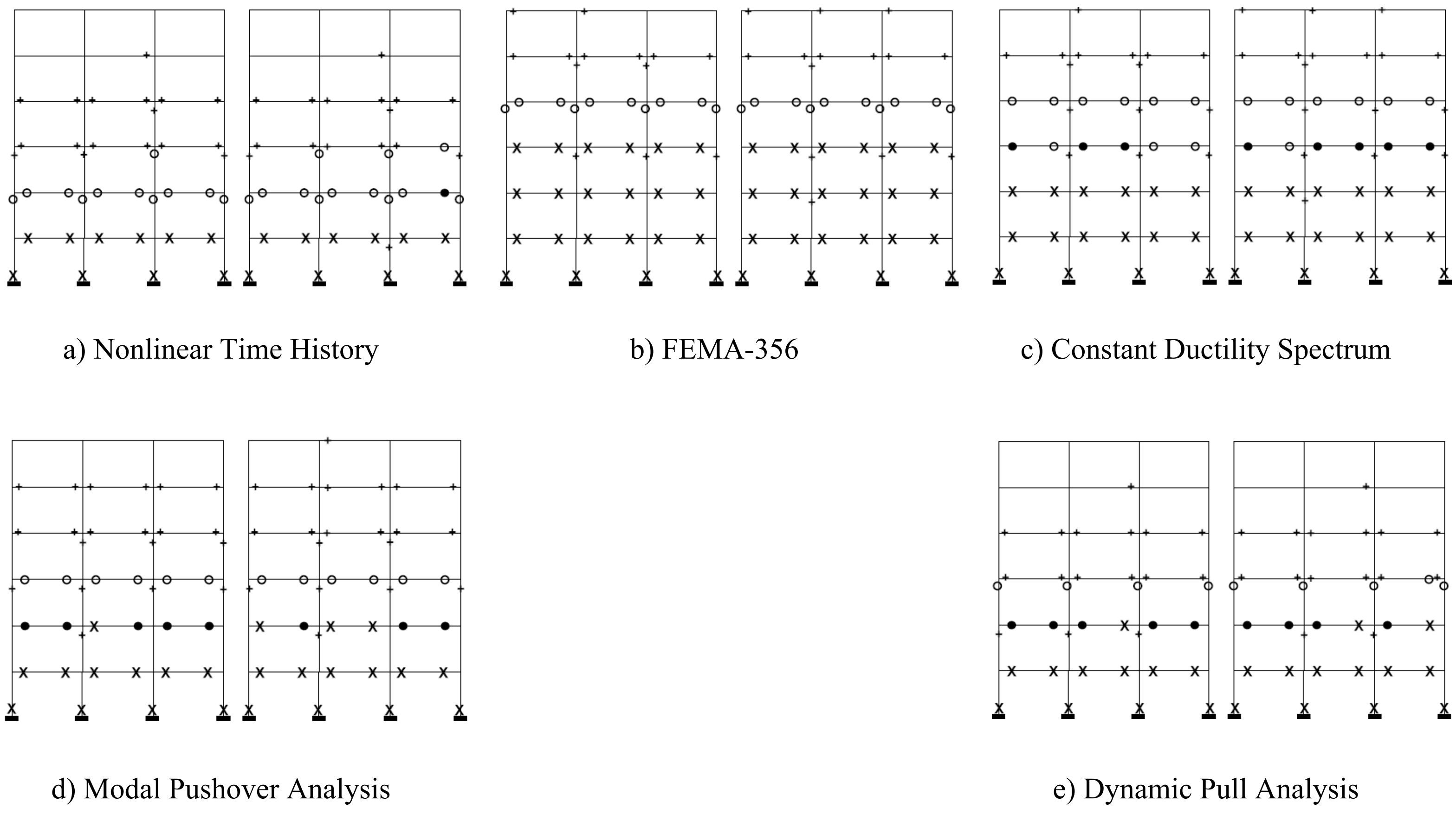

a) Nonlinear Time History

b) FEMA-356

c) Constant Ductility Spectrum

d) Modal Pushover Analysis

e) Dynamic Pull Analysis

Figure 4.18 : Plastic hinge distribution in the six storey frame under Rinaldi-228^{o} ground motion

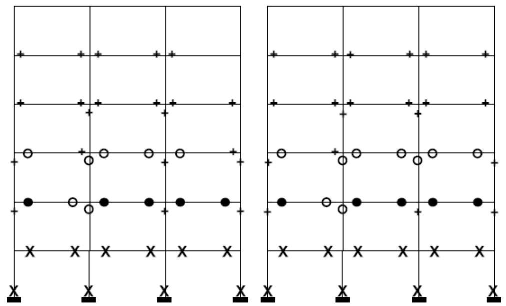

a) Nonlinear Time History

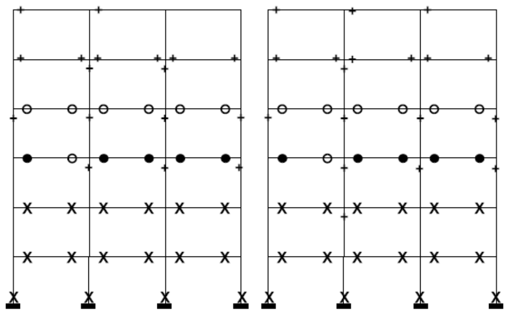

b) FEMA-356

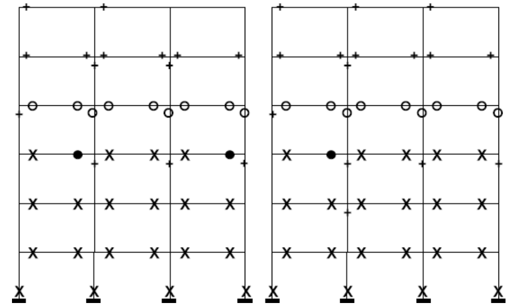

c) Constant Ductility Spectrum

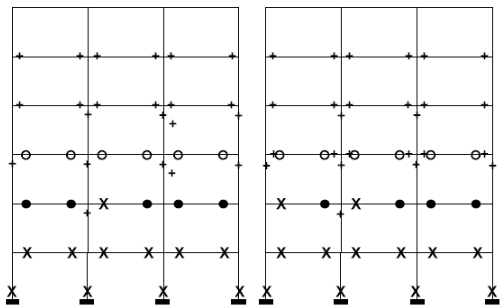

d) Modal Pushover Analysis

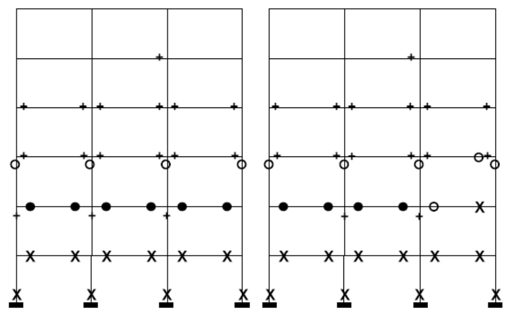

e) Dynamic Pull Analysis

Figure 4.19 : Plastic hinge distribution in the six storey frame under Sylmar-52^{o} ground motion

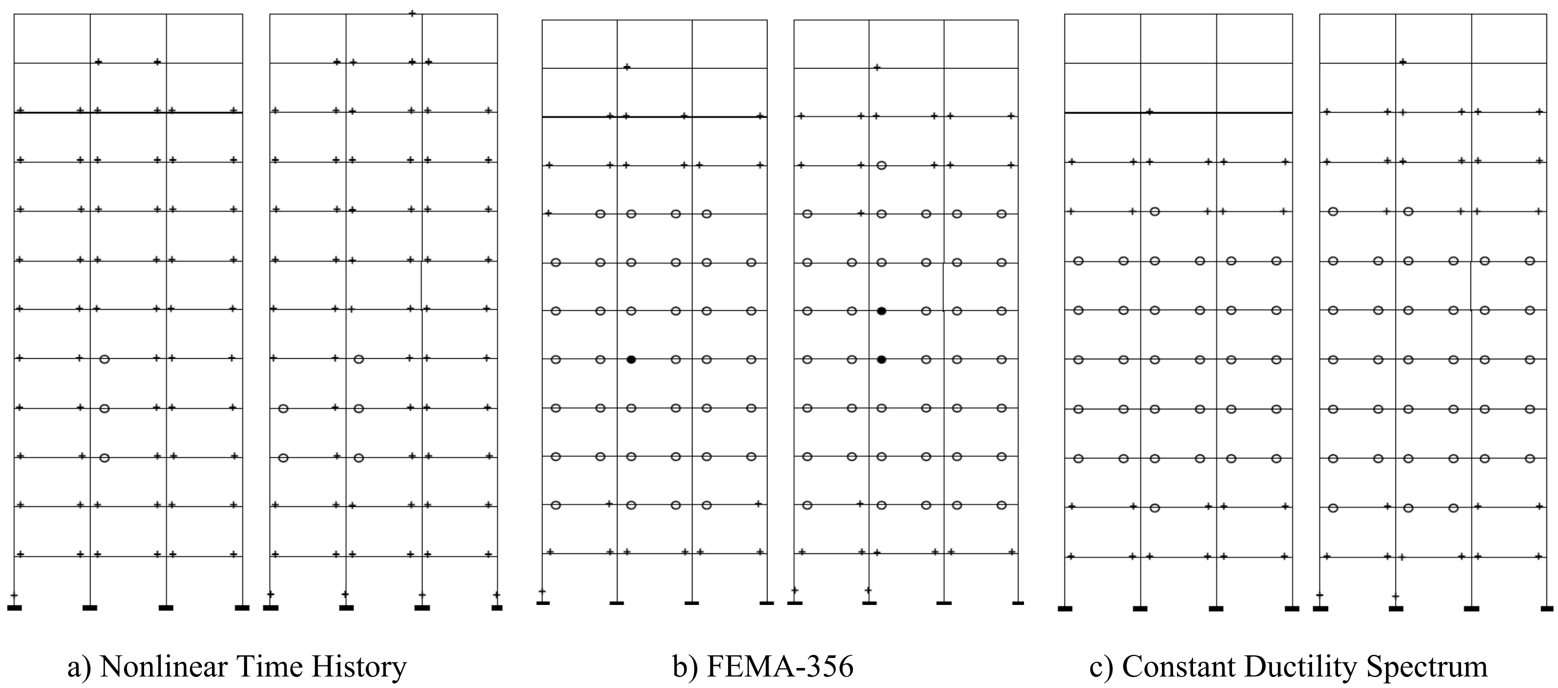

Figure 4.20 : Plastic hinge distribution in the twelve storey frame under Erzincan-EW ground motion

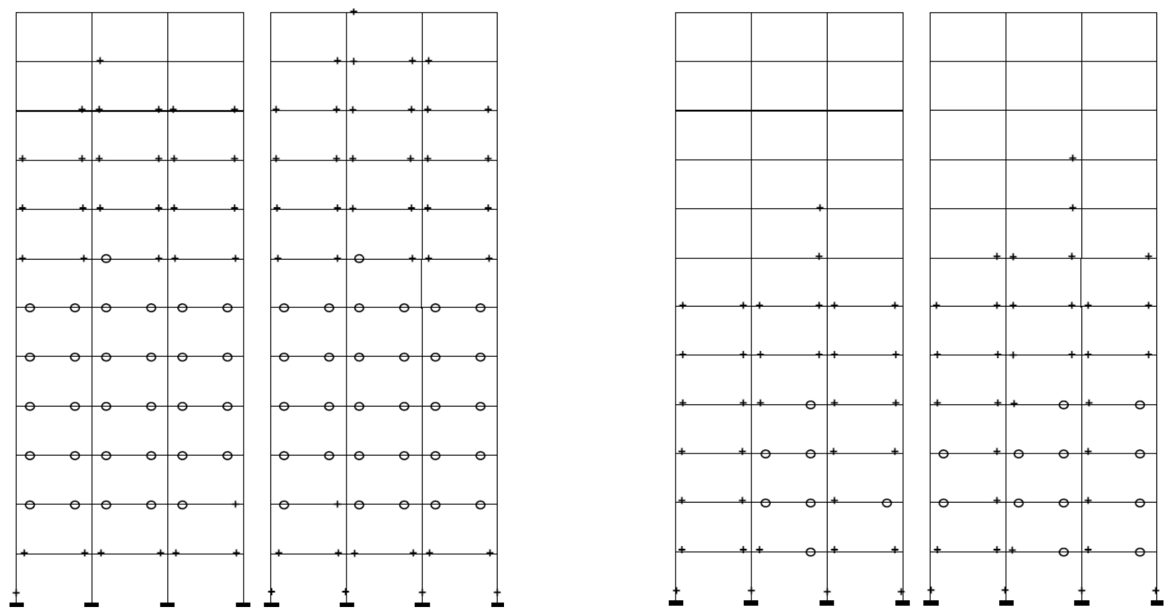

d) Modal Pushover Analysis

e) Dynamic Pull Analysis

Figure 4.21 : Plastic hinge distribution in the twelve storey frame under Erzincan-EW ground motion

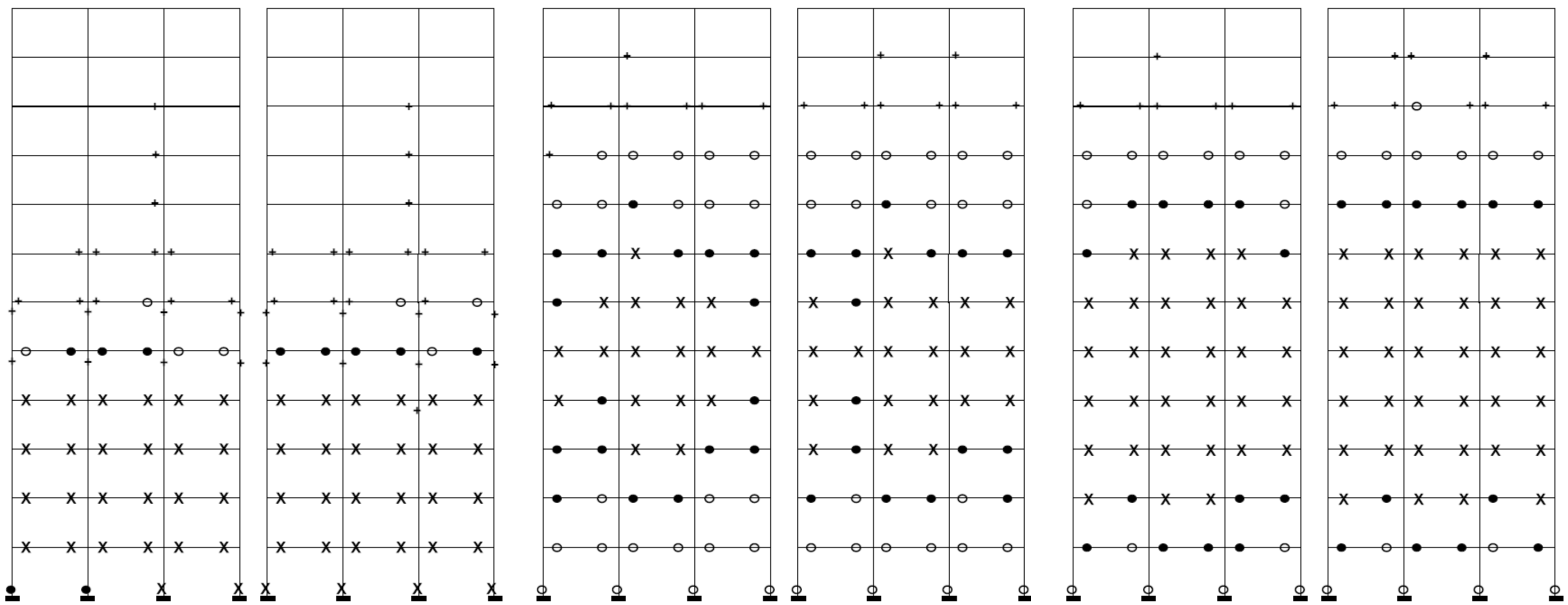

a) Nonlinear Time History b) FEMA-356 c) Constant Ductility Spectrum

Figure 4.22 : Plastic hinge distribution in the twelve storey frame under Rinaldi-228^{o} ground motion

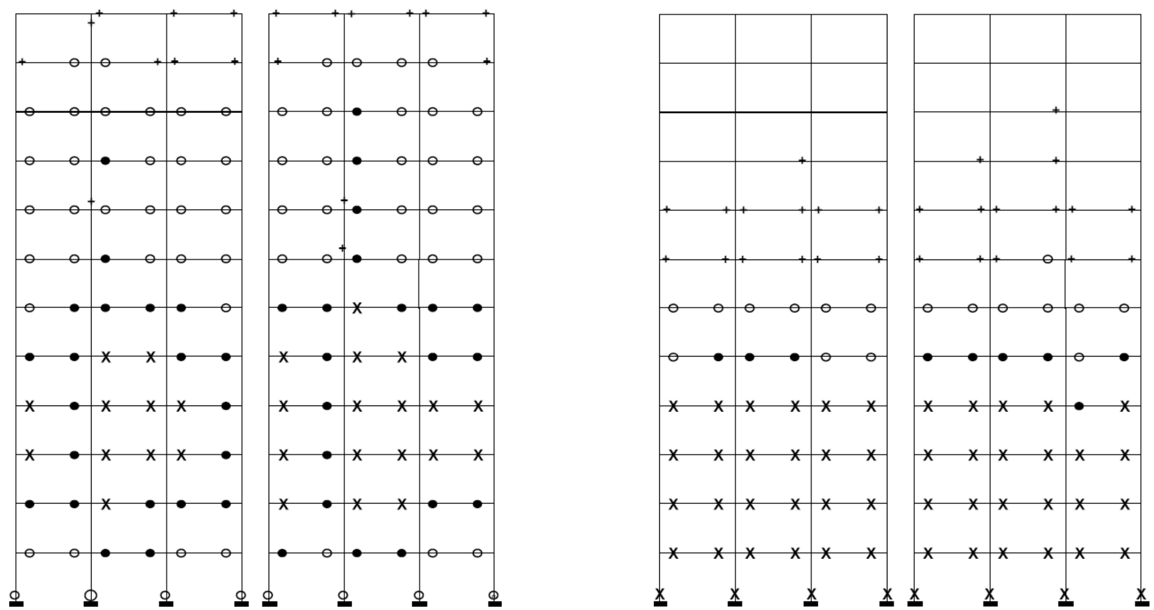

d) Modal Pushover Analysis

e) Dynamic Pull Analysis

Figure 4.23 : Plastic hinge distribution in the six storey frame under Rinaldi-228^{o} ground motion

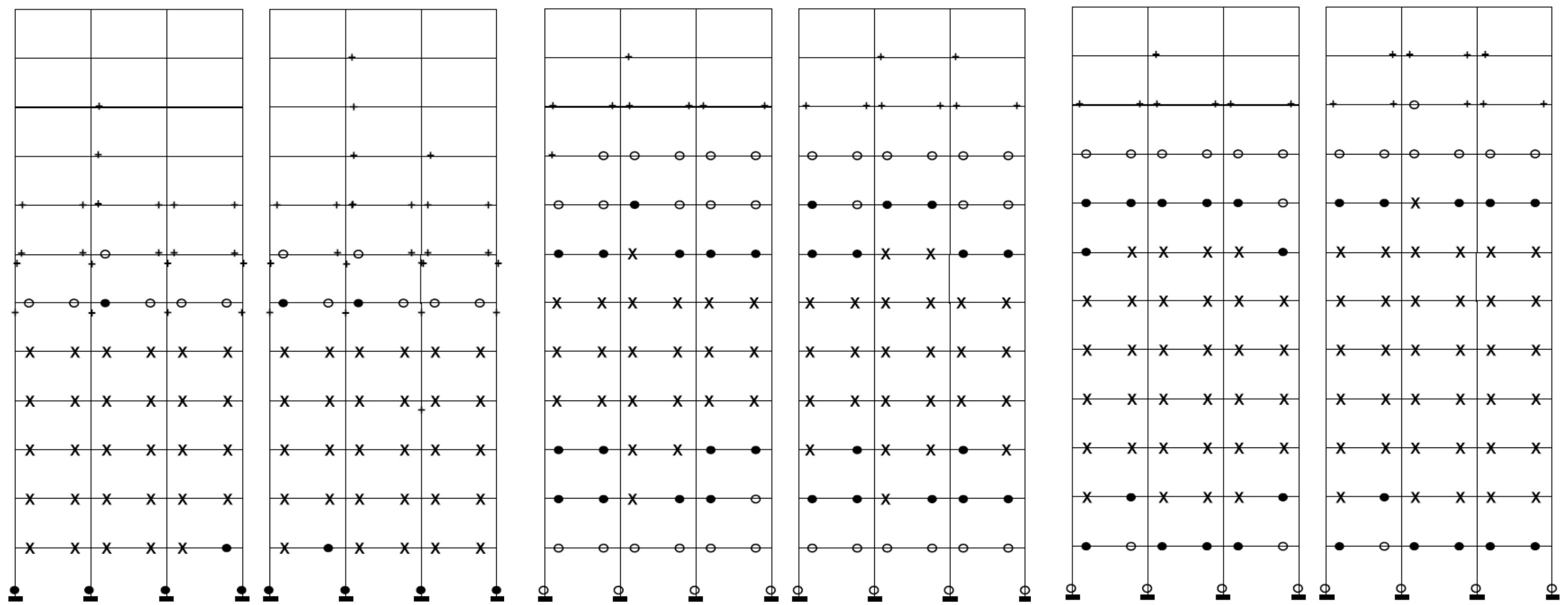

a) Nonlinear Time History b) FEMA-356 c) Constant Ductility Spectrum

Figure 4.24 : Plastic hinge distribution in the twelve storey frame under Sylmar-52^{o} ground motion

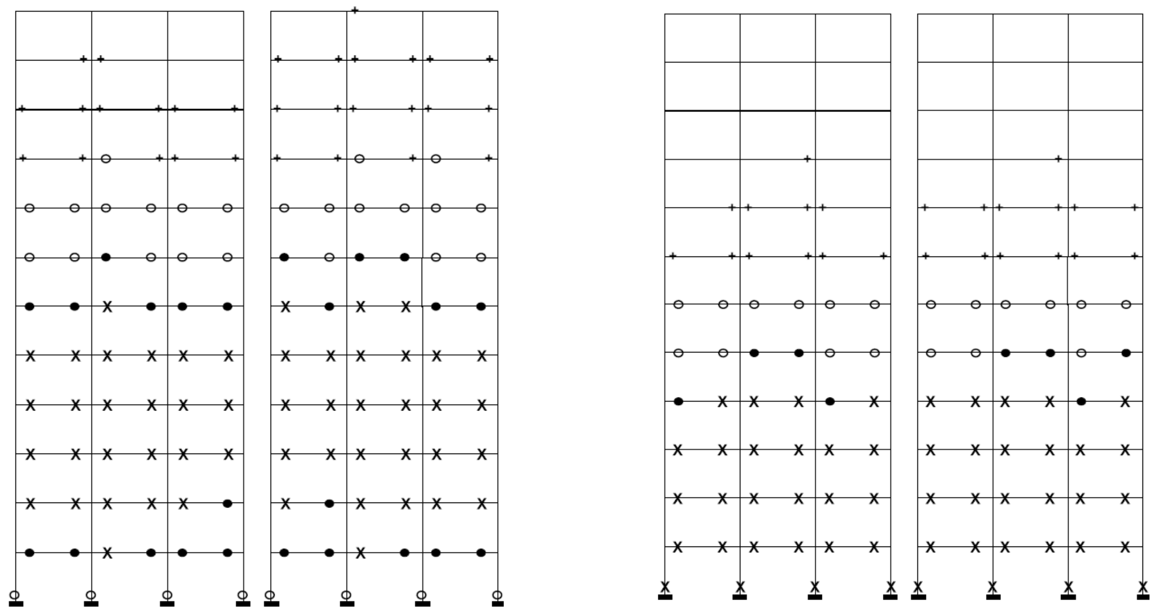

d) Modal Pushover Analysis

e) Dynamic Pull Analysis

Figure 4.25 : Plastic hinge distribution in the six storey frame under Sylmar-52^{o} ground motion

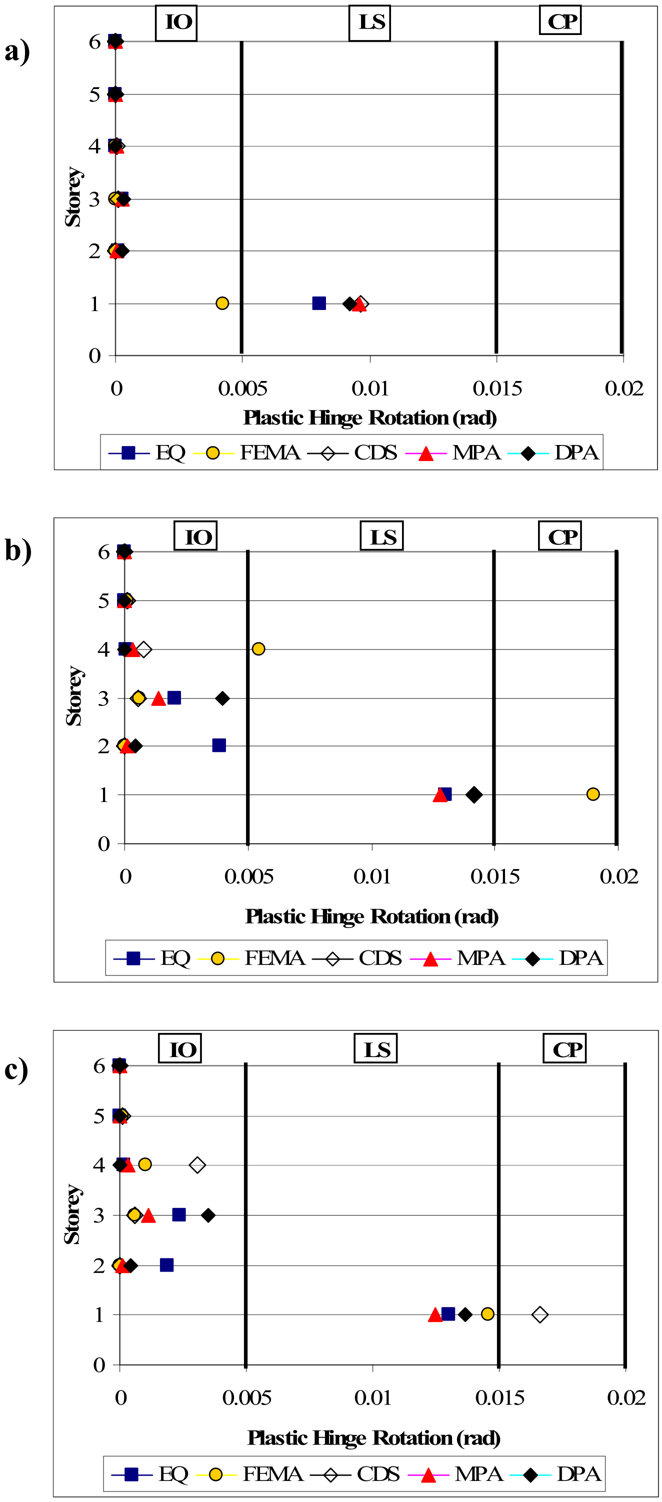

Figure 4.26 : Mean storey plastic hinge rotation results for column ends in the six-storey frame a) Erzincan-EW b) Rinaldi-228^{o} c) Sylmar-52^{o}

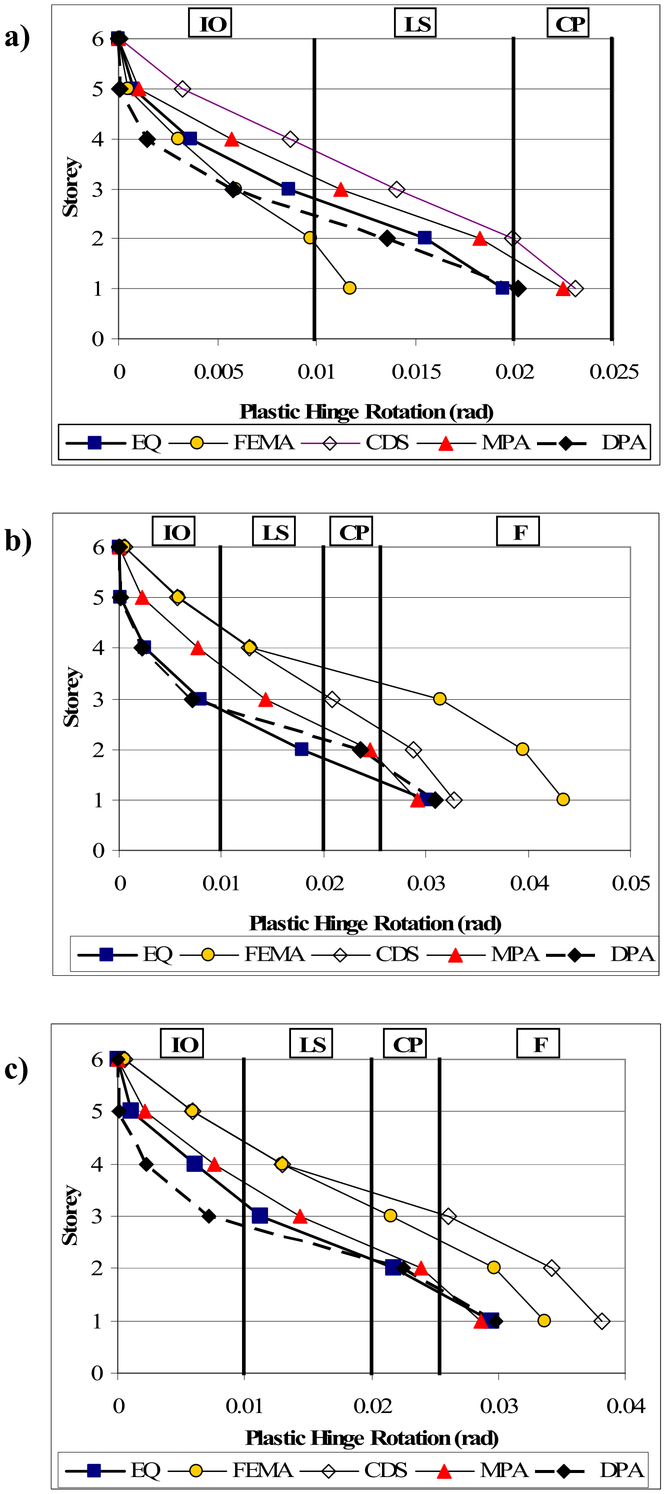

Figure 4.27 : Mean storey plastic hinge rotation results for beam ends in the six-storey frame a) Erzincan-EW b) Rinaldi-228^{o} c) Sylmar-52^{o}

a)

b)

c)

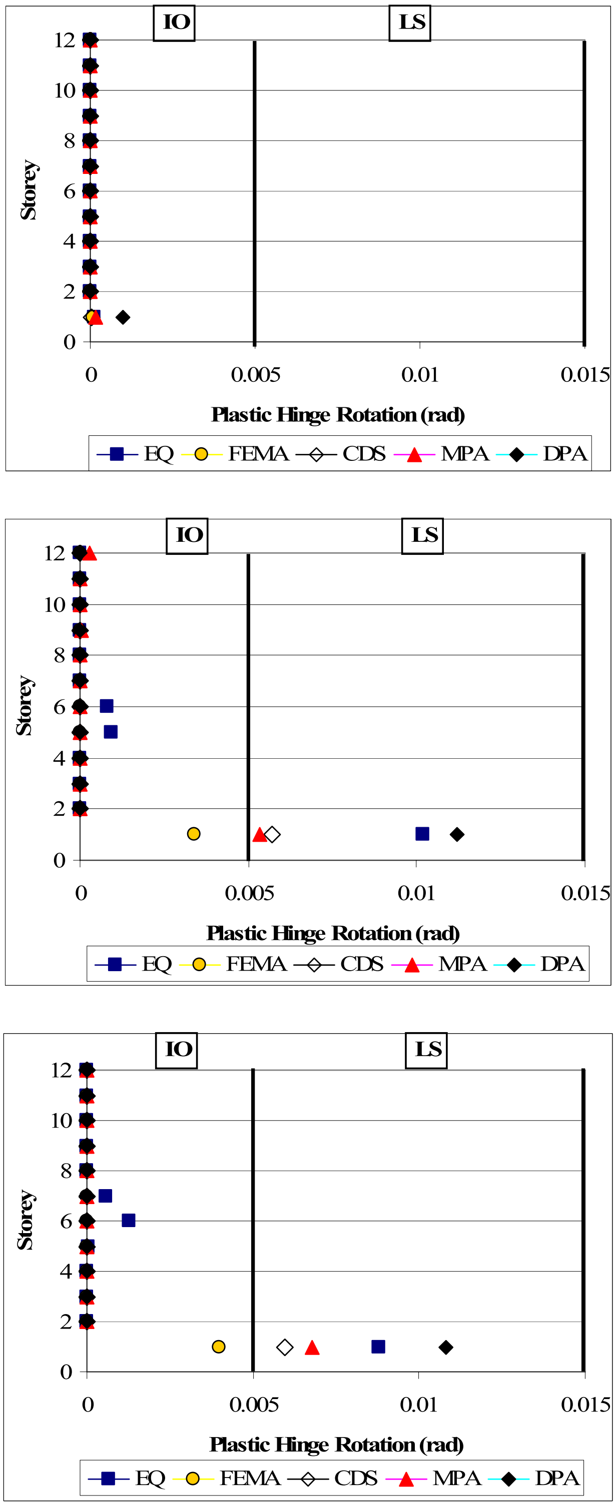

Figure 4.28 : Mean storey plastic hinge rotation results for column ends in the twelve-storey frame a) Erzincan-EW b) Rinaldi-228° c) Sylmar-52°

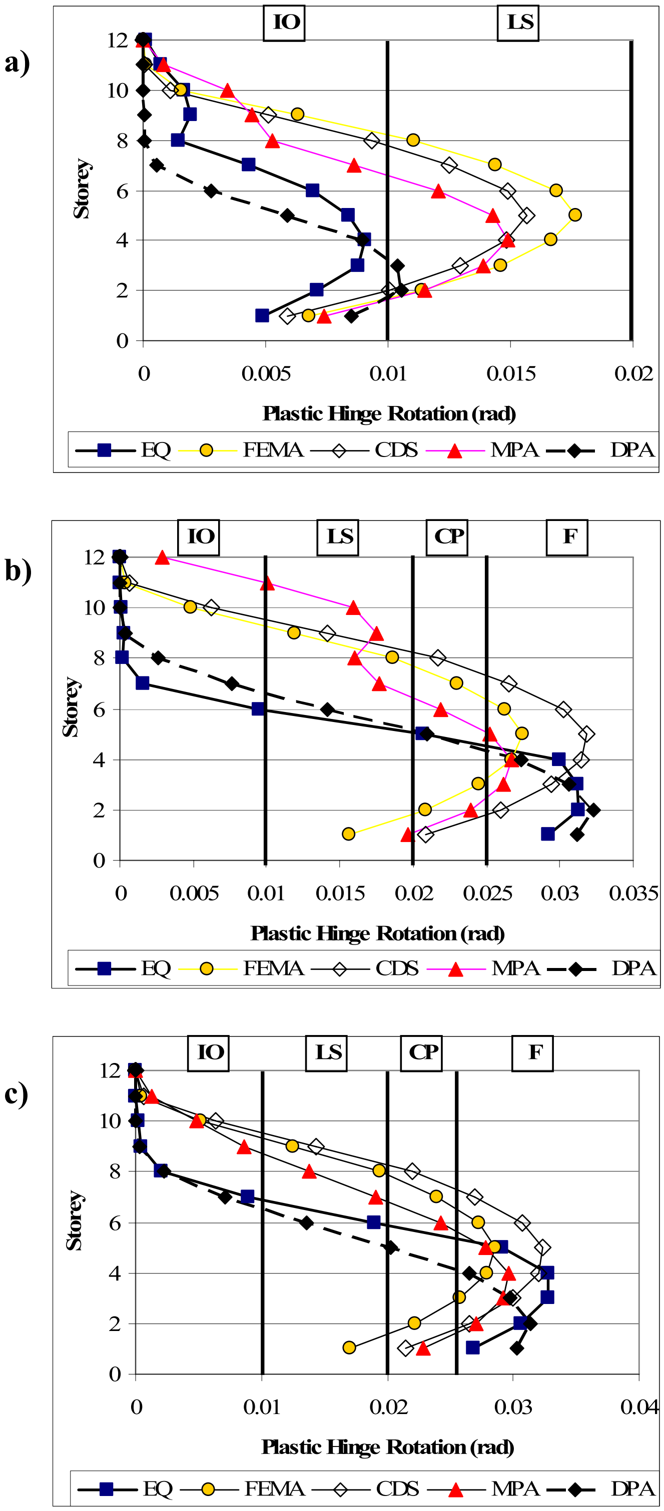

Figure 4.29 : Mean storey plastic hinge rotation results for beam ends in the twelve-storey frame a) Erzincan-EW b) Rinaldi-228° c) Sylmar-52°

CHAPTER 5

SUMMARY and CONCLUSIONS

5.1 Summary

A simple nonlinear dynamic analysis procedure called "Dynamic Pull Analysis" for estimating, the seismic response of multi degree of freedom (MDOF) systems is proposed. Proposed method employs simple inelastic dynamic analysis for calculating the seismic capacity, and a generalized SDOF system approach for calculating the seismic demand. The procedure is applied on a six-story reinforced concrete frame and a twelve-story reinforced concrete frame that were designed according to the regulations of TS-500 (2000) and TEC (1997). The results obtained from the proposed procedure were compared with the results of nonlinear static procedures, which are constant ductility spectrum method (Chopra and Goel, 1999), displacement coefficient method (FEMA-356, 2000) and modal pushover analysis (Chopra and Goel, 2001) obtained under several near-fault ground motion records that have significant velocity and acceleration pulses. These frames were also analyzed by the nonlinear time history analysis under the same ground motions, where the results are used as reference to other methods. Mainly, the deformation demand, interstory drift profiles, base shear capacity, plastic hinge patterns and plastic hinge rotations are examined in detail. Estimated displacement profiles, interstory drifts, plastic hinge rotations and patterns were used for deciding on procedure acceptability and accuracy. All nonlinear static analyses and time history analyses were conducted by using the software Drain-2DX (Allahabadi, 1987).

5.2 Conclusions

The following conclusions are derived from the results obtained in this study. In the following paragraphs, the results of this study will be briefly discussed and the conclusions of the study will be drawn. These conclusions are based on the numerical analyses and literature survey carried out in this study.

- The accuracy of predictions of DPA depend on ground motion characteristics and structural properties as well as the inherent limitations of procedure like using generalized SDOF system approximation for MDOF systems.
- Preliminary evaluations of DPA for nonlinear MDOF systems show that generalized SDOF system approximation is affected by two problems which are the selection of target displacement while obtaining idealized curve and selection of A, the slope of DPR. An iterative implementation is introduced for solving the selection of target displacement problem which affects the shape of capacity curve. In addition, it is suggested to use $A \leq 0.1$ for DPA to eliminate the effect of A on MDOF system to obtain more consistent results.
- According to target displacement predictions of nonlinear case study frames, DPA and MPA (Chopra and Goel, 2001) estimate the probable maximum roof displacements for different near fault ground motion records more accurately than the other nonlinear static procedures which are Displacement Coefficient Method

(FEMA-356, 2000) and Constant Ductility Spectrum Method (Chopra and Goel, 1999). DPA and MPA gives more closer results to exact roof displacement under specific earthquake excitation than other nonlinear static procedures because of including effects of higher mode responses to their solution strategy.

- For analyzing nonlinear MDOF systems, DPA may avoid the engineers from the problem of selecting push pattern. Because all desired response quantities can be obtained by including the entire mode effects in applying a simple acceleration pulse record, DPR.
- Observation of capacity curve plots demonstrate that DPA curve possess higher initial stiffness. Because all modes contribute to the force-deformation response of the system.
- Although proposed procedure gives more closer results to exact response quantities, it usually overestimates the storey displacement demands at lower stories whereas the other methods underestimate the same response.
- Plastic hinge pattern of DPA resembles the hinge pattern of nonlinear time history analysis very successfully. The other procedures foresee more plastic hinges especially at upper stories.
- Only the plastic hinge rotations estimated by DPA are close enough to exact response of beams and columns of the case study frames, compared to all nonlinear static procedures. It should be noted that the basic response parameter in nonlinear seismic assessment is plastic rotation.

5.3 Future Studies

In this study, only two reinforced structure frames and a limited number of strong ground motion records were used. A parametric study containing a larger number of frames with a large number of fundamental periods under a wider set of ground motions will show the accuracy of method better. In addition, validity and applicability of the proposed method is tested on 2-D frames. For this reason, the idea developed through the thesis work may be extended to 3-D. Implementation of the developed procedure on a computer software can be very useful, since it would enable the processing of the DPA procedure in a much shorter time.

REFERENCES

Alavi B., Krawinkler H., 2001, “Effects of Near-Fault Ground Motions on Frame Structures”, Report No.138, John A. Blume Earthquake Engineering Center, Stanford University

Alavi B., Krawinkler H., 2004, “Strengthening of Moment-Resisting Frame Structures Against Near-Fault Ground Motion Effects”, Earthquake Engineering and Structural Dynamics, Vol.33, pp. 707 - 722

Allahabadi R. 1987, “Drain-2DX – Seismic Response and Damage Assessment for 2D structures”, Ph.D. Thesis, University of California at Berkeley, California.

Antoniou S., Pinho P., 2004, “Advantages and Limitations of Adaptive and Non-Adaptive Force-Based Pushover Procedures”, Journal of Earthquake Engineering, Vol.8, No.4, pp. 497 - 522

Applied Technology Council, ATC-19, 1995, “Structural Response Modification Factors”, Redwood City, California.

Applied Technology Council, ATC-40, 1996, “Seismic Evaluation and Retrofit of Concrete Buildings”, Volume 1-2, Redwood City, California

Aydinoglu N.M., and Kacmaz, U., 2002, "Strength Based Displacement Amplification Spectra For Inelastic Seismic Performance Evaluation", Department of Earthquake Engineering Report, No. 2002/2, Kandilli Observatory and Earthquake Research Institute, Bogazici University, Istanbul, Turkey, 32 pages.

Aydinoğlu, N.M., 2003, "An Incremental Response Spectrum Analysis Procedure Based on Inelastic Spectral Displacements for Multi-Mode Seismic Performance Evaluation,", Bulletin of Earthquake Engineering, Vol. 1, Kluwer Academic Publishers, pp.3-36.

.Biggs J., 1964, "Introduction to Structural Dynamics", McGraw-Hill, Inc., New York

Bracci J.M., Kunnath S.K. and Reinhorn A.M., 1997, "Seismic Performance and Retrofit Evaluation of Reinforced Concrete Structures", Journal of Structural Engineering, ASCE, Vol. 123, pp. 3-10.

Chintanapakdee C. and Chopra A.K., 2003, "Evaluation of Modal Pushover Analysis Using Generic Frames", Earthquake Engineering and Structural Dynamics, Vol. 32, pp. 417-442.

Chopra A.K., 1995, "Dynamics of Structures-Theory and Application to Earthquake Engineering", Prentice Hall, New Jersey.

Chopra A.K. and Goel R.K., "Capacity – Demand Diagram Methods for Estimating Seismic Deformation of Inelastic Structures: SDOF Systems", PEER Report 1999/02, Pacific Earthquake Engineering Research Center, University of California, Berkeley.

Chopra A.K. and Goel R.K., "A Modal Pushover Analysis Procedure to Estimating Seismic Demands for Buildings: Theory and Preliminary Evaluation", PEER Report 2001/03, Pacific Earthquake Engineering Research Center, University of California, Berkeley.

Chopra, A.K., and Chintanapakdee, C., 2004, "Inelastic deformation ratios for design and evaluation of structures: single-degree-of-freedom bilinear systems," Journal of Structural Engineering., Vol. 130, No. 9, American Society of Civil Engineers, Reston, Virginia, pp. 1309-1319.

Clough R.W., Johnston S.B., 1996, "Effect of Stiffness Degradation on Earthquake Ductility Requirements", Proceedings of Japan Earthquake Engineering Symposium, Tokyo, Japan, pp. 227-231

Elanshai A.S., 2001, "Advanced Inelastic Static (Pushover) Analysis Procedure for Earthquake Applications", Structural Engineering and Structural Dynamics, 12(1),pp. 51-69.

Ersoy U., 1997, "Reinforced Concrete", Middle East Technical University, Ankara, Turkey.

Fajfar P. and Fischinger M., 1987, “Nonlinear Seismic Analysis of RC Buildings: Implications of a Case Study”, European Earthquake Engineering, pp. 31-43.

Fajfar P. and Gaspersic P., 1996, “The N2 Method for the Seismic Damage Analysis of RC Buildings”, Earthquake Engineering and Structural Dynamics, Vol. 25, pp. 31-46.

Federal Emergency Management Agency (FEMA), 1997, “NEHRP Guidelines for the Seismic Rehabilitation of Buildings”, FEMA-273.

Federal Emergency Management Agency (FEMA), 2000, “Prestandard and Commentary for the Seismic Rehabilitation of Buildings”, FEMA-356.

Freeman S.A., 1998, “Development and Use of Capacity Spectrum Method”, Proceedings of the Sixth U.S. National Conference on Earthquake Engineering, Seattle, Washington.

Goel R.K. and Chopra, A.K., 2005, “Extension of Modal Pushover Analysis to Compute Member Forces”, Earthquake Spectra., Vol. 21, No. 1, Earthquake Engineering Research Institute, Oakland, California, pp. 125-139

Gupta B., 1999, “Enhanced Pushover Procedure and Inelastic Demand Estimation for Performance-Based Seismic Evaluation of Buildings”, Ph.D. Dissertation, University of Central Florida, Orlando, FL.

Gülkan P. and Sozen M.A., 1974, "Inelastic Responses of Reinforced Concrete Structures to Earthquake Motions", Journal of the American Concrete Institute, Vol. 71, pp. 604-610.

İnel M., Tjhin T. and Aschheim A.M., 2003, "The Significance of Lateral Load Pattern in Pushover Analysis", İstanbul Fifth National Conference on Earthquake Engineering, Paper No: AE-009, İstanbul, Turkey.

Jacobsen L.S., 1960, "Damping in Composite Structures.", Proceedings of the Second World Conference on Earthquake Engineering, Vol.2, pp 1029 – 1044, Tokyo & Kyoto, Japan.

Jan T.S., Liu M.W. and Kao Y.C., 2004, "An Upper-Bound Pushover Analysis Procedure for Estimating the Seismic Demands of High-Rise Buildings", Engineering Structures, Vol. 26, pp. 117-128.

Krawinkler H. and Seneviratna G.D.P.K., 1998, "Pros and Cons of a Pushover Analysis of Seismic Performance Evaluation", Engineering Structures, Vol.20, pp. 452-464.

Lawson R.S., Reinhorn A.M. and Lobo R.F., 1994, "Nonlinear Static Pushover Analysis - Why, When and How?", Proceedings of the 5th US National Conference on Earthquake Engineering, Chicago, Vol. 1, pp. 283-292.

Mahaney J.A., Paret T.F., Kehoe B.E. and Freeman S.A., 1993, “The Capacity Spectrum Method for Evaluating Structural Response During Loma Prieta Earthquake”, 1993 National earthquake Conference, Memphis, TN

Mander, J.B., Priestley, M.J.N., Park, R. 1988, “Theoretical Stress-Strain Model for Confined Concrete”, Journal of Structural Division (ASCE), 114(8), 1804-1826.

Mahmoud M. and Hachem, P.E., 2004, “BISPEC: Interactive Software for the Computation of Unidirectional and Bidirectional Nonlinear Earthquake Spectra” [online]. Available from URL: http://www.ce.berkeley.edu/~hachem/bispec

Miranda E., 2000, “Inelastic Displacement Ratios for Structures on Firm Sites”, Journal of Structural Engineering, Vol. 126, pp. 1150-1159.

Miranda E. and Ruiz-García J., 2002,” Evaluation of Approximate Methods to Estimate Maximum Inelastic Displacement Demands”, Earthquake Engineering and Structural Dynamics, Vol. 31, pp. 539-560.

Mwafy A.M. and Elnashai A.S., 2001, “Static Pushover versus Dynamic Analysis of R/C Buildings”, Engineering Structures, Vol. 23, pp. 407-424.

Nassar A.A. and Krawinkler H., 1991, “Seismic Demands for SDOF and MDOF Systems”, Report No.95, John A. Blume Earthquake Engineering Center, Stanford University.

Newmark N.M. and Hall W.J., 1982, “Earthquake Spectra and Design”, Earthquake Engineering Research Institute, Berkeley, CA.

Nonlinear Dynamic Time History Analysis of Single Degree of Freedom Systems (NONLIN), developed by Dr. Finley A. Charney, Advanced Structural Concepts, Golden, Colorado and Schnabel Engineering, Denver, Colorado.

Paret T.F., Sasaki K., Eilbeck D.H., Freeman S.A., 1996, “Approximate Inelastıc Procedures to Identify Failure Mechanisms From Higher Mode Effect”, Eleventh World Conference on Earthquake Engineering, Paper No. 966 Acapulco, Mexico

PEER (2005) Documentation on the New Generation Attenuation (NGA) Project. http://peer.berkeley.edu/lifelines/nga.html and http://peer.berkeley.edu/nga/index.html

Prakash V., Powell G.H., 1992, “Drain-2DX, Version 1.02, User Guide”, Department of Civil Engineering, University of California, Berkeley, California.

Prakash V., Powell G.H., Campbell S., 1993, “Drain-2DX Base Program Description and User Guide Version 1.10”, Department of Civil Engineering, University of California, Berkeley, California.

Ramirez, O. M., Constantinou, M. C., Whittaker, A. S., Kircher, C. A., Johnson, M. W., and Chrysostomou, C. Z., 2003, “Validation of the 2000 NEHRP Provisions' equivalent lateral force and modal analysis procedures for buildings with damping systems", Earthquake Spectra, Vol. 19, No. 4, Earthquake Engineering Research Institute, Oakland, California, pp. 981-999

Rodrigez-Marek A., "Near fault site response", Ph.D. thesis, Department of Civil and Environmental Engineering, University of California, Berkeley, Fall 2000

Rosenblueth E. and Herrera I., 1964, "On a Kind of Hysteretic Damping", Journal of Engineering Mechanics Division ASCE; 90, pp.37-48.

Ruiz-Garcia, J., and Miranda, E., 2003, "Inelastic displacement ratios for evaluation of existing structures," Earthquake Engineering & Structural Dynamics, Vol. 32, No. 8, pp. 1237-1258

Sasaki F., Freeman S. and Paret T., 1998, "Multi-Mode Pushover Procedure (MMP)-A Method to Identify the Effect of Higher Modes in a Pushover Analysis", Proc. 6th U.S. National Conference on Earthquake Engineering, Seattle, CD-ROM, EERI, Oakland.

Somerville P., Smith N., Graves R, and Abrahamson N., 1997, "Modification of Empirical Strong Ground Motion Attenuation Relations to Include the Amplitude and Duration Effects of Rapture Directivity", Seismological Research Letters, Vol. 68, No.1, pp. 180-203

Somerville P., 1998, "Development of an Improved Ground Motion Representation for Near Fault Ground Motions", SMIP98 Seminar on Utilization of Strong-Motion Data, Oakland, CA, SeismoSoft, 2004, SeismoSignal A computer program for signal processing of strong motion data" [online]. Available from URL: http://www.seismosoft.com.

Shibata A. and Sozen M.A., 1976, “Substitute-Structure Method for Seismic Design in RC”, Journal of the Structural Division, ASCE, Vol.102, pp. 1-17.

Takeda T., Sözen M.A. and Nielson N.N., 1970, “Reinforced Concrete Response to Simulated Earthquakes”, Journal of Structural Division, ASCE, Vol. 96, pp. 2557-2573.

Turkish Earthquake Code: Specifications for the Buildings to be constructed in Disaster Areas, 1998, Ministry of Public Works and Settlement, Ankara, Turkey.

Turkish Standard Institute, 2000, “TS-500 Requirements for Design and Construction of Reinforced Concrete Structures”.

Vamvatsikos D., Conell C.A., 2002, “Incremental Dynamic Analysis”, Earthquake Engineering and Structural Dynamics, 31(3), pp. 491-514

Velestos A. , Newmark N. and Chelapati C., 1965 , “Deformation Spectra for Elastic and Elastoplastic System Subject to Ground Shock and Earthquake Motions”, Proceeding, Third World Conference on Earthquake Engineering, Vol2, New Zealand

Vidic, T., Fajfar, P. and Fischinger, M., 1994, “Consistent Inelastic Design Spectra: Strength and Displacement, Earthquake” Engineering and Structural Dynamics, 23(5), pp. 507-521.

Wilson E. L., Farhoomad I., Bathe K.J., 1973, “Nonlinear Dynamic Analysis of Complex Structures”, Earthquake Engineering and Structural Dynamics, Vol 1, pp. 241-252.

APPENDIX A

BILINEARIZATION PROCESS OF FEMA-273

In Appendix A, a simple procedure which is proposed by Chopra and Goel (2001) is explained step by step for obtaining bilinear capacity curve.

1. Apply force distribution incrementally and record the base shears and associated roof displacements. System should push beyond the target roof displacement in the selected mode.
2. Define the anchor point, B, of the bilinear curve at the target roof displacement u_{rno} and V_{bno} are the base shear at point B
3. By using any type of integration method, calculate the area under the actual pushover curve, A_{pn}
4. Estimate the yield base shear, V^{i}_{bny}
5. According to FEMA-273 procedure, calculate the initial slope, k^{i}_{n} and u^{i}_{rny} of idealize curve by connecting a straight line between point O and point $V_{bny,0.6}$ which gives the secant stiffness at the base shear equals to 60% of the yield base shear

$$k_n^i = \frac{0.6 \cdot V_{bny}^i}{u_{rn,0.6}^i} \tag{A.1}$$

$$u^i_{rny} = \frac{V^i_{bny}}{k^i_n} \tag{A.2}$$

6. Draw the curve OAB by connecting the three points, O, A, B with straight line segments to obtain idealized bilinear curve

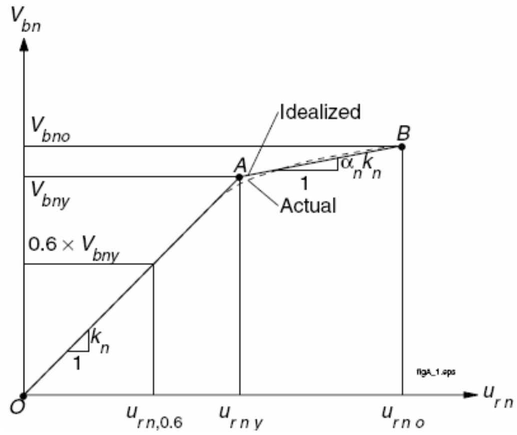

Figure A.1: Idealization of pushover curve

Calculate the post yielding strain-hardening ratio, α^i_n

$$\alpha^i_n = \frac{(V_{bno} - V^i_{bny}) - 1}{(u_{bno} - u^i_{bny}) - 1} \tag{A.3}$$

7. Calculate area under new bilinearized curve, OAB, A^i_{bn}

$$\alpha^i_n = \frac{(V_{bno} - V^i_{bny}) - 1}{(u_{bno} - u^i_{bny}) - 1} \tag{A.4}$$

8. Calculate error, E;

$$E = \frac{(A^i_{bn} - A_{pn})}{A_{pn}} \cdot 100 \tag{A.5}$$

9. If error does not exceed some pre-specified tolerance, bilinearized curve is acceptable, if not iterations are necessary.

If not calculate,

$$V_{bny}^{i+1} = V_{bny}^{i} \cdot \left(\frac{A_{pn}}{A_{bn}^{i}}\right) \tag{A.6}$$

10. And replace i+1 with i, recalculate steps 5 to 10

APPENDIX B

MODELLING WITH DRAIN-2DX

B.1 Modelling with Drain-2DX

In this study for the modelling purpose, DRAIN-2DX (Allahabadi, 1987) which is a general-purpose computer program for static and dynamic analysis of inelastic plane structures is used. By the help of this program nonlinear static and nonlinear time history analyses can be performed. Mode shapes and periods can be calculated for any stressed state of structure. Linear response spectrum analyses can also be performed for the unstressed state.

DRAIN-2DX contains six types of frame element models. The description of element models is as follows (Powel, 1993):

Type 01: Truss Element to model truss bars, simple columns and nonlinear support springs

Type 02: Beam-Column Element to model beams and beam-columns of steel and reinforced concrete type by using lumped plasticity approach.

Type 04: Simple Inelastic Connection Element to model structural connections with rotational and/or translational flexibility

Type 06: Elastic panel element to model only elastic behavior of rectangular panels with extensional, bending and/or shear stiffness.

Type 09: Link Element to model inelastic bar element with initial gap or axial force.

Type 15: Fiber Beam-Column Element to model inelastic steel, reinforced concrete and composite steel-concrete members.

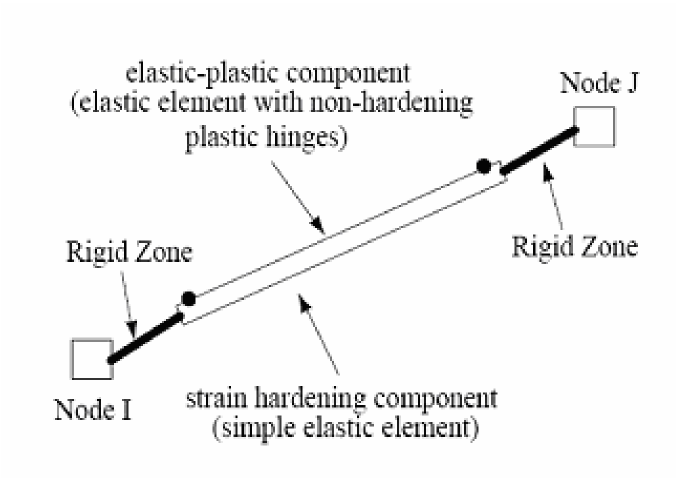

Figure B.1 : Geometry of "Type 02" Element (Allahabadi, 1987)

For modelling the inelastic components of case studies, “Type 2” element is used. According to user manual of program (Prakash et al 1993), "Type 02" element consists of an elastic member with two rigid plastic hinges that are defined at member ends and rigid end zones (Figure B.1). These hinges represent nonlinear behaviour of members in other words; all nonlinearity is concentrated on these member end plastic hinges. For beams, member specific bilinear moment-curvature relationships (Figure B.2) for both positive and negative bending must be defined. For columns besides bending relationship, member specific interaction diagrams that are composed of a series of straight-line segments to idealized form of smooth interaction diagrams must be defined**.** (Figure B.3) The behavior in shear is assumed to be elastic and it is not possible to consider nonlinear shear effects. That means all nonlinear calculations are carried by using moment values on members. In addition, inelastic axial force effect neglected.

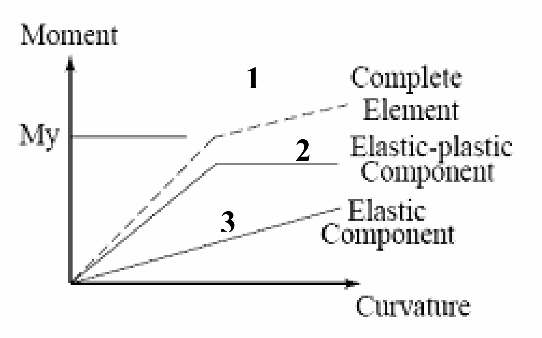

Figure B.2 : Moment-Curvature Relationship of "Type 02" Element (Allahabadi, 1987)

For defining the structural system in DRAIN-2DX, a formatted input file must be filled. This file contains geometry, mass distribution, strength, stiffness and loading data of the structure and appropriate inelastic parameters that are interaction diagram and moment curvature diagram of structural members. After preparing the input file, just adding the simple commands end of file, any type of analysis like pushover analysis, nonlinear time history analysis, eigenvalues analysis etc. can be conducted. However, it is suggested that especially before starting any type of nonlinear analysis, gravity analysis must be carried to obtain more realistic results. In this segment of analysis, only defined gravity loads are applied to system. Moreover, for an analysis option, geometric nonlinearity can be considered through P-delta effects by adding a geometric stiffness matrix to the stiffness matrix of each element. The geometric stiffness matrix is changed at each event in a pushover analysis and time history analyses. Nevertheless, in this study, this second order effect is not considered thorough the analysis of case study frames. More detailed explanation about preparing input file and element descriptions can be found in user manual (Prakash et al 1993).

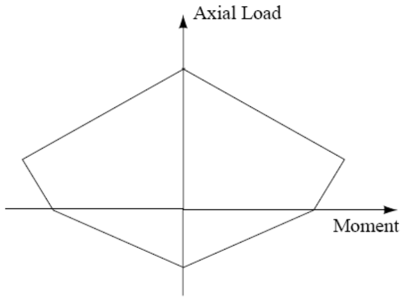

Figure B.3 : Reinforced Concrete Column Interaction Diagrams of Columns for "Type 02" Element (Allahabadi, 1987)

The program performs the pushover analysis and time history analysis after the analysis phase called the “Gravity” analysis. In the “Gravity” analysis, the structure is analyzed under the gravity forces only. The program does not continue for the pushover analysis if plastic hinges occur during the “Gravity” analysis.

B.2 Plastic Hinge Calculation in Drain-2DX

In deformation-controlled pushover that is used in study and nonlinear time history analysis is used in this study if flexural yielding occurs inside a step or at the end of a step, the stiffness matrix has to be modified. The program only considers yielding at the element ends due to flexure.

B.2.1 Modification of Stiffness Matrix

The local stiffness matrix for a prismatic element with the degrees of freedom is illustrated in Figure B.4.

$$
\begin{pmatrix}
E\cdot\frac{A}{L} & 0 & 0 & -E\cdot\frac{A}{L} & 0 & 0 \\
0 & 12\cdot E\cdot\frac{I}{L^3} & 6\cdot E\cdot\frac{I}{L^2} & 0 & -12\cdot E\cdot\frac{I}{L^3} & 6\cdot E\cdot\frac{I}{L^2} \\
0 & 6\cdot E\cdot\frac{I}{L^2} & 4\cdot E\cdot\frac{I}{L} & 0 & -6\cdot E\cdot\frac{I}{L^2} & 2\cdot E\cdot\frac{I}{L} \\
-E\cdot\frac{A}{L} & 0 & 0 & E\cdot\frac{A}{L} & 0 & 0 \\
0 & -12\cdot E\cdot\frac{I}{L^3} & -6\cdot E\cdot\frac{I}{L^2} & 0 & 12\cdot E\cdot\frac{I}{L^3} & -6\cdot E\cdot\frac{I}{L^2} \\
0 & 6\cdot E\cdot\frac{I}{L^2} & 2\cdot E\cdot\frac{I}{L} & 0 & -6\cdot E\cdot\frac{I}{L^2} & 4\cdot E\cdot\frac{I}{L}
\end{pmatrix}
$$

Figure B.4 : Local degrees of freedom for a prismatic beam-column element

Drain 2DX is capable of making pushover analysis of structures composed of elements with bilinear moment curvature relationship (Prakash et al., 1992, Prakash et al., 1993).

In Figure B.2, line 1 is the moment curvature relation of the element. At this stage, an assumption is made and the moment curvature relation (1) is decomposed into components (2) and (3). After flexural yielding occurs at an element end; considering only component 2, the stiffness matrix of the element is reduced to a 5*5 matrix using the fact that the yielding end cannot carry moment any longer. 5*5 matrix is completed by adding a row and column of 0's for the yielding degree of freedom and modified 6*6 matrix for component 2 is formed. The modified 6*6 matrices for elements with only I end yielding and with only J end yielding are shown in Figure B.5 (a) and (b) respectively. For component 3, the local stiffness matrix is formed using the EI value as the slope of line 3 (this value is input to the program as strain hardening ratio). The two stiffness matrices are added to calculate the final local stiffness matrix of the yielding element.

If both ends of an element yield; for component 2 the stiffness matrix is reduced to a 4*4 matrix using the fact that both ends can not carry moments any longer; 2 rows and columns of 0's are added to the 4*4 matrix to form the modified stiffness matrix. The stiffness matrix of the element becomes the stiffness matrix of a truss element; it is shown in Figure B.6. For component 3, the local stiffness matrix is formed using the EI value as the slope of line 3. The two stiffness matrices are added to calculate the final local stiffness matrix of the yielding element.

$$\begin{pmatrix} E\cdot\frac{A}{L} & 0 & 0 & -E\cdot\frac{A}{L} & 0 & 0 \\ 0 & 3\cdot E\cdot\frac{I}{L^3} & 0 & 0 & -3\cdot E\cdot\frac{I}{L^3} & 3\cdot E\cdot\frac{I}{L^2} \\ 0 & 0 & 0 & 0 & 0 & 0 \\ -E\cdot\frac{A}{L} & 0 & 0 & E\cdot\frac{A}{L} & 0 & 0 \\ 0 & -3\cdot E\cdot\frac{I}{L^3} & 0 & 0 & 3\cdot E\cdot\frac{I}{L^3} & -3\cdot E\cdot\frac{I}{L^2} \\ 0 & 3\cdot E\cdot\frac{I}{L^2} & 0 & 0 & -3\cdot E\cdot\frac{I}{L^2} & 3\cdot E\cdot\frac{I}{L} \end{pmatrix}$$

a)

$$\begin{pmatrix} E\cdot\frac{A}{L} & 0 & 0 & -E\cdot\frac{A}{L} & 0 & 0 \\ 0 & 3\cdot E\cdot\frac{I}{L^3} & 3\cdot E\cdot\frac{I}{L^2} & 0 & -3\cdot E\cdot\frac{I}{L^3} & 0 \\ 0 & 3\cdot E\cdot\frac{I}{L^2} & 3\cdot E\cdot\frac{I}{L} & 0 & -3\cdot E\cdot\frac{I}{L^2} & 0 \\ -E\cdot\frac{A}{L} & 0 & 0 & E\cdot\frac{A}{L} & 0 & 0 \\ 0 & -3\cdot E\cdot\frac{I}{L^3} & -3\cdot E\cdot\frac{I}{L^2} & 0 & 3\cdot E\cdot\frac{I}{L^3} & 0 \\ 0 & 0 & 0 & 0 & 0 & 0 \end{pmatrix}$$

b)

Figure B.5 : The stiffness matrices for an element that flexural yielding occurs a) at End I, b) at End J with the degrees of freedom in Figure B.1

The new local stiffness matrices for the elements are used to form the global stiffness matrices of the elements and the global stiffness matrices are assembled to form the new stiffness matrix of the structure, and the new stiffness matrix is used in the next step (if hinging occurs inside a step, in the rest of the step).

$$\begin{pmatrix} E\cdot\frac{A}{L} & 0 & 0 & -E\cdot\frac{A}{L} & 0 & 0 \\ 0 & 0 & 0 & 0 & 0 & 0 \\ 0 & 0 & 0 & 0 & 0 & 0 \\ -E\cdot\frac{A}{L} & 0 & 0 & E\cdot\frac{A}{L} & 0 & 0 \\ 0 & 0 & 0 & 0 & 0 & 0 \\ 0 & 0 & 0 & 0 & 0 & 0 \end{pmatrix}$$

Figure B.6 : The stiffness matrix for an element whose ends yield in flexure

B.2.2 Calculation of Plastic Rotations In Case Only One End Yields

The slope deflection equation for the I end of a prismatic element (Figure B.7) is

$$M_I = \frac{2\cdot E\cdot I}{L}\cdot(2\cdot\theta_I + \theta_J + \frac{3\cdot\Delta}{L}) \qquad \text{(B.1)}$$

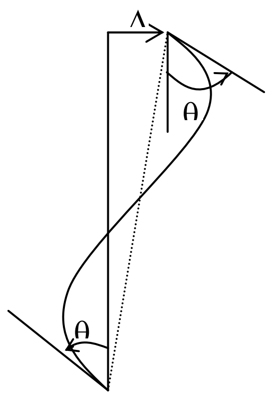

Figure B.7 : Deformation of a prismatic element used in slope deflection equation

Considering component 2 of the moment curvature relation in Figure B.2, M_I stays constant after yielding (M_I=0 for the inelastic range). Equating M_I to 0;

$$\theta_I = -\frac{\theta_J}{2} - \frac{3 \cdot \Delta}{2 \cdot L} \quad \text{(B.2)}$$

In EqB.2, θ_I is the rotation of the plastic hinge about the joint (Figure B.8); the minus sign at the right hand side indicates that the rotation is clockwise. In addition, the joint itself makes a rotation (component 3 contributes to that rotation). Plastic rotation is equal to the sum of these rotations (Figure B.8). Plastic rotation in one step of the pushover analysis is equal to

$$\theta_I + \frac{\Delta}{L} + \frac{1}{2} \cdot (\theta_J + \frac{\Delta}{L}) \quad \text{(B.3)}$$

Here, θ_I and θ_J are the increments of the joint rotations at the I and J ends of the element respectively, and Δ is the increment in lateral displacement between the J and I ends of the element (Figure B.6).

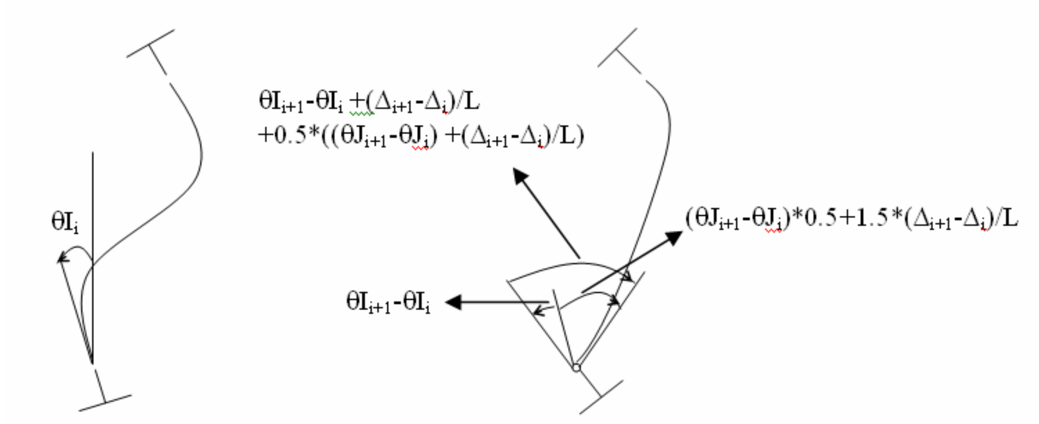

Deformed shape at step i (no yielding) | Deformed shape at step i+1 (yielding at end I)

Figure B.8 : Calculation of plastic rotations in case only one end yields

B.2.3 Calculation of Plastic Rotations In Case Both Ends Yields

The slope deflection equations for the I and J ends of a prismatic element is

$$M_I = \frac{2 \cdot E \cdot I}{L} \cdot (2 \cdot \theta_I + \theta_J + \frac{3 \cdot \Delta}{L}) \tag{B.4}$$

$$M_J = \frac{2 \cdot E \cdot I}{L} \cdot (2 \cdot \theta_J + \theta_I + \frac{3 \cdot \Delta}{L}) \tag{B.5}$$

Considering component 2 of the moment curvature relation; compatibility requires θ_I to be equal to θ_J, since the element will remain straight.

Equating M_I and M_J to 0, $\theta_I = \theta_J = -\Delta/L$ (minus sign indicates that the rotation is clockwise). This is the rotation of the plastic hinge about the joint (Figure B.7). In addition, the joint itself makes a rotation (component 3 contributes to that rotation). Plastic rotation is equal to the sum of these rotations (Figure B.9).

Plastic rotation in one step of the pushover analysis at the I end is;

$$\theta_I + \frac{\Delta}{L} \tag{B.6}$$

Plastic rotation in one-step of the pushover analysis at the J end is;

$$\theta_J + \frac{\Delta}{L} \tag{B.7}$$

In EqB.6 and B.7, θ_I and θ_J are the increments of the joint rotations at the I and J ends of the element respectively, and Δ is the increment in lateral displacement between the J and I ends of the element (Figure B.9).

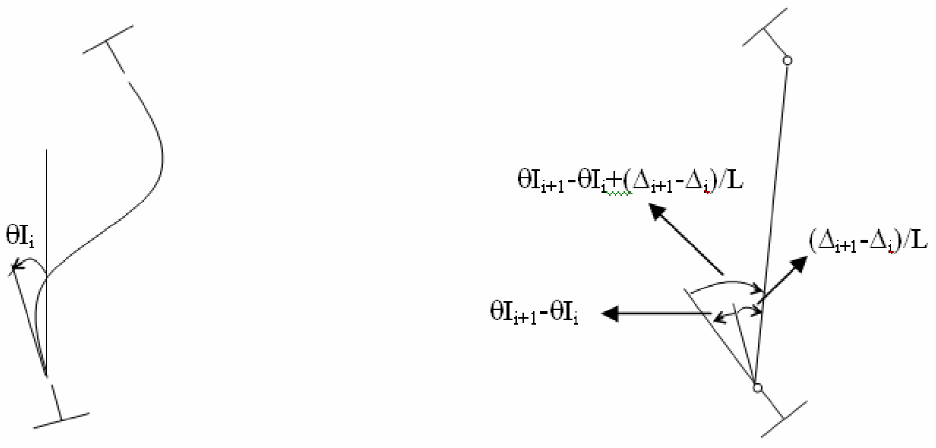

Deformed shape at step i (no yielding) | Deformed shape at step i+1 (yielding at both ends)

Figure B.9 : Calculation of plastic rotations when both ends yield

B.3 Materials' Models

Main factor influencing behaviour of concrete is lateral confinement. The term confinement refers the influence that lateral reinforcement exercises on concrete, which leads to a modification of the compression stress state from uniaxial to multiaxial. The presence of confinement has favorable effect on the strength, as well as ductility factor of concrete.

For stress-strain relationship of concrete, Mander Concrete Model (Mander et al., 1988) is used, while obtaining member moment-curvature relations for structural members. Obtaining concrete stress – strain diagrams by Mander Model is composed of following formulas:

$$f_c = \frac{f'_{cc} \cdot x \cdot r}{r - 1 + x^r} \tag{B.8}$$

$$x = \frac{\varepsilon_c}{\varepsilon_{cc}} \tag{B.9}$$

$$r = \frac{E_c}{E_c - E_{sec}} \tag{B.10}$$

$$E_c = 5000 \cdot \sqrt{f'_{co}} \tag{B.11}$$

$$E_{sec} = \frac{f'_{cc}}{\varepsilon_{cc}} \tag{B.12}$$

$$\varepsilon_{cc} = \varepsilon_{co} \cdot \left[1 + 5 \cdot (\frac{f'_{cc}}{f'_{co}} - 1) \right] \tag{B.13}$$

$$\varepsilon_{co} \cong 0.002 \tag{B.14}$$

$$f'_{cc} = f'_{co} \cdot (-1.254 + 2.254 \cdot \sqrt{1 + \frac{7.94 \cdot f_e}{f'_{co}}} - 2\frac{f_e}{f'_{co}}) \tag{B.15}$$

$$f_e = k_e \cdot \rho \cdot f_{yw} \tag{B.16}$$

$$k_e = \frac{(1 - \sum_{i=1}^{n} \frac{(w_i)^2}{(6 \cdot b_c \cdot d_c)}) \cdot (1 - \frac{s}{2 \cdot b_c}) \cdot (1 - \frac{s}{2 \cdot d_c})}{(1 - \rho_{cc})} \tag{B.17}$$

$$\varepsilon_{cu} = 0.004 + \frac{1.4 \cdot \rho_s \cdot f_{yw} \cdot \varepsilon_{su}}{f'_{cc}} \tag{B.18}$$

where

f'_{cc} is compressive strength of confined concrete

f'_{co} is unconfined concrete compressive strength

f_e is unconfined effective lateral confining stress

f_{yw} is yield strength of transverse reinforcement

k_e is confinement effectiveness coefficient

ρ is ratio of the volume of transverse confining steel to the volume of confined concrete core in x-direction

w_i is ith clear distance between adjacent longitudinal bars

b_c , d_c = core dimensions to centerlines of perimeter hoop and $b_c > d_c$

s is center to center spacing or pitch of spiral or circular hoop

ρ_{cc} is ratio of area of longitudinal reinforcement to area of section

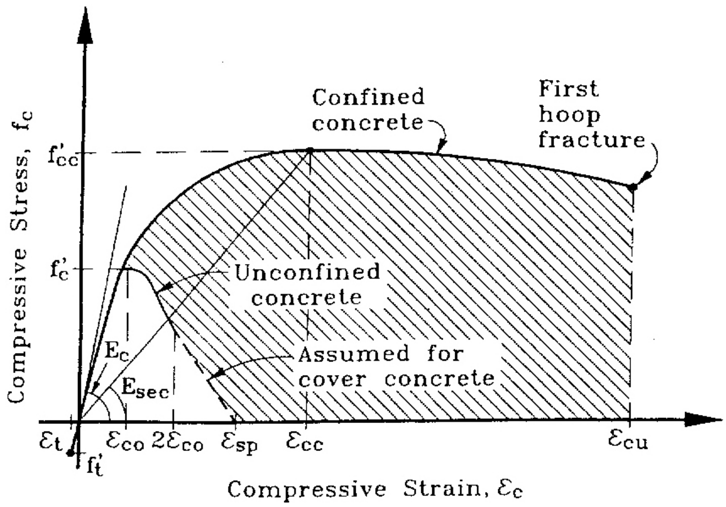

Figure B.10 : Mander Concrete Model, (Mander et al., 1988)

For the reinforcement steel stress – strain model following formulation is used.

$$E_s = 2 \cdot 10^5 \text{ Mpa} \tag{B.19}$$

$$
\begin{aligned}
f_s &= E_s \cdot \varepsilon_s && \text{if} \quad (\varepsilon_s \le \varepsilon_{sy}) \\
f_s &= f_s && \text{if} \quad (\varepsilon_y < \varepsilon_s \le \varepsilon_{sh}) \\
f_s &= f_u - (f_u - f_y) \cdot \frac{(\varepsilon_{su} - \varepsilon_s)^2}{(\varepsilon_s - \varepsilon_{sh})^2} && \text{if} \quad (\varepsilon_{sh} < \varepsilon_s \le \varepsilon_{su})
\end{aligned}
\qquad \text{B.20)}
$$

In thesis work, bilinear stress strain curves is used for reinforcement steel; in other words, f_u is assumed to be equal f_y.

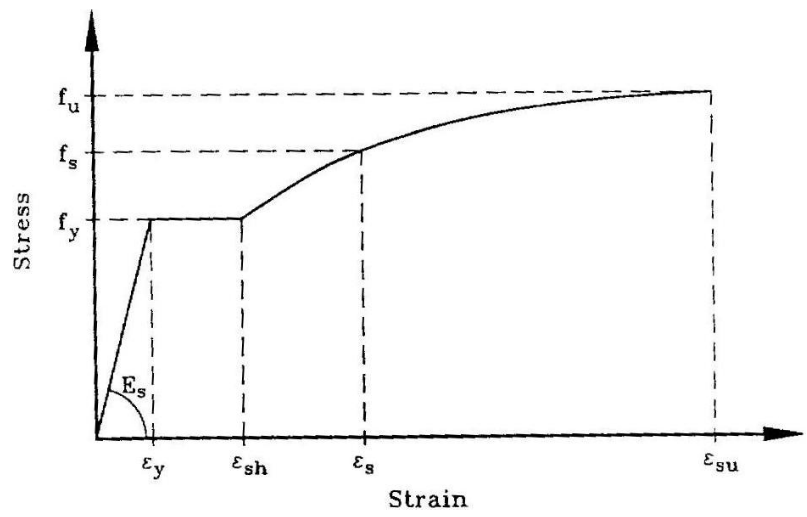

Figure B.11 : Stress – strain model for steel

B.4 Obtaining Moment-Curvature Relations

For each member, moment – curvature curves must be converted to moment – rotation curves by following formulas:

$$\theta_y = \frac{K_y \cdot L_p}{6} \tag{B.21}$$

$$\theta_u = \frac{(K_u - K_y)}{L_p} \tag{B.22}$$

where

K_y is yield curvature of moment – curvature curve

K_u is ultimate curvature of moment – curvature curve

L_p is plastic hinge length of section

L_p is plastic hinge length of section which is taken as half of the cross-section depth

θy is yield rotation

θu is ultimate rotation

APPENDIX C

DYNAMIC RESPONSE OF LINEAR SDOF SYSTEMS TO DYNAMIC PULL RECORD

C.1 Response to Dynamic Pull Record

The response of SDOF systems to earthquake excitation is a classical topic in structural dynamics. In this part of study, results for response of linear SDOF system to dynamic pull record (DPR) is presented, including concept of equivalent viscous damping.

Including viscous damping the equation of motion of SDOF systems to earthquake excitation is

$$m \cdot \ddot{u}(t) + c \cdot \dot{u}(t) + k \cdot u(t) = -m \cdot \ddot{u}_g(t) \tag{C.1}$$

This equation is to be solved subject to the initial conditions

$$u(0) = 0 \quad \dot{u}(0) = 0 \tag{C.2}$$

Damping coefficient and natural frequency are

$$c = 2 \cdot \zeta \cdot m \cdot \omega_n \tag{C.3}$$

$$\omega_n = \sqrt{\frac{k}{m}} \qquad \text{(C.4)}$$

According to Figure 3.1 following relation can be used for defining ground acceleration for DPR

$$\ddot{u}_g(t) = A \cdot t \qquad \text{(C.5)}$$

After inserting previous relations to equation of motion, linear second order differential equation becomes,

$$\ddot{u}(t) + 2 \cdot \varsigma \cdot \omega_n \cdot \dot{u}(t) + \omega_n{}^2 \cdot u(t) = -A \cdot t \qquad \text{(C.6)}$$

Steady state solution of equation of motion is of the form

$$u_s(t) = c_1 \cdot t + c_2 \qquad \text{(C.7)}$$

Transitient part of solution of equation of motion is of the form

$$u_t(t) = e^{-\zeta \cdot \omega_n \cdot t}(c_3 \cdot \sin(\omega_D \cdot t) + c_4 \cdot \cos(\omega_D \cdot t)) \qquad \text{(C.8)}$$

where

$$\omega_D = \omega_n \cdot \sqrt{1-\zeta^2} \qquad \text{(C.9)}$$

Total response of SDOF system is summation of transition part and steady state responses.

$$u(t) = u_s(t) + u_t(t) \qquad \text{(C.10)}$$

By imposing the initial conditions to obtain the final result, unknown coefficients, c_1, c_2, c_3 and c_4, become

$$c_1 = -\frac{A}{\omega_n^2}$$

$$c_2 = \frac{2 \cdot \varsigma \cdot A}{\omega_n^2}$$

$$c_3 = \frac{A \cdot (1 - 2 \cdot \varsigma^2)}{\omega_n^2 \cdot \omega_D} \qquad \text{(C.11)}$$

$$c_4 = \frac{2 \cdot \varsigma \cdot A}{\omega_n^3}$$

Finally inserting the found coefficients to transition and steady state solutions of equation of motion, response of linear SDOF system becomes

$$u_t(t) = \frac{A}{\omega_n^{\ 2}} \cdot e^{(-\zeta \cdot \omega_n \cdot t)} \cdot \left(\cdot (\frac{(1 - 2 \cdot \zeta^2)}{\omega_D}) \cdot \sin(\omega_D \cdot t) - \frac{2 \cdot \zeta}{\omega_n} \cdot \cos(\omega_D \cdot t) \right) \text{(C.12)}$$

$$u_s(t) = \left(-\frac{A \cdot t}{\omega_n^{\ 2}} \right) + \left(\frac{2 \cdot \zeta \cdot A}{\omega_n^{\ 3}} \right) \qquad \text{(C.13)}$$

C.2 Acceleration Response Spectrum of Dynamic Pull Record

$$\ddot{u}_{tot}(t) = \ddot{u}_g(t) + \ddot{u}(t) \qquad \text{(C.14)}$$

According to Figure 3.1 following relation can be used for defining ground acceleration

$$\ddot{u}_g(t) = A \cdot t \qquad \text{(C.15)}$$

Differentiating response of SDOF system, $u(t)$, twice gives,

$$\ddot{u}(t) = -A \cdot e^{(-\varsigma \cdot \omega_n \cdot t)} (\frac{\sin(\omega_D \cdot t)}{\omega_D}) \qquad \text{(C.16)}$$

After inserting ground and relative acceleration relations to total acceleration equation, following expression is obtained.

$$\ddot{u}_{tot}(t) = A \cdot t \cdot (1 - (e^{(-\varsigma \cdot \omega_n \cdot t)} \frac{\sin(\omega_D \cdot t)}{\omega_D \cdot t})) \tag{C.17}$$

Absolute maximum values of $\ddot{u}_{tot}(t)$ are obtained when t is equal to t_d which is called target time. A plot of absolute maximums as a function of natural vibration period makes acceleration response spectrum (Figure 3.4).

$$Sa(\omega_n) = \left| A \cdot t_d \cdot (1 - (e^{(-\varsigma \cdot \omega_n \cdot t_d)} \frac{\sin(\omega_D \cdot t_d)}{\omega_D \cdot t_d})) \right| \tag{C.18}$$